COMSAT Laboratories

Volume I

Technology Assessment

PHASED-ARRAY-FED ANTENNA CONFIGURATION STUDY

Submitted to

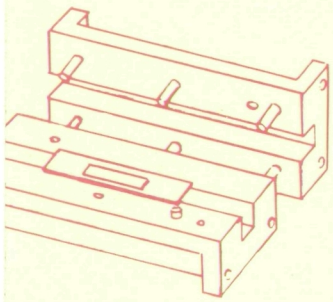

NASA Lewis Research Center
21000 Brookpark Road
Cleveland, Ohio 44135

Under Contract NAS3-23250

October 1983

COMSAT Laboratories
Clarksburg, Maryland 20871

1 Report No	2 Government Accession No	3 Recipient's Catalog No
CR168231		

4 Title and Subtitle	5 Report Date
Phased-Array-Fed Antenna Configuration Study Volume I - Technology Assessment	October 1983
	6 Performing Organization Code

7 Author(s)	8 Performing Organization Report No
R. M. Sorbello, A. I. Zaghloul, B. S. Lee, S. Siddiqi B. D. Geller, H. I. Gerson, D. N. Srinivas	
	10 Work Unit No

9 Performing Organization Name and Address	11 Contract or Grant No
Communications Satellite Corporation COMSAT Laboratories Clarksburg, Maryland	NAS3-23250
	13 Type of Report and Period Covered Contract Report

12 Sponsoring Agency Name and Address	14 Sponsoring Agency Code
National Aeronautics & Space Administration Washington, D.C. 20546	

15 Supplementary Notes

NASA Lewis Research Center
Technical Manager, Jerry Smetana, M.S. 54-5

Space Communications Division
Cleveland, OH 44135

16 Abstract

The present status of the technologies for phased-array-fed dual reflector systems is reviewed in this volume. The report addresses the different aspects of these technologies, including optical performances, phased array systems, problems encountered in phased array design, beamforming networks, MMIC design and its incorporation into waveguide systems, reflector antenna structures, and reflector deployment mechanisms. The report offers a comprehensive literature survey on each of these subjects.

17 Key Words (Suggested by Author(s))	18 Distribution Statement
Antenna, Satellite Communications, Dual Reflector, Array Feed, MMIC Active Array	Unclassified - Unlimited

19 Security Classif (of this report)	20 Security Classif (of this page)	21 No of Pages	22 Price*
Unclassified	Unclassified	157	

* For sale by the National Technical Information Service, Springfield, Virginia 22161

PHASED-ARRAY-FED ANTENNA CONFIGURATION STUDY

VOLUME I
TECHNOLOGY ASSESSMENT

by

R. M. Sorbello
A. I. Zaghloul
B. S. Lee
S. Siddiqi
B. D. Geller
H. I. Gerson
D. N. Srinivas

Submitted to

NASA Lewis Research Center
21000 Brookpark Road
Cleveland, OH 44135

Under Contract NAS3-23250

October 1983

COMSAT Laboratories
Clarksburg, Maryland 20871

Page intentionally left blank

Pages II — VI

Page intentionally left blank

Table of Contents

Table of Contents (Cont'd)

Table of Contents (Cont'd)

List of Illustrations

List of Illustrations (Cont'd)

List of Illustrations (Cont'd)

List of Tables

1. INTRODUCTION

The design of a phased-array-fed, dual-reflector antenna system requires a comprehensive understanding of different areas of antenna and microwave technology. This volume, Technology Assessment, presents COMSAT's effort performed under Task I of the phased-array-fed antenna configuration study. This assessment is based on thorough knowledge of current technology and a logical prediction of future trends. Seven areas of significance are covered under this task. The present status of each area, including a survey of related literature, is addressed in detail. Based on this status, a technology trend is discussed for each area.

Section 2 compares the main optical systems used for satellite communications applications. These include a single reflector system, Cassegrain/Gregorian- and Schwarzschild-type dual reflector systems, and systems fed by phased arrays.

Section 3 addresses topics related to phased array design. It assesses the present status of phased-array-fed reflector systems and direct radiating phased arrays, and then presents the design aspects of phased array and array elements. A survey of the studies on mutual couplings and on different lens types is also included.

Section 4 discusses different types of beam-forming networks (BFNs) and examines their main components: power dividers, phase shifters, switches, and polarizers. This section also briefly discusses BFN controllers.

The availability of microwave integrated circuits (MICs) and monolithic MICs (MMICs) is the most significant factor in the potential use of phased arrays for satellite communications. Section 5 gives the present status of MIC and MMIC technology, including the packaging of MMICs into waveguide systems through special waveguide/MMIC transitions.

The mechanical aspects of reflector system design are presented in Sections 6 and 7. Different reflector surfaces are discussed in Section 6, with assessments of surface tolerances, thermal distortions, and the resultant beam pointing errors. The materials used in reflector fabrication are also mentioned. Section 7 discusses current deployment techniques and the associated sources of error.

2. LARGE SCANNING REFLECTOR ANTENNAS

2.1 PARABOLIC REFLECTORS

Parabolic reflectors have been the most commonly used antennas in modern satellite applications. These antennas are light in weight, simple in configuration, and easily generate scanned spot beams or multiple beams. To achieve beam scanning, the feeds are displaced in the focal plane from the focal point such that the energy is reflected at an angle from the boresight. To generate multiple beams, a feed cluster is located on the focal plane or on the optimum feed locus surface. Usually, these feeds are arranged in a lattice form to optimize the feed aperture area.

Since a parabolic surface is a perfect collimating device only for a feed located on the focal point, a beam scanned from the boresight direction experiences degradation caused by phase aberrations resulting from feed displacement. This degradation always limits the scan range of the reflectors. To determine how far a parabolic reflector can scan, or to improve its scan range, the effects of aberration on the performance of a parabolic reflecting system must be investigated. Studies in this area have been extensive and can be traced back to the classical theory of aberrations in optical systems [2-1]-[2-3].

In the area of antenna problems, the original experimental work that investigated the scanning characteristics of parabolas was done by Silver and Pao [2-4]. Kelleher and Coleman [2-5] also performed experiments and derived the theoretical expression for the coma term. Lo [2-6] developed the formulas for the beam deviation factor, which relates the beam reflection

angle to the angular displacement of the feed. A more extensive analysis was performed by Sandler [2-7], who predicted the scan beam pattern by using the current distribution method and the scalar diffraction theory.

Ruze [2-8] developed the approximate formulas to predict beam shift and degradation of a paraboloid with an offset feed. His analysis was based on the scalar plane wave theory and series expansion of the phase function. Even though the approximation in his analysis is valid only for limited scanned angles, his work made a significant contribution by presenting the scan characteristics of the offset-fed paraboloid in both simple formulations and useful graphic curves. A more general treatment of the aberration and dispersion of a parabola was reported by Afifi [2-9].

For larger feed displacements, Imbriale et al. [2-10] utilized both the vector current method and the scalar aperture theory to evaluate scan performance. They concluded that the vector theory is required to accurately predict the peak gain and coma lobe levels for large scan angles.

Recently, Mrstik investigated the scan limits of large parabolas [2-11]. By minimizing the variance of the path lengths, the scan angle can be expressed in terms of feed position and antenna geometry such as focal length and aperture diameter. Scan loss can be estimated by using rms phase error. If the acceptable scan loss is specified, the scan limit of a paraboloid can be determined.

To avoid aperture blockage effects, most reflectors used in current satellites are offset parabolas. A typical offset parabola configuration is shown in Figure 2-1. Unfortunately, only a limited number of studies dealing with the scan performance of offset parabolic reflectors are available in the literature. A detailed analysis of the radiation patterns of offset reflectors with offset feeds was given by Rudge [2-12]. Two

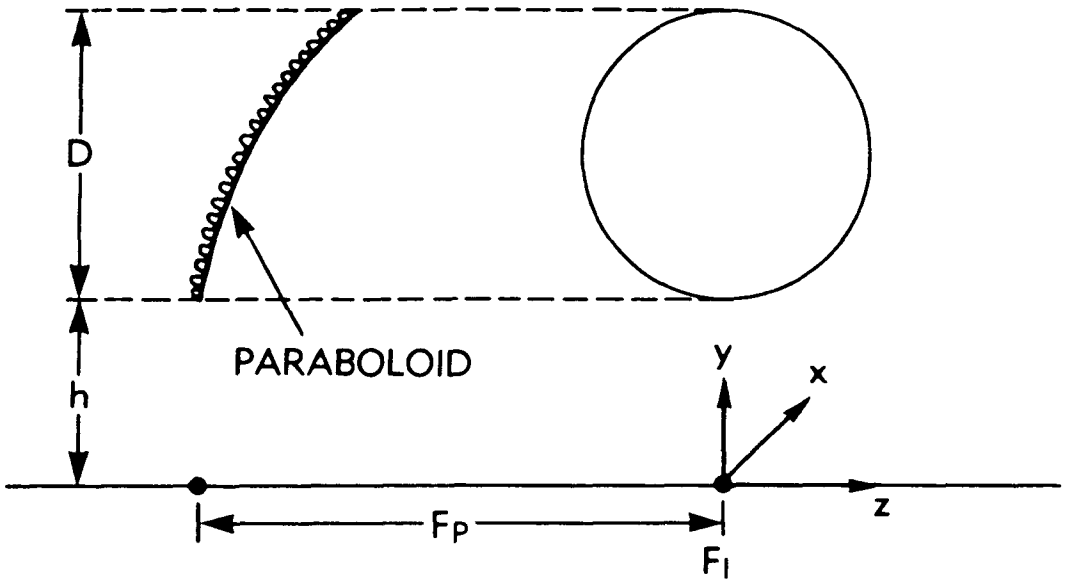

Figure 2-1. Geometry of the Single Offset Reflector

theoretical models were described to predict co-pol and cross-pol patterns, as well as the effects of moderate lateral feed displacements.

Ingerson and Wong presented the focal region characteristics of offset parabolic reflectors [2-13]. They defined the offset axis as the line through the focal point that bisects the subtended angle of the reflector at the focal point in the plane of symmetry. The offset focal plane was defined as the plane perpendicular to the offset axis and containing the focal point. These definitions are useful in arranging multiple feeds in a multiple beam system. However, the optimum feed pointing axis does not usually coincide with the offset axis, and the optimum feed loci generally form a curved surface instead of the offset focal plane [2-14]. A recent study of the optimum feed locus for parabolic reflectors [2-15], found that the optimum feed pointing axis is almost midway between the offset axis and the line connecting the focal point and the

center point of the reflector. The beam deviation factor derived from a symmetrical system reported in Reference 2-13 does not take into account the unsymmetric curvature of the surface, which in reality generates upper scan beams with BDF > 1 and lower scan beams with BDF < 1 in the offset plane. Ingerson [2-16] also presented the scan characteristics of the offset reflector in terms of beam scan loss and sidelobe structures based on numerical and measured data.

Recently, Zaghloul and Persinger [2-17] presented a study on the INTELSAT VI antenna subsystem. Their analysis of the two candidate antennas for various zone coverages demonstrated the scanning performance of the parabolic reflectors as multiple beam antennas in a practical application. A review of the beam scanning of paraboloidal antennas resulting from lateral feed displacement was given in a recent antenna handbook by Rudge et al. [2-18]. The effects of beam scanning can be readily seen from the H-plane pattern of a paraboloid, as shown in Figure 2-2.

The scanning capability of parabolic reflectors is restricted by phase aberrations resulting from feed displacements. Thus, it is desirable to correct the phase error and reduce the beam distortion so that the scan range can be extended. A number of studies have described different approaches to this problem. Takeshima [2-19] employed a defocusing technique to compensate the phase errors; Lonx and Martin [2-20] applied the focal plane array technique to correct the aberration; and Rudge and Witners [2-21] achieved wide angle beam steering by adjusting the feed movement along a given locus to match the focal region fields of an off-axis incident plane wave. However, these approaches are difficult, if not impossible, to implement in satellite antenna systems.

A more promising way to improve scan beam performance is to use a cluster feed instead of a single element feed. A

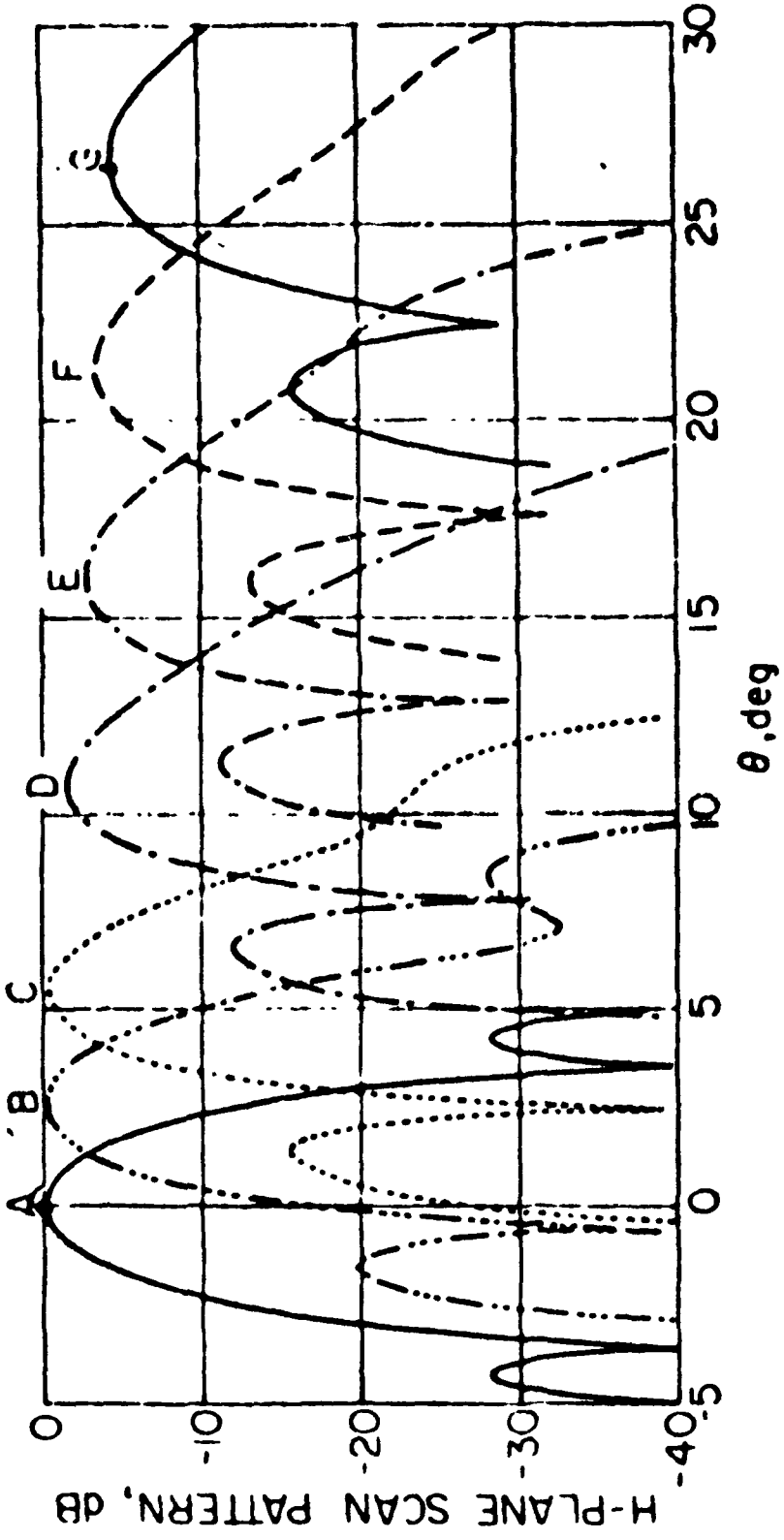

Figure 2-2. H-Plane Pattern of a Paraboloid Illuminated by a Laterally Defocused TE_{11} Feed [2-18]

cluster consists of multiple elements arranged, for example, in circular layers. To maintain an appropriate crossover level of component beams, some feed elements may need to be shared by adjacent clusters. To determine horn size and element spacing, Balling et al. [2-22] synthesized a "clean" beam by constructing the cluster feed to minimize the sidelobes and cross polarization of the feed patterns. As this effect is achieved, the array factor function for the feed cluster is forced to a minimum at the edge of the reflector. The scan beam quality in a reflector system using feed clusters can be optimized by choosing nonuniform excitation coefficients which minimize the phase error on the reflector aperture. Galindo-Israel et al. [2-23] used the sequential current method to synthesize the excitations for a laterally displaced feed cluster. This compensates the aperture phase distortion caused by feed displacement.

Phase aberrations can also be reduced by using a long focal length. Zaghloul and Persinger [2-17] have demonstrated the effect of different focal lengths on scanned beam degradation. Figure 2-3 shows the 4-dB contours of the scanned beams of two single offset reflectors with f/D = 0.9 and 1.4, respectively. It can be seen that the system with shorter focal length has more beam distortion for larger scanning. However, the use of large f/D increases the physical dimension of the antenna and may cause a package problem. Also, bigger horns are needed to generate narrower feed patterns to reduce spillover. These will add weight to the system and cause blockage. For applications that require a large aperture to generate narrow beams with high gain, the scan range in degrees would be small, since the scanning capability is given by beamwidths. DiFonzo [2-24] has discussed the fundamental optical performance of a single offset reflector in terms of diameter, antenna beamwidth, and beam isolation. Further study is required to determine the optical limitation of beam scanning for single offset reflectors as aperture sizes increase.

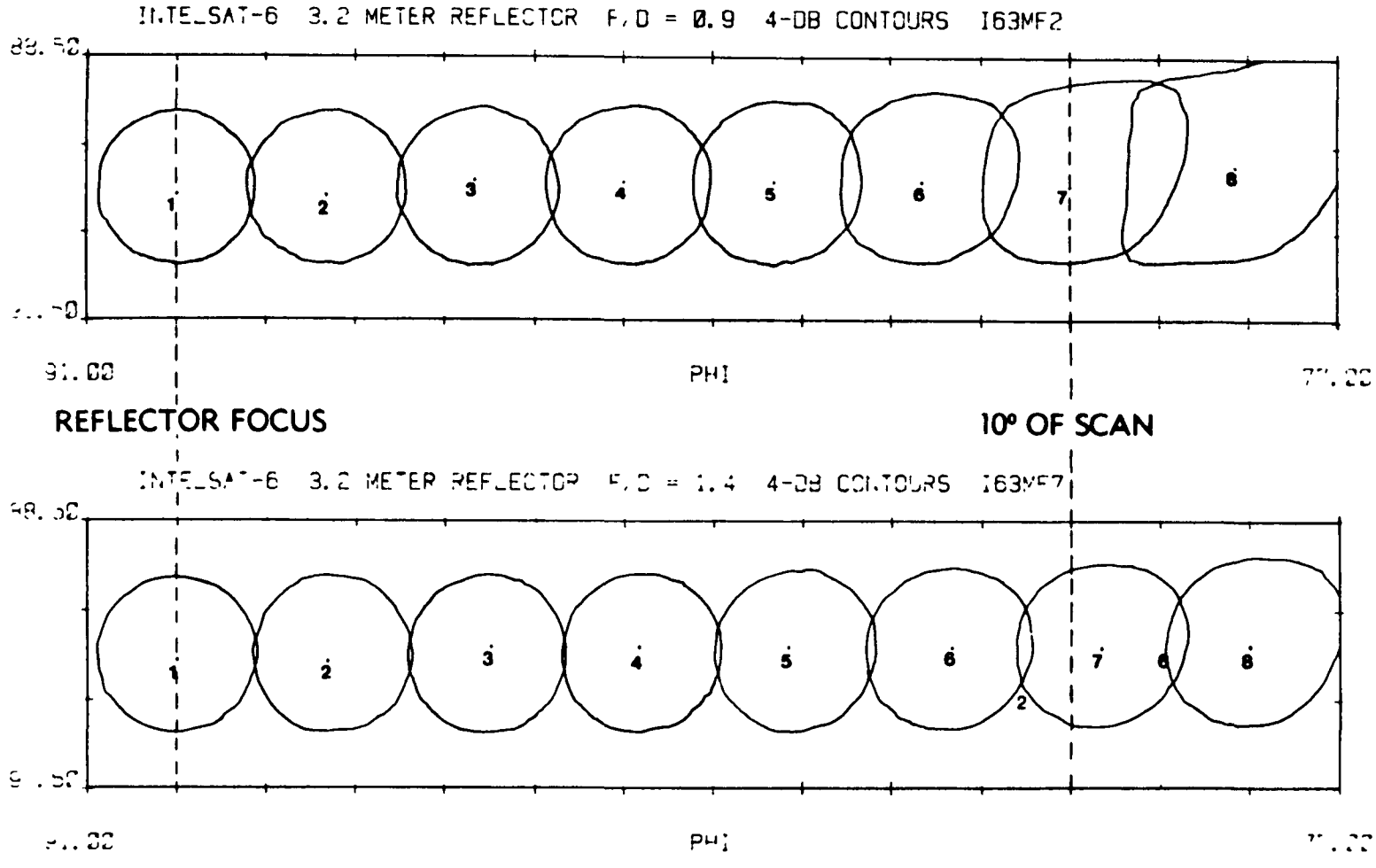

Figure 2-3. Component Beam Scan Performance for f/D = 0.9 and 1.4 [2-17]

2.2 CASSEGRAIN/GREGORIAN REFLECTOR SYSTEMS

As future satellite communications systems require high resolution of signal transmissions, dual-reflector antennas may be able to generate narrow beams with high gain, while maintaining good isolation spatially and by polarization. Compared with single parabolic reflectors, dual-reflector systems usually have larger equivalent f/D ratios. Also, the additional degree of design freedom implied by the use of two reflecting surfaces may yield better cross polarization, beam squint, and beam scanning performance.

The most popular dual-reflector systems are Cassegrain and Gregorian, as illustrated in Figure 2-4. Hannan [2-25] published the first comprehensive analysis of Cassegrain antennas derived from classical optical concepts. He introduced the concept of equivalent parabola based on geometrical optics and obtained reasonably good results by analyzing the equivalent parabola in place of the Cassegrain system. The geometrical relationship of these two antennas is illustrated in Figure 2-5. White and DeSize [2-26] defined the focal length of the equivalent parabola as the main reflector focal length times magnification, which is the ratio of the long and short focal lengths of the hyperbola. The equivalent parabola concept technique is also used by Wong [2-27] to predict the scan performance of a Cassegrain system. His conclusion is that the equivalent parabola concept only produces negligible error for beam squints up to four beamwidths. However, Griss and Ries [2-28] found severe differences between the Cassegrain system and the equivalent parabola for large defocusing by investigating the aperture phase in the form of a series expansion. Recently, Rahmat-Samii and Galindo-Israel [2-29] observed, based on numerical data, that the equivalent parabola concept can be used to determine the location of the displaced feed and to define the local optimal focal plane for small scan angles.

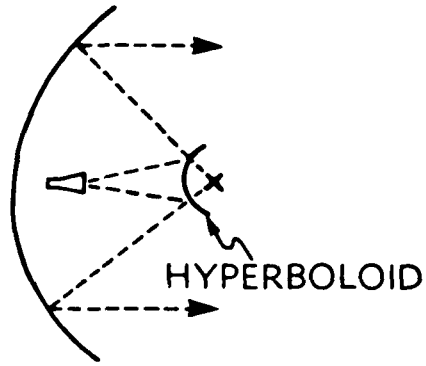

(a) CASSEGRAIN ANTENNA

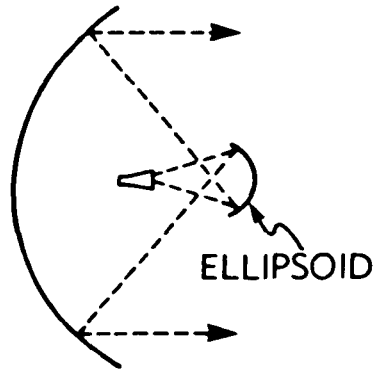

(b) GREGORIAN ANTENNA

Figure 2-4. Geometries of Symmetrical Dual-Reflector Antennas

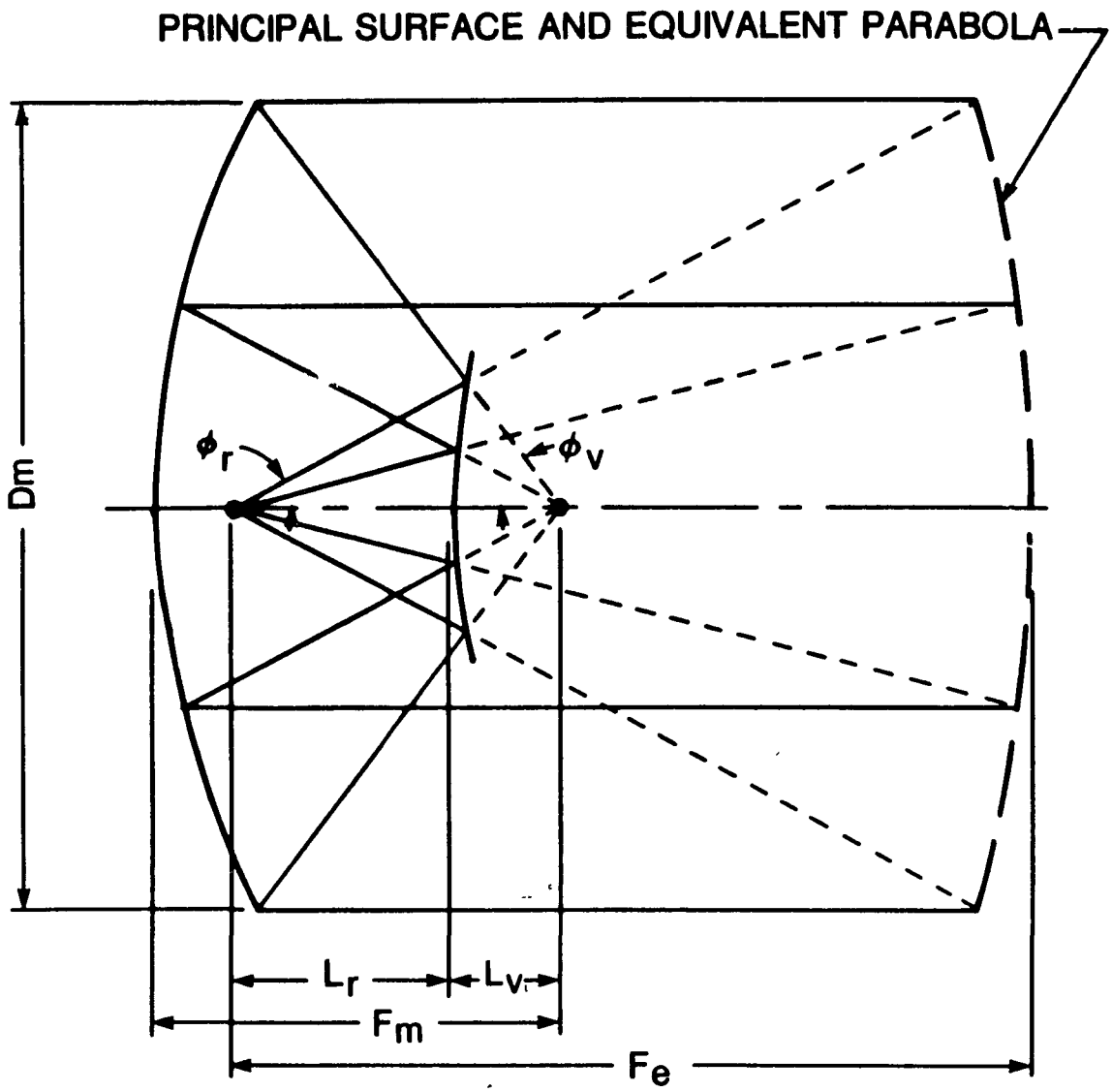

Figure 2-5. Geometry of the Cassegrain Antenna and Its Equivalent Parabola [2-25]

DiFonzo and Lee [2-30] compared the calculated scan patterns of a Cassegrain antenna and its equivalent parabola. Their results confirm that the equivalent parabola always predicts less degradation, as shown in Figures 2-6 and 2-7. In fact, even for small scanning, this concept should only be used as a simplified tool to design or analyze the antennas. More accurate results should be obtained by using the actual two-reflector model, so that the diffraction and depolarization effects of the subreflector are included.

To evaluate the scattered field from the subreflector, Rusch [2-31] employed the physical optics (PO) approach, which integrates the induced current density over the subreflector surface. In this way, the spillover field can be accurately predicted. On the other hand, Potter [2-32] used the spherical wave expansion technique, which generates more efficient aperture distributions and improves subreflector impedance matching. As long as the scattered field from the subreflector is known, the secondary pattern can be computed, as in the single reflector case. However, two surface integrations would be required to compute the secondary pattern, which would be time-consuming and expensive.

In recent years, the geometrical theory of diffraction (GTD) [2-33],[2-34], which is an efficient high-frequency technique, has been used to calculate the subreflector fields; while PO is used to compute the secondary pattern. One of the earliest papers that applied GTD to Cassegrain reflector system was presented by Mentzer and Peters [2-35], who used GTD in a two-dimensional model to calculate the far-out sidelobes of a symmetrical system. Sorensen and Rusch [2-36] evaluated the scattered fields of a Cassegrain subreflector in a defocused system by GTD. Adatia [2-37] also used GTD to investigate the diffraction effects in the offset Cassegrain antenna. He found that for small subreflectors (less than 20λ), the diffracted fields from the subreflector contribute significantly to the secondary pattern in the sidelobe region.

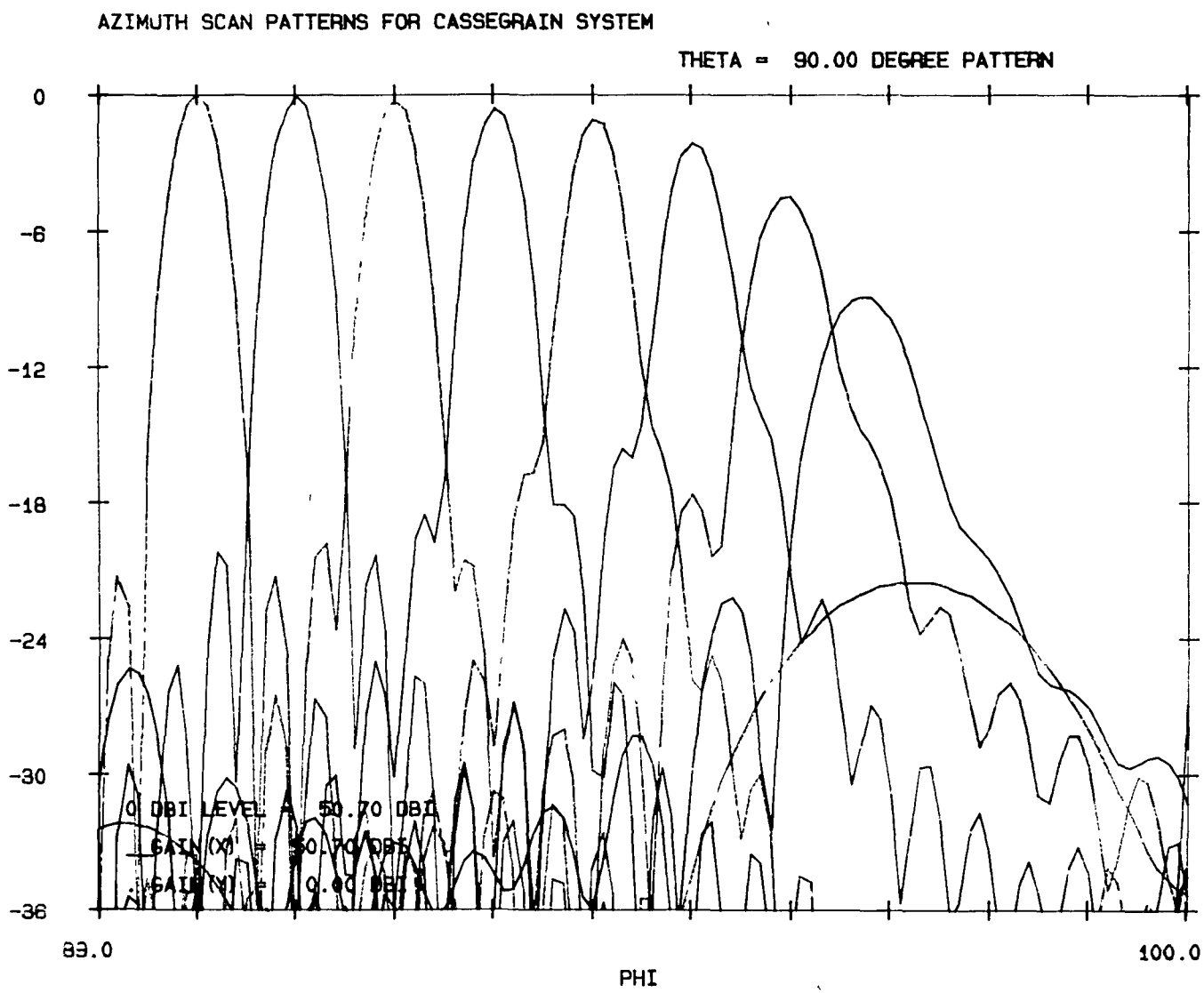

Figure 2-6. Azimuth Scan Patterns for the Cassegrain System [2-30]

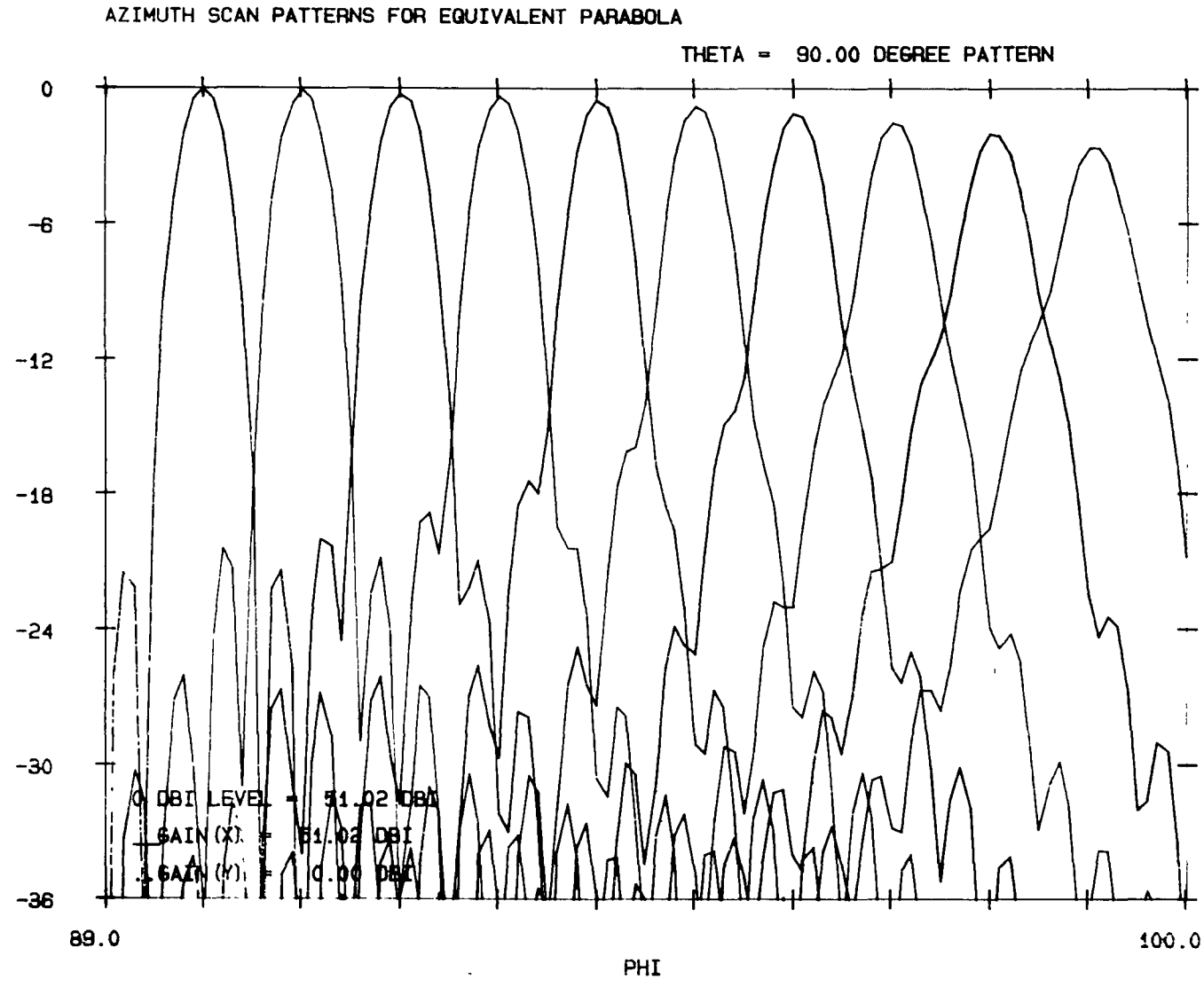

Figure 2-7. Azimuth Scan Patterns for the Equivalent Parabola [2-30]

The offset Cassegrain and Gregorian antennas (see Figures 2-8 and 2-9) were proposed by Graham [2-38] and Yokoi et al. [2-39] independently. In addition to avoiding subreflector blockage, an appropriate arrangement of the two offset reflectors may cancel the cross-pol components caused by each individual reflector surface and thus allow certain degrees of cross-pol control and sidelobe suppression. The radiation characteristics of both the offset Cassegrain and Gregorian antennas have been discussed extensively [2-40]-[2-42].

A detailed study of these two types of reflectors was performed by Akagawa [2-43] for spacecraft antenna applications. Numerical data that relate f/D, eccentricity, beamwidths, sidelobe and cross-pol levels, etc., were presented to demonstrate the tradeoff of system performance with respect to antenna parameters. Mizuguchi et al. [2-44] investigated the characteristics of an offset Gregorian reflector both theoretically and experimentally. Their results showed that the sidelobe levels of their designed antenna were lower by 3 $\cong$ 5 dB than those of a comparable offset Cassegrain antenna. They also showed that cross-pol can be eliminated by the proper choice of axis orientation.

Beam scanning characteristics of offset Cassegrain or Gregorian antennas have not been investigated extensively in the past. However, this topic has drawn more attention in recent years. Akagawa and DiFonzo [2-45] computed the gain loss vs beam scan for an offset Gregorian antenna, and Rahmat-Samii and Galindo-Israel [2-29] studied the scan performance of an offset Cassegrain system. Both these studies show that, for small scans, the scan loss curve follows that of the equivalent parabola; whereas, for large scans, the deviation is substantial.

In regard to the aberration caused by feed displacements, Ohm and Gans [2-46] first applied a numerical analysis technique to evaluate the effect on an offset nonparaxial Cassegrain system.

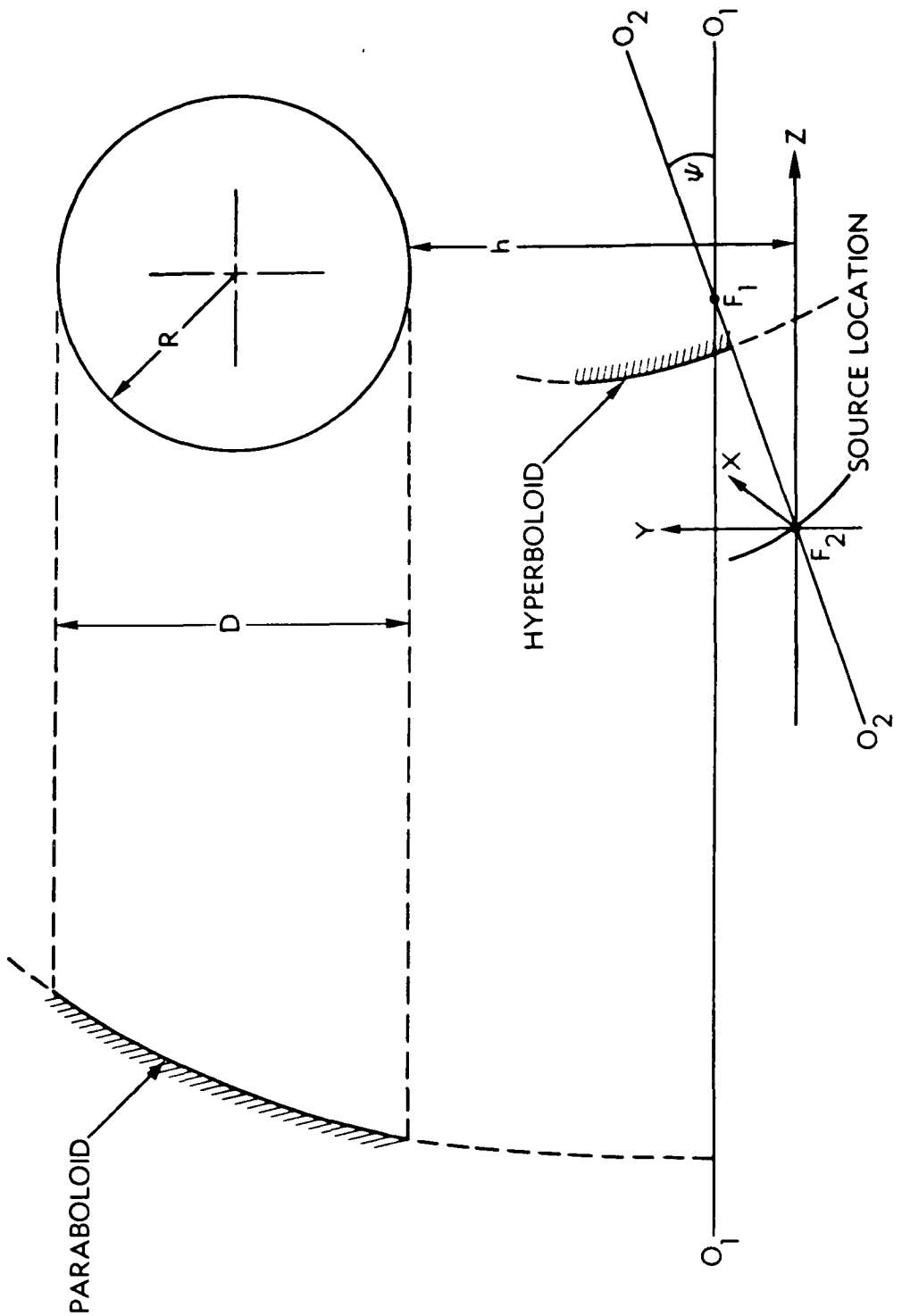

Figure 2-8. Geometry of the Offset Cassegrain Antenna

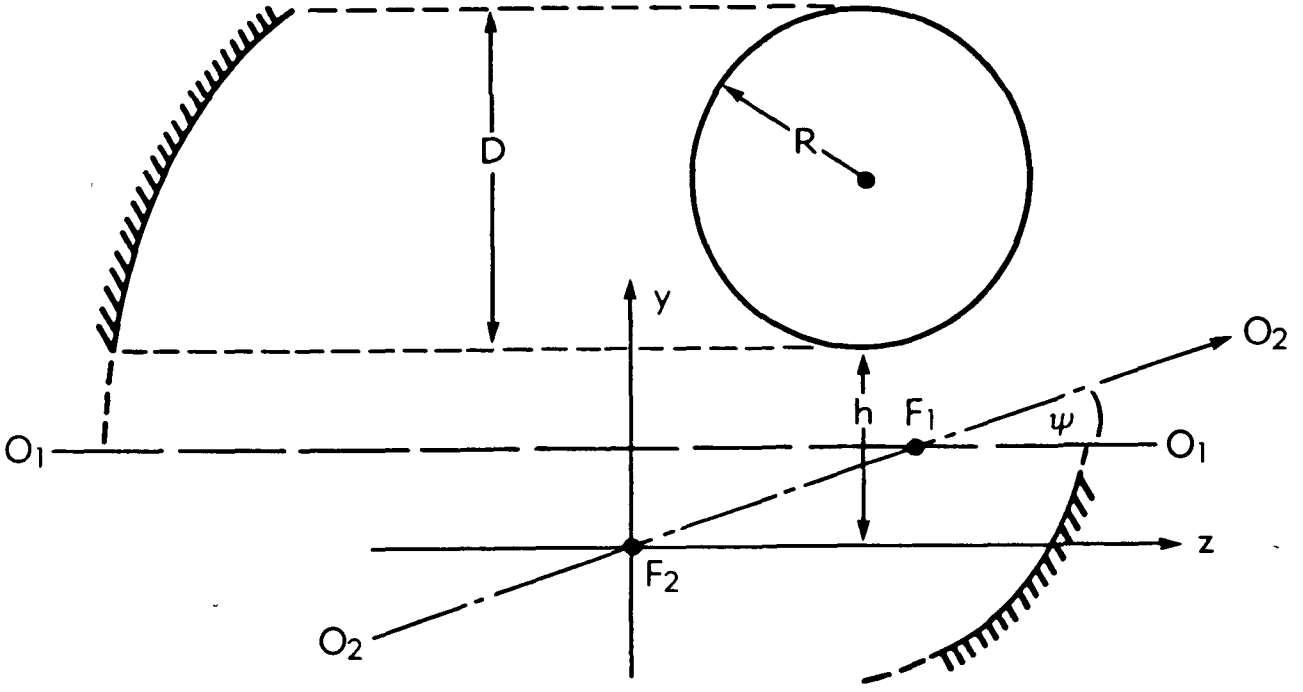

Figure 2-9. Geometry of the Offset Gregorian Antenna

Ohm [2-47] then extended the study and calculated the gain degradation due to astigmatism. More recently, a theoretical derivation of the aberrations in Cassegrain and Gregorian antenna was done by Dragone [2-48], who explicitly derived the various aberration components attributable to astigmatism, coma, etc. He also showed the effect of aberrations on aperture efficiency, as well as the conditions that optimize performance. These results are useful for designing a scanning dual-reflector system.

2.3 SCHWARZSCHILD REFLECTOR SYSTEMS

One of the advantages of using dual-reflector systems is that they have longer equivalent focal lengths, which reduce the phase error and thus have less degradation on scanned beams. However, the coma aberration is still the major cause of pattern distortion for small feed displacement in the Cassegrain and Gregorian systems. One way to reduce the coma aberration is to have the optical system satisfy the Abbé sine condition, which is given by $H = F \sin \alpha$, where the parameters H and α are defined in Figure 2-10 and F is a constant independent of H.

The Schwarzschild antenna system shown in Figure 2-10 resembles a Cassegrain system with the reflector profiles as transcendental curves, which fulfills the Abbé sine condition. Thus, the primary coma does not exist in a Schwarzschild system for small scan angles. Both graphical and analytical methods were used to discover the reflector profile curves that would satisfy not only the Abbé sine condition but also other ray optics requirements in designing a microwave scanning antenna. These requirements include equal path lengths from the source to the specific wavefront plane and Snell's law at each reflector surface. Ponomarev [2-49] devised an iterative graphical method of generating Schwarzschild

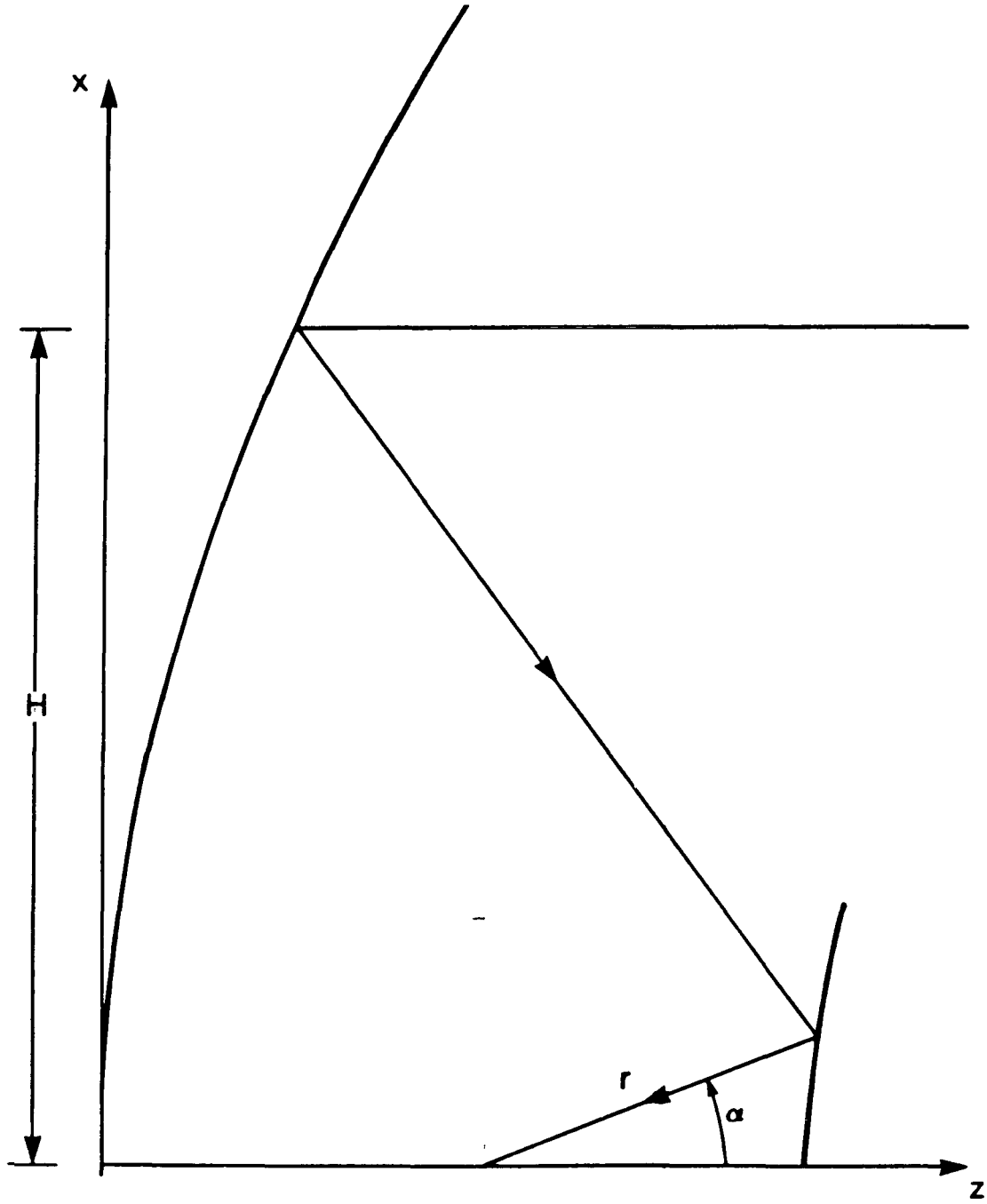

Figure 2-10. Geometry of the Schwarzschild Antenna

profiles. His approach ignores the path length constraint and explicitly applies Snell's law at the main reflector. Unfortunately, the choice of the arbitrary starting points is crucial in the design of the profiles. Furthermore, it is difficult to determine the final reflector diameters, the separation between reflectors, and the illumination requirements before beginning the iterations.

An analytical approach to this problem proves to be more useful. White and DeSize [2-50] derived the solution of the profile equations by solving the equations of the constraints of the optical system. Ray tracing and integration techniques were used to evaluate the antenna radiation patterns which show that the scan performance of the Schwarzschild system is superior to that of the conventional Cassegrain system for small to moderate scan angles (up to $\pm 5^{\circ}$). It was also found that the allowable scan range decreases as the magnification increases. For larger scan angles, the improvement in performance is not as significant, since the coma effects become as pronounced in the Schwarzschild antenna as in the Cassegrain system. An overcompensated system has been designed for larger angle scanning. In this system, the profile of the primary reflector deviates further from that of the Cassegrain system.

Claydon [2-51] gave a detailed analysis of the Schwarzschild antenna, in which a ray tracing method was used to analyze the image region fields, scanning efficiency, and other scanning characteristics. He recommended the use of Schwarzschild systems if the primary reflector is larger than 100λ. Balling et al. [2-22] also reviewed the Schwarzschild system and discussed the coma coefficient.

A design procedure for Schwarzschild systems was reported by van de Sande et al. [2-52]. Formulas for the aperture field and antenna efficiency were derived, and investigation of the geometrical configurations was based on the parametric description

of the reflector surfaces proposed by Roberts [2-53]. The closed-form expressions obtained for the aperture distortion and gain factor show that design of the Schwarzschild antenna system can be simple and easy.

Recently, Rappaport [2-54] compared the coma coefficients of a single paraboloid, a Cassegrain, and a Schwarzschild antenna. He showed that the coma coefficient of the Schwarzschild antenna approaches zero at the focus with zero slope, as illustrated in Figure 2-11. The curves in this figure also confirm that the Schwarzschild antenna is superior to the other two antennas when the scan angle is small. Rappaport's investigation also revealed that use of the Gregorian configuration of the Schwarzschild system to minimize the subreflector blockage resulted in an increase in the overall package size. His findings showed that this design offers excellent scanning possibilities without the overwhelming blockage problems of standard Schwarzschild systems.

2.4 CONFOCAL PARABOLOIDAL REFLECTOR SYSTEMS

A confocal parabolic reflector system, which consists of two reflectors with the same f/D fed by a plane wave source, has long been used in microwave antenna applications. One of the early works was by Hogg and Semplak [2-55], who studied the near-field Cassegrain configuration and compared its performance with that of the standard Cassegrain antennas. Since the near field of a plane wave feed is collimated and of uniform phase, less spill-over is expected in this system than in the standard Cassegrain configuration with comparable dimensions. In their experimental model, Hogg and Semplak used a horn reflector antenna as the plane wave feed, as shown in Figure 2-12. Fitzgerald [2-56] also reported on a near-field Cassegrain system and showed that this

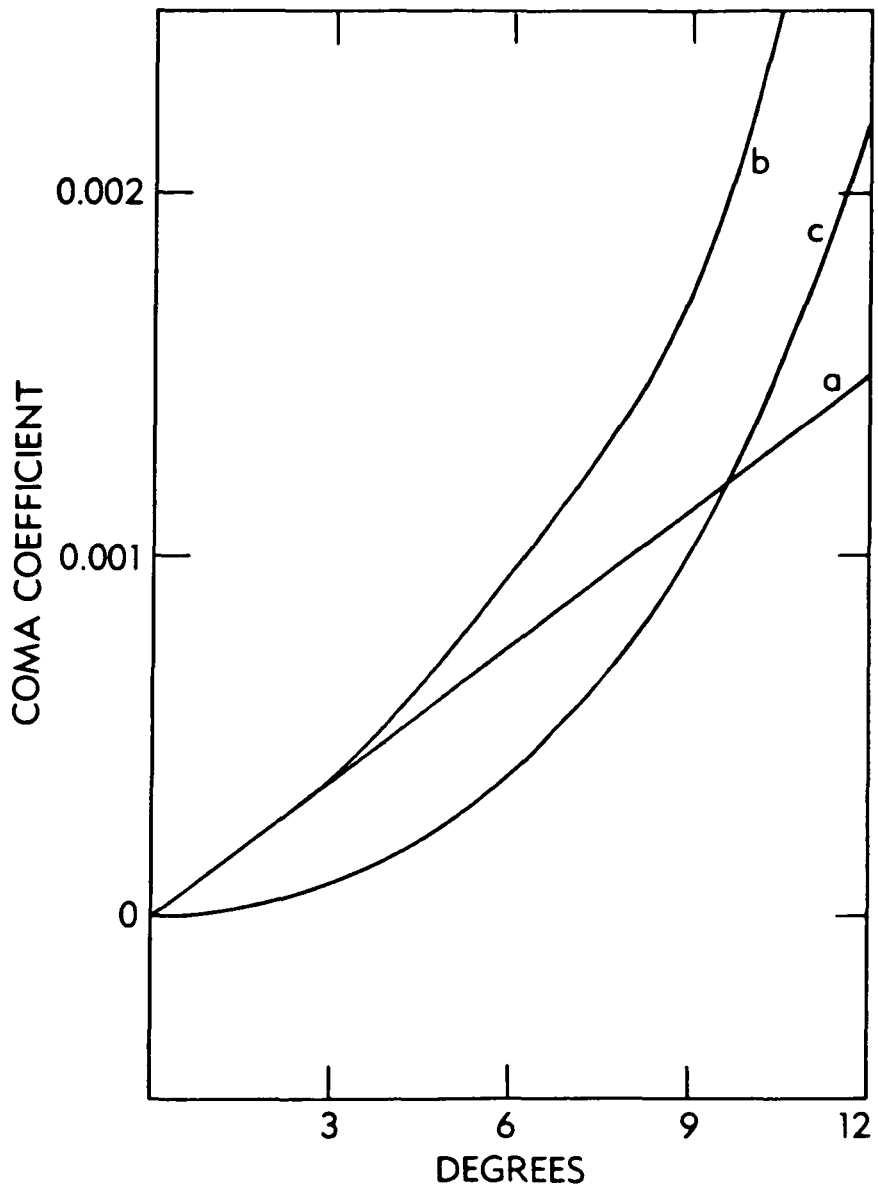

Figure 2-11. Comparison of Coma Aberration for Three Reflector Antennas: (a) Paraboloid, (b) Cassegrain, and (c) Schwarzschild [2-54]

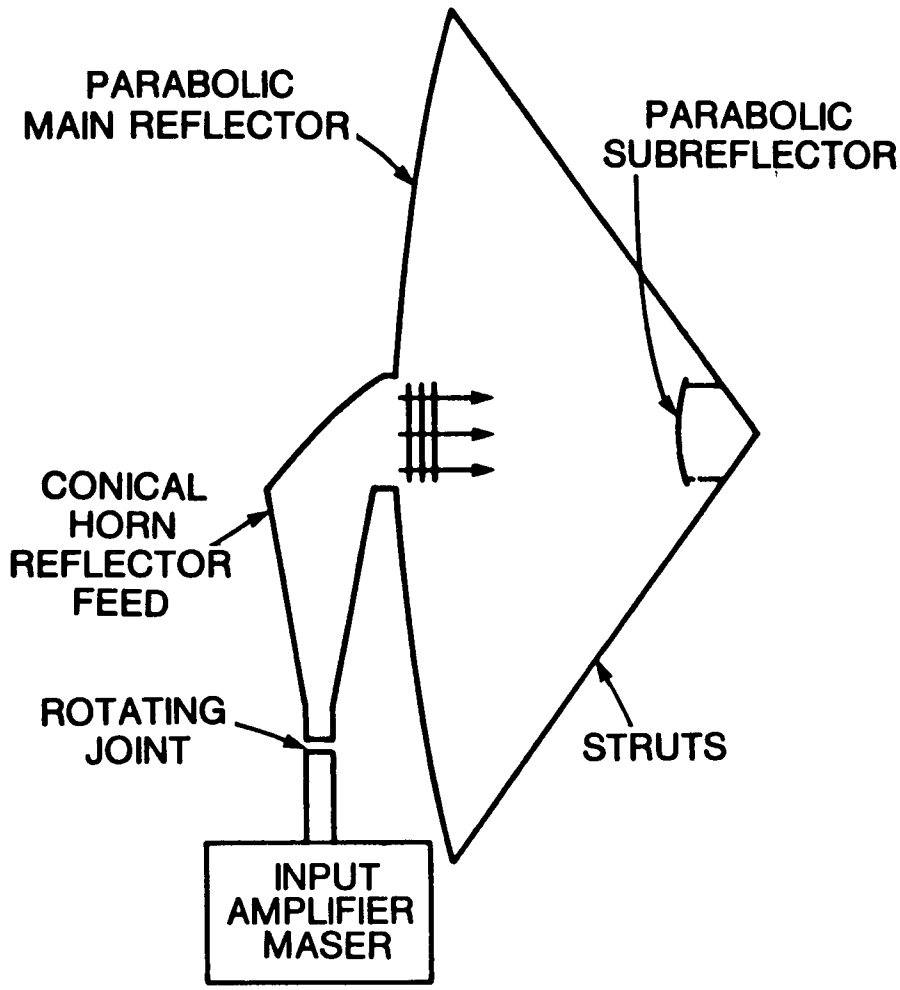

Figure 2-12. Near-Field Cassegrain Antenna Fed by a Horn Reflector [2-55]

system combines high resolution with the performance capabilities of an electronically scanned array over a limited scan range.

To avoid subreflector blockage, offset geometry of a confocal reflector system was proposed by Dudkovsky [2-57]. Shahill et al. [2-58] first investigated the off-axis properties of this system. Fitzgerald [2-59] performed an extensive study on the offset near-field Gregorian system illustrated in Figure 2-13. His analysis was based on a ray tracing procedure from the plane wave source to the sub-reflector and then to the main reflector. Scalar diffraction theory was then used to calculate the secondary pattern. Although Fitzgerald assumed an ideal plane wave source in his computation, the calculated results were in good agreement with measurements and demonstrated that the offset Gregorian system performed exceptionally well for limited scan applications. Figure 2-14 shows the computed scanned patterns in the horizontal plane of a typical near-field Gregorian system. A tradeoff discussion of the antenna parameters, such as reflector sizes, magnification factor, and array position, was also given.

Kreutel and DiFonzo [2-60] have also investigated the characteristics of the offset near-field Cassegrain and Gregorian systems. They established some simple relations between the physical parameters, such as aperture diameters and magnification factor, and the electrical parameters, such as gain, beamwidth, and average sidelobe levels. These expressions have proved to be useful in confocal reflector system design.

Chen and Tsandoulas [2-61] developed a time-delayed space-fed phase array feed for the confocal Gregorian system. In comparison to the conventional subarrayed wideband corporate feed, this wideband space feed offers such advantages as better gain performance, lower amplitude quantization lobes, and grating lobes. Woo and Cramer [2-62] employed a phased array feed as the plane

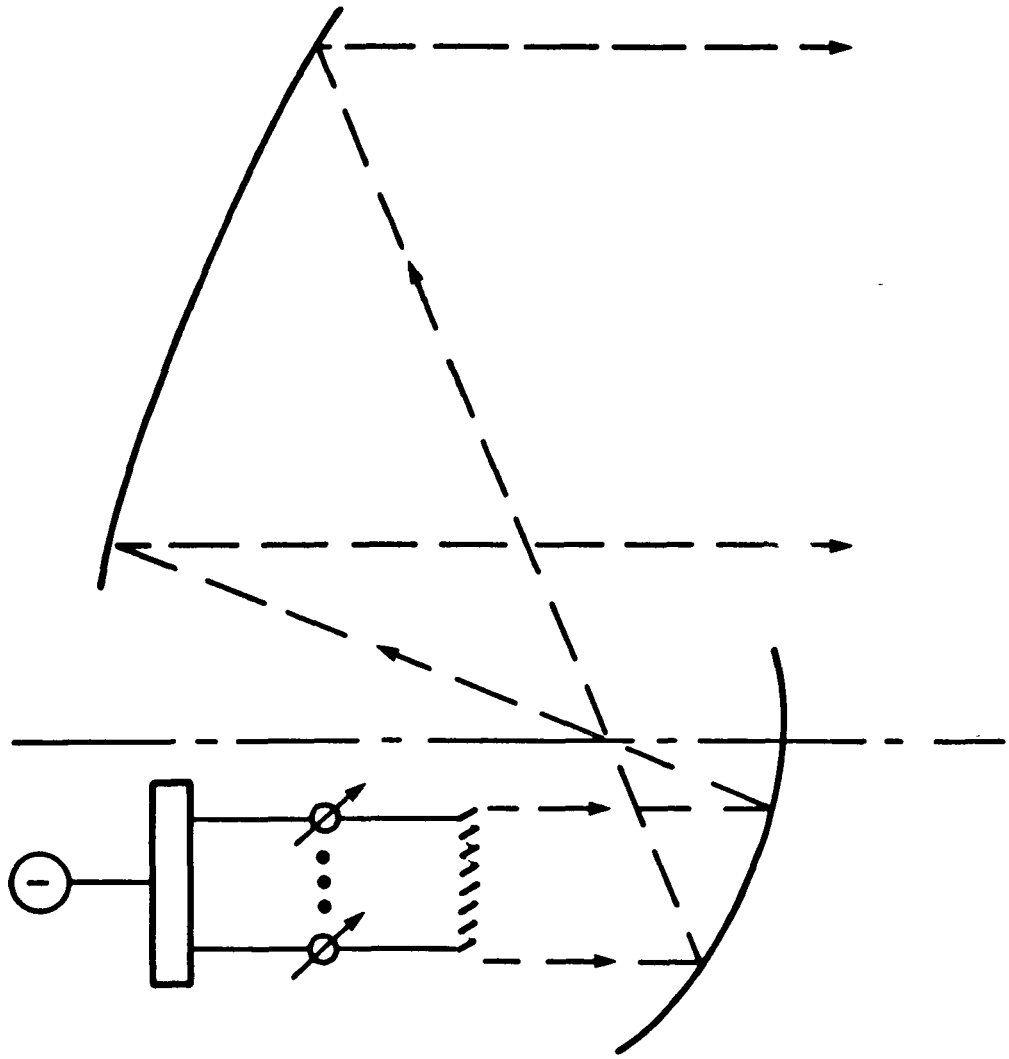

Figure 2-13. Geometry of the Offset Near-Field Gregorian Antenna [2-59]

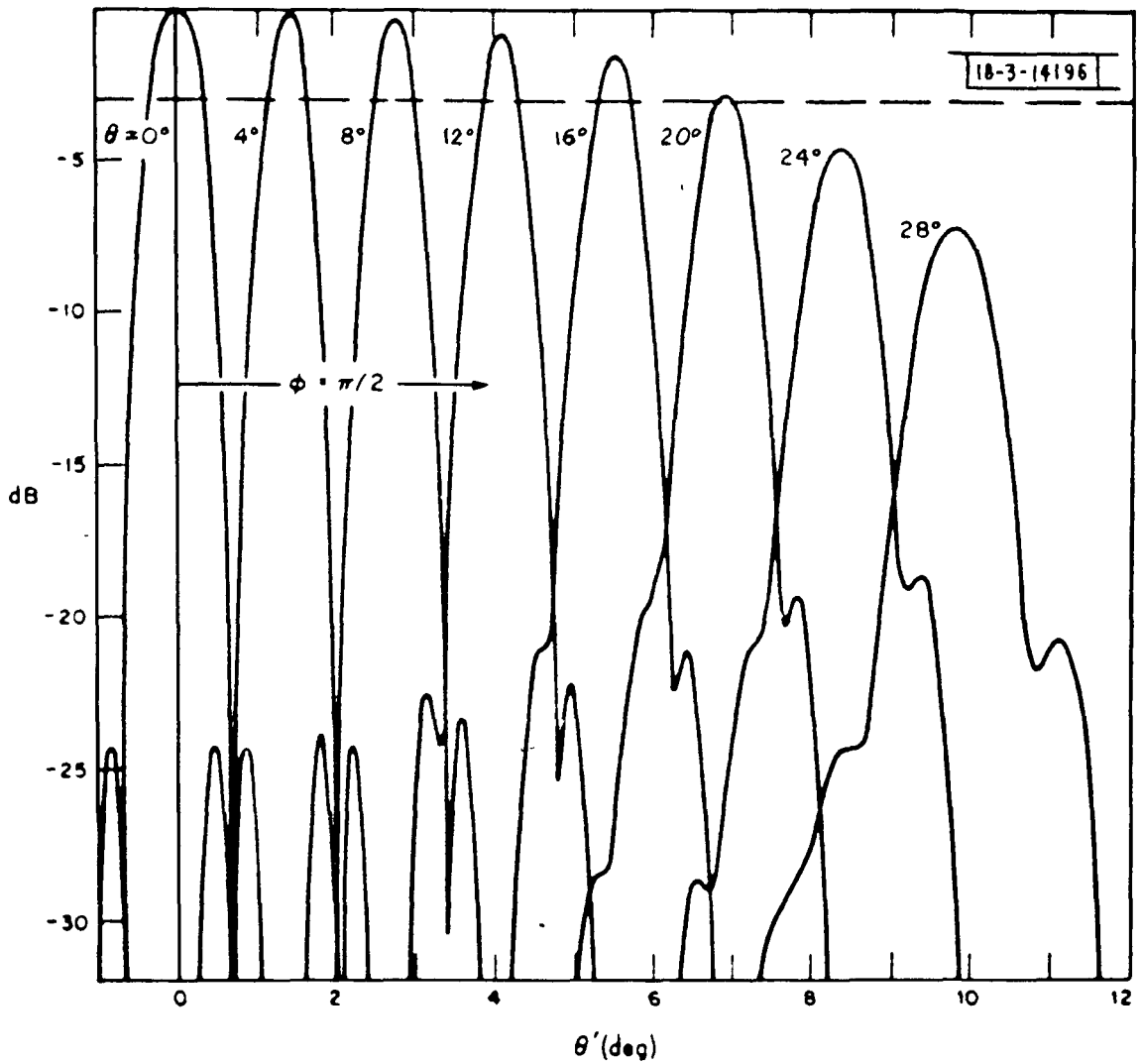

Figure 2-14. Computed Horizontal Scanned Plane Pattern of the Near-Field Gregorian System [2-59]

wave source for a near-field Cassegrain antenna system to obtain limited beam scanning.

Dragone and Gans [2-63] proposed a near-field Gregorian system for satellite communications applications. They introduced the concept of conjugate elements relating the main reflector aperture and the phased array plane. When this condition is satisfied, maximum efficiency of illumination for the main reflector is obtained, and the field on the main reflector aperture is simply the image of the field on the array aperture. By using this concept, the optimal position of the array can be determined and the main reflector deformation can be corrected by adjusting the time delay of the array element corresponding to the conjugate deformed element on the reflector surface. Dragone and Gans also introduced a third hyperbolic reflector between the two paraboloidal surfaces to increase the distance between the feed and the subreflector for polarization or frequency diplexing.

Based on the geometrical optics analysis in Reference 2-63, Dragone and Gans have designed a compact antenna system suitable for generating a scanning beam for satellite communications in the CONUS [2-64]. The antenna has a Gregorian arrangement with a filter placed in the focal plane of the main reflector to reduce the effect of the grating lobes from the feed array. This results in a smooth field distribution mapping between the array aperture and the main aperture.

Recently, Woo [2-65] developed three array-fed reflector antenna systems for beam scanning, power amplification, and multiple beam applications. An offset near-field Gregorian configuration was chosen for the multiple beam antenna design, which generates multiple beams that can be scanned simultaneously. Measured data from the model antenna verify that simultaneous beam scanning is achieved. Also, an analysis of the offset near-field Gregorian system by Hwang and Han [2-66] has shown that the

secondary beam is depolarized as the beam scans from the reflector axis, and the depolarization is proportional to the amount of the offset of the system.

2.6 FUTURE DEVELOPMENTS IN REFLECTOR OPTICS FOR BEAM SCANNING

Among the alternative reflector systems that are designed to cover CONUS, the Schwarzschild antenna and the phased-array fed confocal parabolic system deserve further investigation. The Schwarzschild antenna, which does not have primary coma for small to moderate angle scanning, offers better scan performance than other focal region feed systems with a single focal point. Unfortunately, the Schwarzschild system has not been widely used because the profiles of the reflectors are transcendental curves. A simple mathematical or numerical model that describes the profile curves is required to make this antenna easy to design and analyze. Rappaport [2-54] has employed a fourth-order least-squares polynomial to approximate the profiles; however, sizable errors for the subreflector were still present. Another worthwhile area of exploration is to find the optimum feed locus surface for multiple feed systems.

The phased array fed confocal parabolic antenna system also has great potential for spot beam and multiple beam applications. It possesses the scan capability of a large phased array and is relatively light in weight. Unlike other parabolic systems, it does not have the coma effect caused by the phase aberration when the beam is scanning. However, beam scan loss and distortion still exist in the secondary patterns because of other aberration effects. Two approaches can be applied to correct the phase error. One is to shape the subreflector surface so that equal path lengths

can be maintained from a source to a plane wavefront perpendicular to the scan direction. The other approach is to synthesize the array aperture distribution corresponding to a nonaxial incident plane wave. Tilting both the phased array and the subreflector array may improve the cross-pol performance of the antenna, as suggested in Reference 2-67 for a conventional Cassegrain system.

3. PHASED ARRAY RELATED TOPICS

3.1 PHASED-ARRAY-FED REFLECTOR SYSTEMS

An imaging reflector system with a small phased array as the feed array has been designed and studied at Bell Laboratories [3-1]. Figure 3-1 shows some of the details of this configuration. The 12/14-GHz system covers the continental United States (3° x 7°) and uses a Gregorian arrangement of two paraboloids with a magnification factor of seven. This results in a scanning range of 21° x 49° at the array level. To reduce the grating lobes in this design, a filter was placed in the focal plane of the main reflector. A simpler method of controlling the modes in the radiating apertures of the feed horns has been proposed by Amitay and Gans [3-2],[3-3]. Since the dominant contributor to the blind spots is the resonance of the TM_{12} mode, the horn taper is chosen to effectively short circuit this mode at the array aperture. An experimental model was built to verify the theoretical results.

A frequency diplexer has been proposed for the Bell Labs system [3-4] to allow the same reflectors to be used at both transmit and receive frequencies. The periodic structure of the diplexer surface is shown in Figure 3-2. The diplexer is designed to pass 14-14.5 GHz and reflect 11.7-12.2 GHz with incident scan angles of 40° → 60° into the E-plane, and -20° → 20° into the H-plane. Figure 3-3 shows the transmission and return losses across the two frequency bands. The experimental diplexer model showed an insertion loss of 2 dB, most of which was caused by ohmic dissipation.

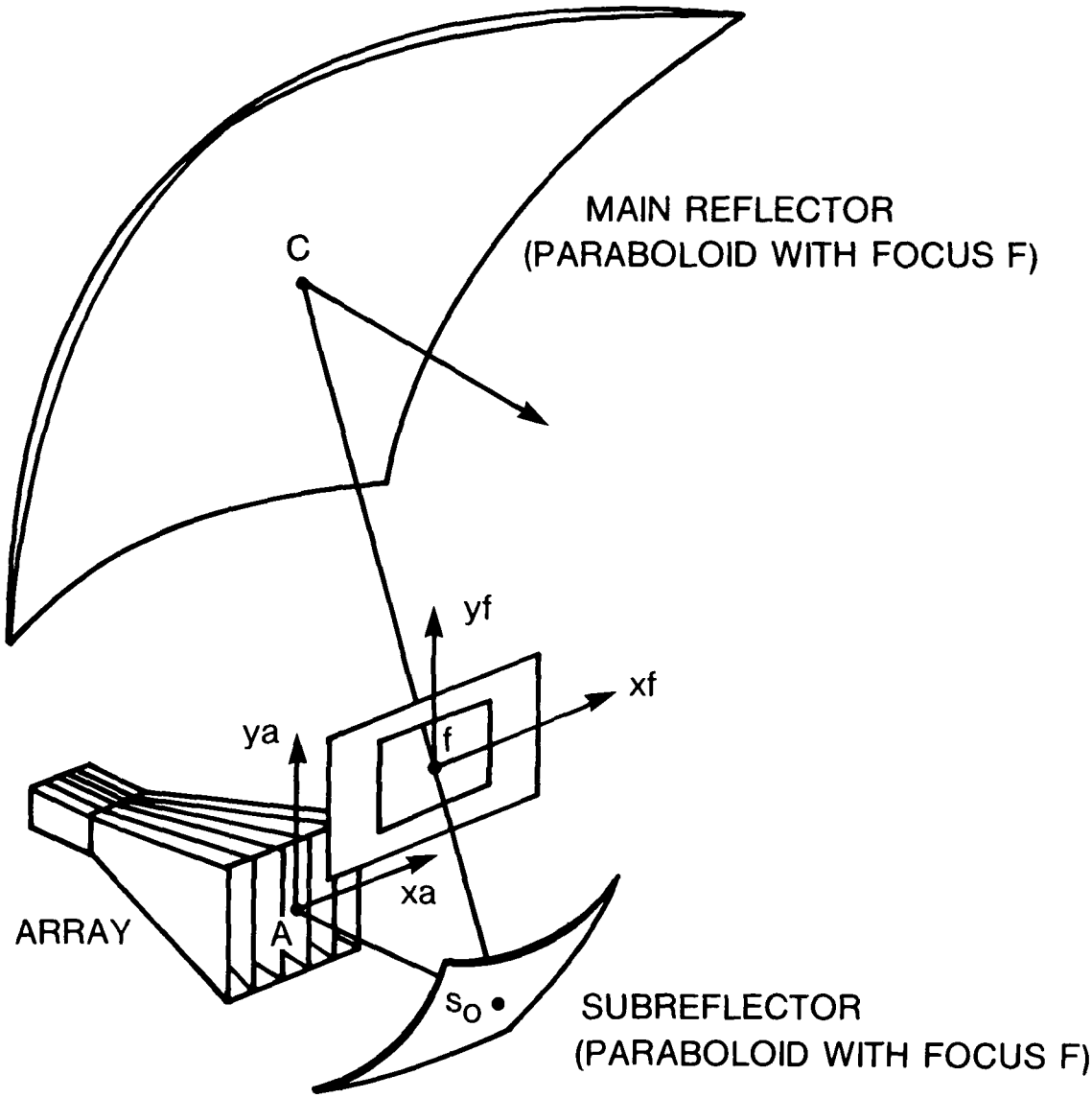

Figure 3-1. Gregorian Arrangement Combined With an Array [3-1]

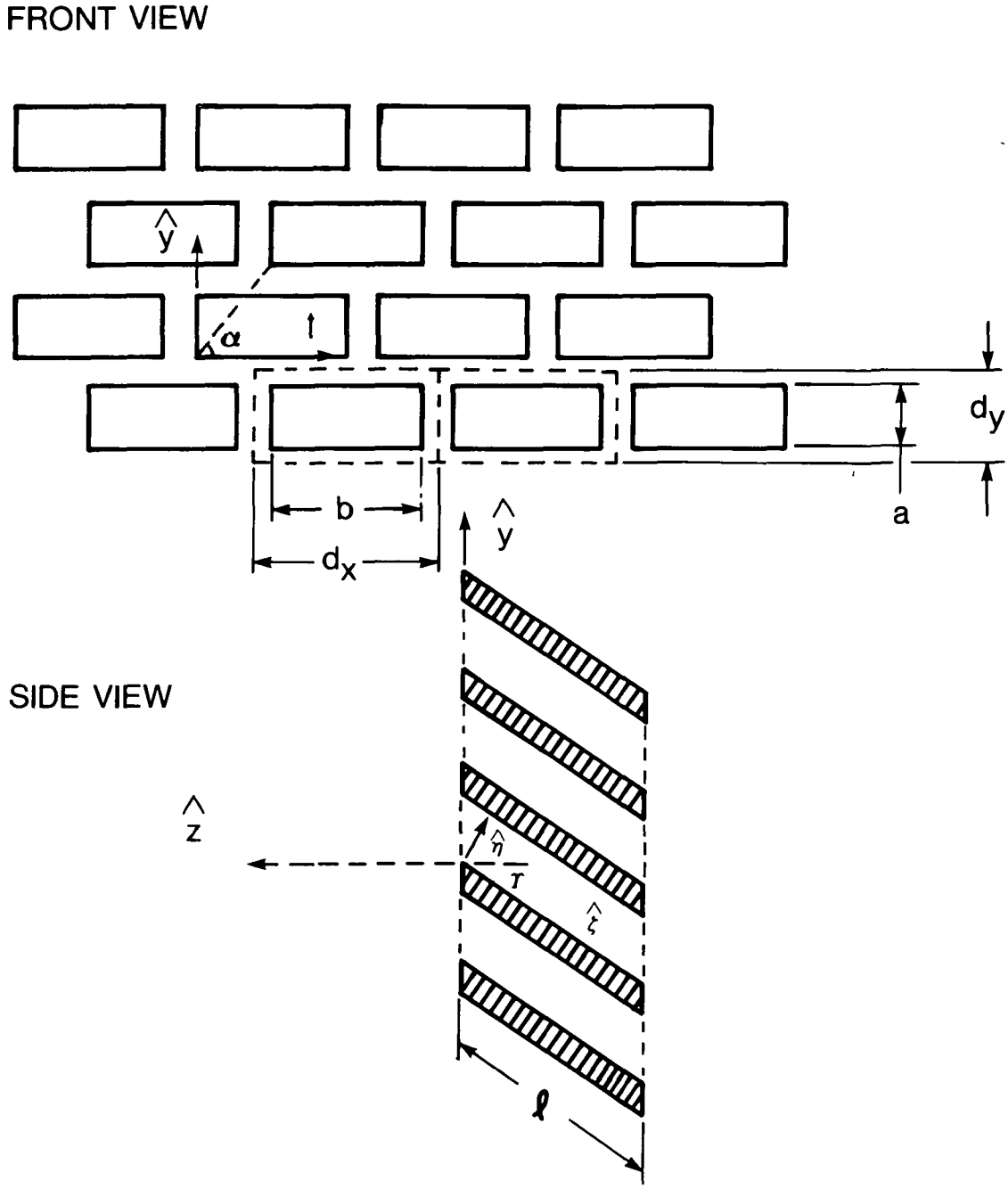

Figure 3-2. Waveguide Array Diplexer [3-4]

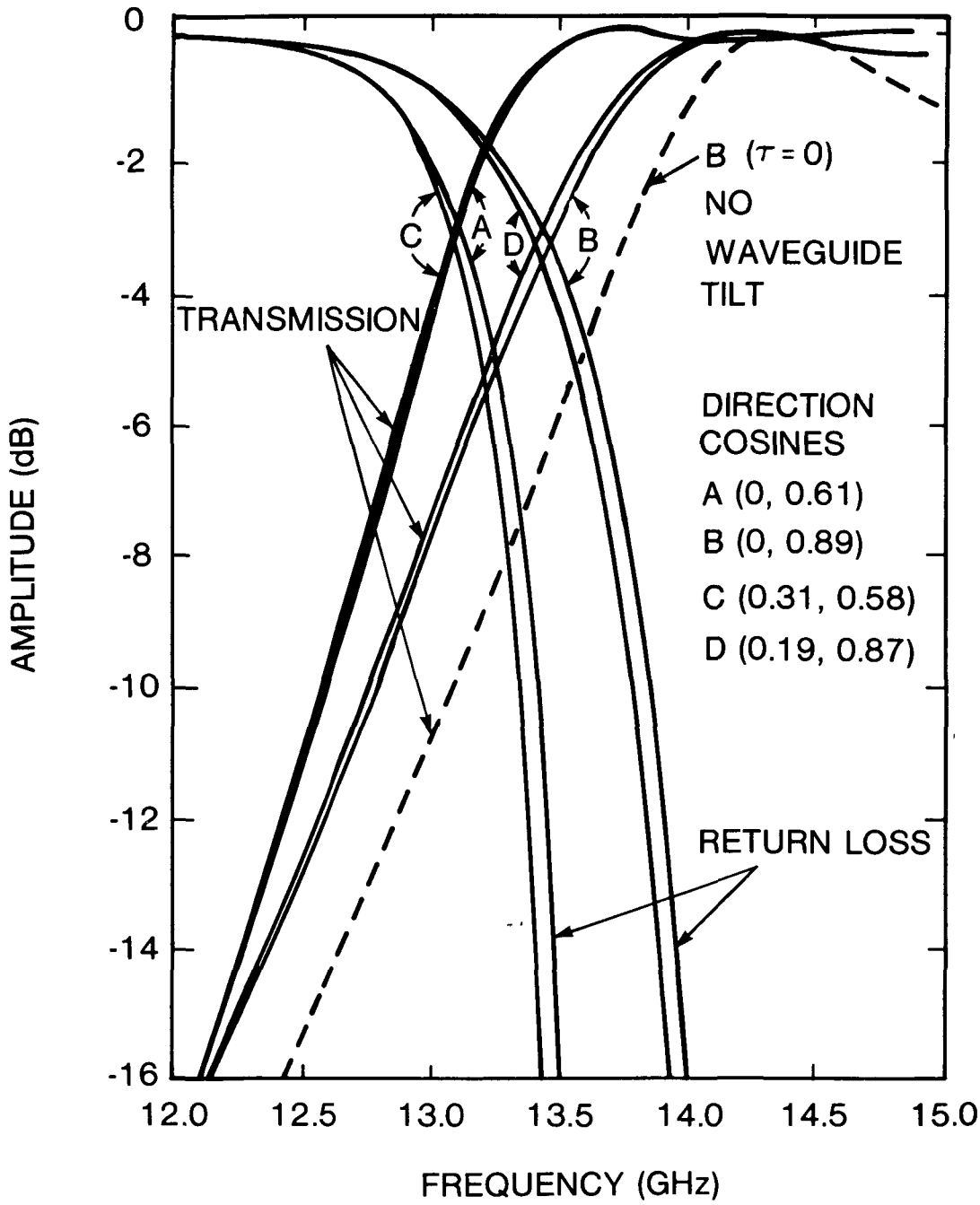

Figure 3-3. Optimal Diplexer Transmissivity [3-4]

In a separate effort, a phased-array-fed system has been developed at the Jet Propulsion Laboratory [3-5]. The X-band symmetric Cassegrain system is designed for deep space and near-earth communications, and the radiating elements are relatively small ($0.702\lambda \times 0.702\lambda$), with interelement spacing of 0.927λ. Failure of one or several units in the array resulted in a 1- to 2-dB reduction in antenna gain.

In an earlier attempt to use dual-reflector systems for phased arrays, Chen and Tsandoulas [3-6] proposed a Gregorian configuration to spatially feed a phased array, as shown in Figure 3-4. This was meant to be an alternative to corporate feed systems. Because of the large size of the phased array, this configuration is not suitable for satellite applications.

3.2 DIRECT RADIATING PHASED ARRAYS

Numerous papers have been published on the general subject of direct radiating phased arrays. Few, however, have proposed using phased arrays for satellite communications, because of weight and feed network complexity considerations. For example, in Reudink and Yeh [3-7], the pattern of a 104-element array covers the entire CONUS region. The elements are rectangular waveguides $19.1\lambda \times 8.2\lambda$. The dimensions were chosen so that the grating lobes would fall outside the coverage region at all scanning angles. Details of the feed network or the effects of mutual couplings were not given.

The fundamental concepts of phased arrays have been described in early papers and books [3-8]-[3-12]. A review paper by Stark [3-13] summarized the early developments of phased arrays, mainly for large arrays suitable for phased-array radar. A recent

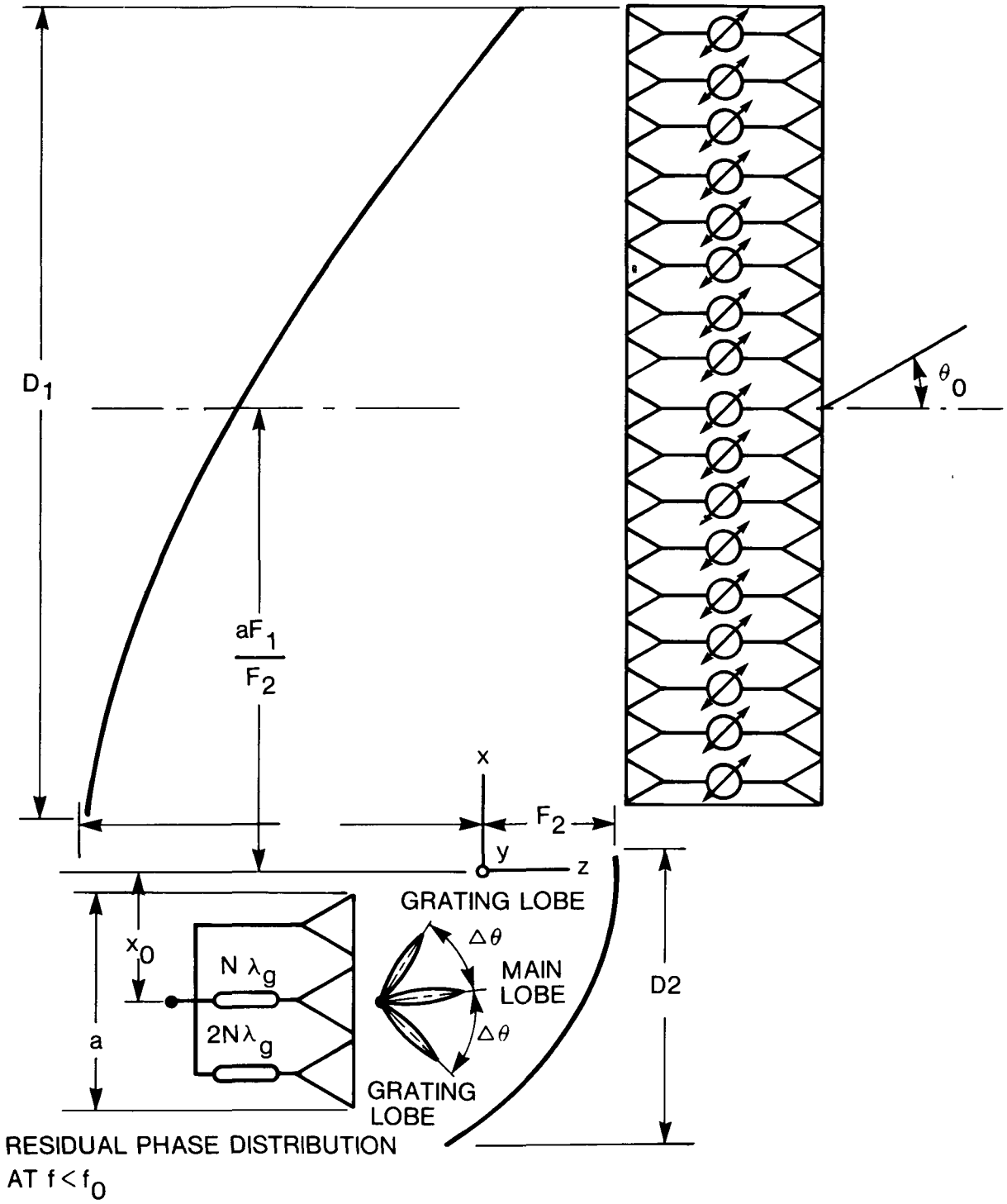

Figure 3-4. Geometry of a Time-Delayed Space-Fed Phased Array [3-6]

paper by Mailloux [3-14] extended the review to include such special-purpose array techniques as conformal and printed-circuit arrays, wide-angle scanning arrays, techniques for limited sector coverage, and antennas with dramatically increased pattern control features such as low-sidelobe, adaptively controlled patterns. This paper also presents a tutorial review of theoretical developments and contains a comprehensive list of references on phased arrays spanning more than 25 years.

3.3 DESIGN ASPECTS OF PHASED ARRAYS

One limiting factor in the design of phased arrays is the emergence of grating lobes in the coverage region. Although choosing the element spacing to be less than certain values can guarantee the absence of grating lobes within the coverage region, it is sometimes necessary to exceed these values to achieve smoother scanning. Examples of methods proposed to control the grating lobes are given in References 3-15 through 3-17.

Mailloux et al. [3-15],[3-16] achieved grating lobe reduction by controlling the amplitude and phase of higher order odd modes to produce an element pattern null at the nearest grating lobe in the plane of scan. Perturbation of the element positions by random Gaussian distribution around the nominal periodic locations has been used to reduce the grating lobe levels [3-17].

Another significant factor in the design of phased arrays is the occurrence of blind spots in the pattern. It has been shown that a sharp dip, or a null for infinite arrays, occurs in the scanning pattern of a phased array at an angle closer to broadside than the angle at which an endfire grating lobe exists. This is known as the blindness phenomenon. At this angle, a complete mismatch occurs as a result of the accumulation of mutual coupling

effects. Bates [3-18] showed, by measurements on an array covered by a plexiglass sheet, that the dips occur when the refractive index of the array region is greater than that of the free space region. He introduced the definition of the "internal grating lobes," which result from the existing surface waves. In discussing surface wave coupling, Allen [3-19] restricted the element spacings to the region of large reflection coefficients outside the desired scan volume.

Farrell and Kuhn [3-20] used modal theory to analyze periodic rectangular arrays and proved the existence of pattern nulls at angles close to those obtained from experimental results. Their analysis was generalized to rectangular grid arrays in a subsequent paper [3-21]. Figure 3-5 shows the verification of null existence using the modal theory, as compared to experimental results.

Hannan [3-22] announced the discovery of an array surface wave in a simulator, and Frazita [3-23] demonstrated the existence of blindness by using the grating lobe series [3-24]. The direct effects of mutual coupling accumulation were discussed by Lechtreck [3-25] for the case where a relationship is given between the critical scan angle at which the dip occurs and the phase of the mutual coupling coefficients.

In an equivalent network analysis based on the modal theory and the unit-cell technique, Knittel, Hessel, and Oliner [3-26] considered an infinite slot array covered with a dielectric slab and proved the occurrence of the null at an angle less than the endfire grating lobe angle for the nonzero slab thickness cases. They also introduced the concept of the leaky wave as a true mode of the actual array. The leaky wave radiates at an angle close to that of the element pattern null. Knittel also showed [3-27] that the blindness effect is directly related to the cut-off conditions of the next higher waveguide mode and

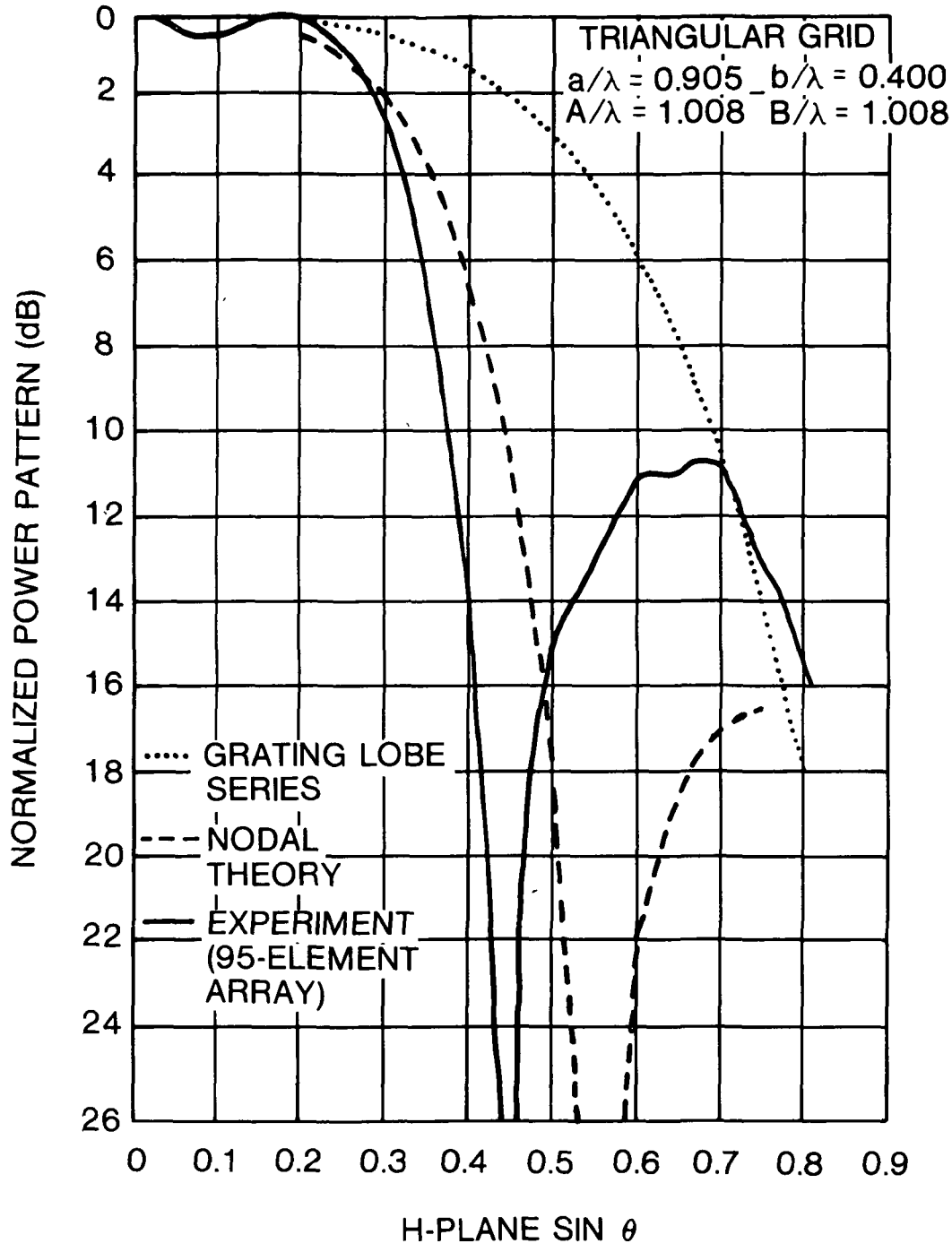

Figure 3-5. Normalized Power Pattern--Comparison of Theory and Experiment for a Triangular Grid, H-Plane Scan [3-21]

unit-cell mode. Figure 3-6 shows the association of the blindness condition and unity reflection coefficient, $|\Gamma|$, with the cutoff mode for an array covered with dielectric slab.

Lo and Agarwal [3-28] proved that the use of random arrays results in a great reduction, if not a complete removal, of the blindness. Similar results can also be obtained by slightly perturbing the element positions about their nominal periodic locations [3-29]. Figure 3-7 shows the filling in of the pattern nulls with different levels of random perturbations.

Hannan and Litt [3-30] have suggested using a capacitive ground plane to speed up the wave radiated along the ground plane. This eliminates surface wave effects and hence the scanning pattern nulls. A practical method for implementing this concept was presented by Hessel and Knittel [3-31]. Figure 3-8 shows the reflection coefficient for different levels of capacitive loading where complete reflection is eliminated before endfire grating lobe directions. Lee and Jones [3-32] showed that the introduction of aperture irises can remove radiation nulls in the element pattern.

Another limiting factor in phased array design is the scanning granularity dependence on the phase shifter steps in the beam forming network. The effect of this limitation on array performance has been discussed in the literature [3-33],[3-34].

3.4 DESIGN ASPECTS OF ARRAY ELEMENTS

Early procedures to design phased array elements were divided mainly into small-array procedures [3-35]-[3-37] and simulator procedures [3-38],[3-39], both of which relied on measurements to design the element and its matching network. Advances in the ability to accurately compute the active reflection coefficient of waveguide elements have made possible reliable

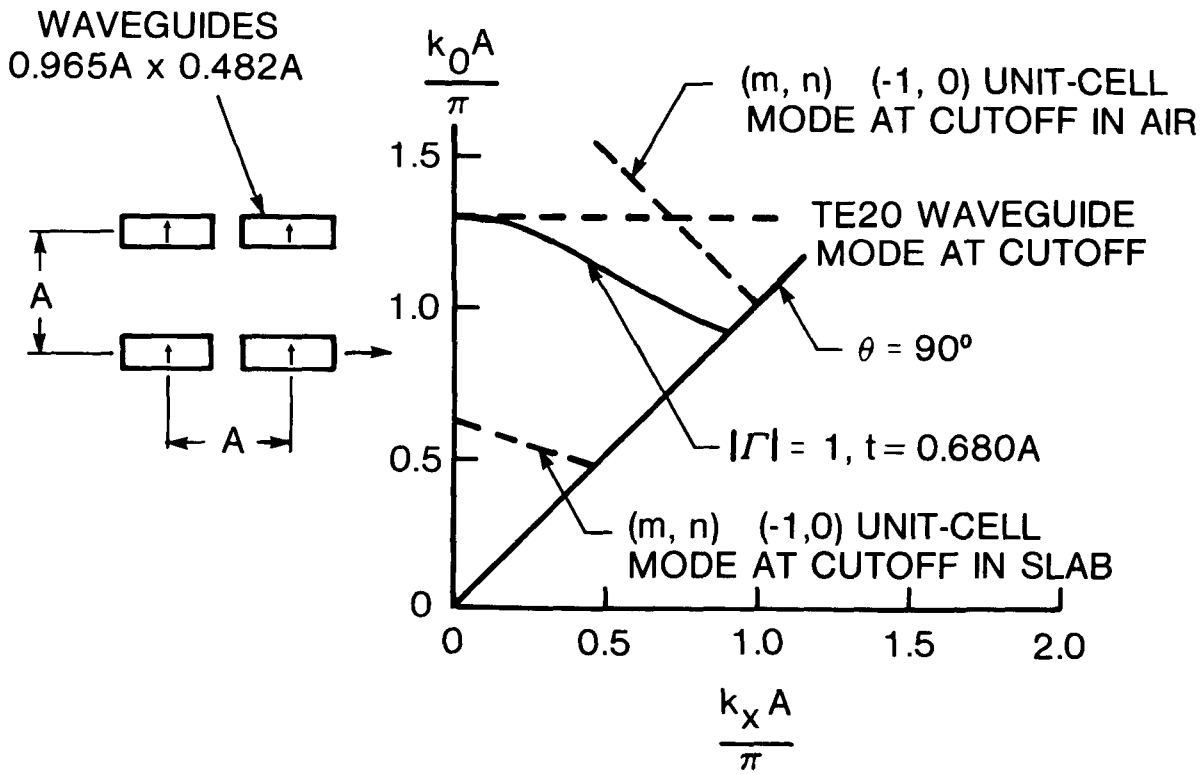

Figure 3-6. Unity Reflection Coefficient Curve for a Rectangular Lattice Array Covered by Dielectric Slab: H-Plane Scan [3-27]

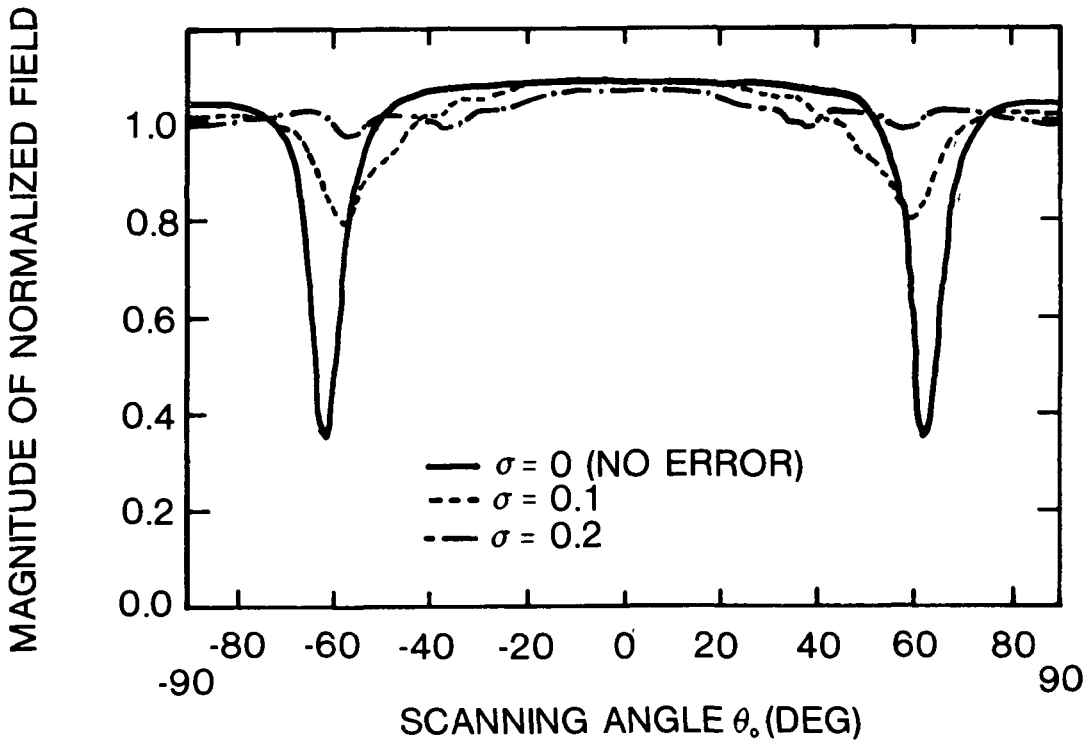

Figure 3-7. Typical Array Patterns for Arrays Subject to Positioning Errors (Number of elements = 51, nominal element spacings = 0.5λ) [3-29]

GLE GRATING LOBE AT ENDFIRE

MGE MAIN LOBE AND GRATING LOBE AT EQUAL ANGLES FROM BROADSIDE

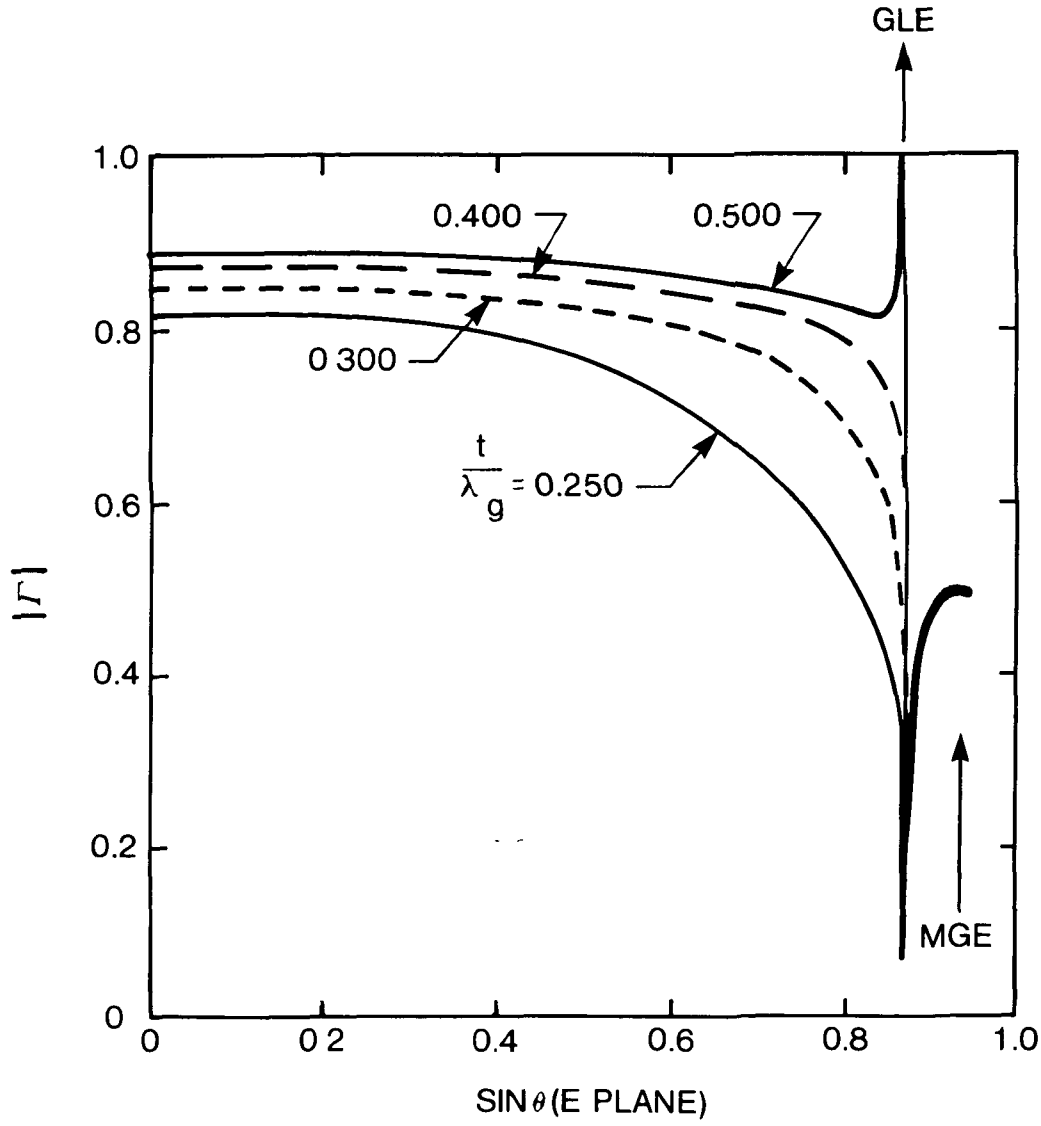

Figure 3-8. Reflection Coefficient Magnitude for Capacitive Loading [3-31]

and more efficient procedures for element design. Diamond and Knittel discussed such a procedure [3-40]. First, the element lattice and shape are chosen. Then, the reflection coefficients are calculated and used to optimize the element aperture dimensions within the imposed constraints. The element matching network is determined by computations, and the final design is confirmed by measurements in a single H-plane simulator.

The choice of element shape is generally determined by the type of application. Several examples have appeared in the literature for dual polarization arrays (Figure 3-9), low cross-polar waveguide horns (Figure 3-10), and low sidelobe horns (Figure 3-11). In cases where large-aperture elements are required, a design procedure for rectangular horns was introduced by Amitay and Gans [3-3]. Other types of elements that have attracted attention in recent years are stripline and microstrip elements. Hall and James have surveyed design techniques for such arrays [3-44]. Microstrip elements generally have a narrow bandwidth, but offer the advantages of low cost and light weight.

3.5 MUTUAL COUPLING CONSIDERATIONS

Mutual coupling effects have been viewed as essential in the analysis and design of phased arrays. As pointed out earlier, the accumulation of mutual couplings leads to blind spots in the array pattern. All the methods reported in the literature for the analysis of phased arrays account explicitly or implicitly for mutual couplings. The element-by-element method [3-45] of phased array analysis employs direct knowledge of interelement mutual effects. This technique was used to analyze large arrays of dipoles [3-46]-[3-48], current sheets [3-49], coaxial horn antennas [3-25], and waveguides [3-50], [3-51]. Another approach

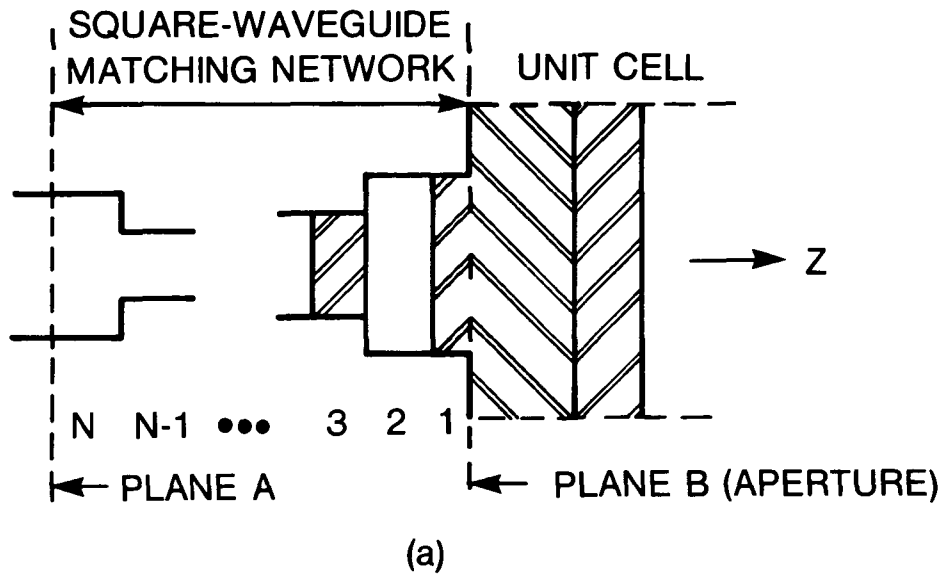

(a) Element Geometry

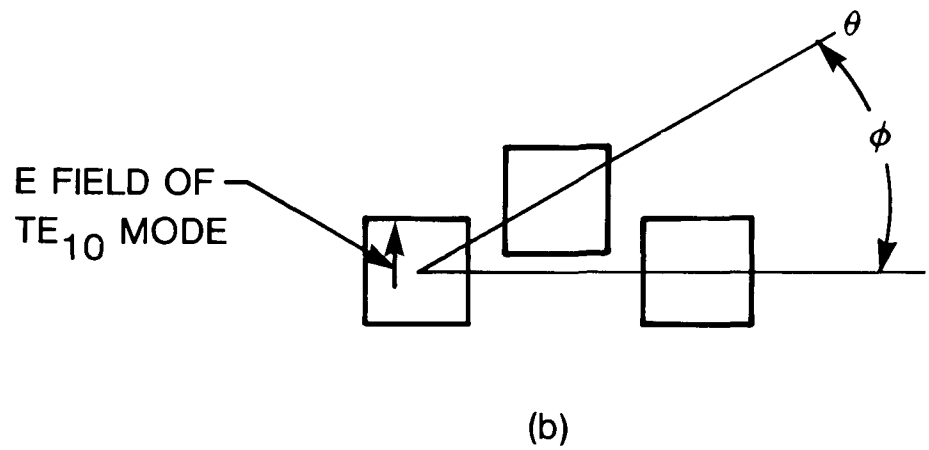

(b) Element Lattice (Rectangular or triangular)

Figure 3-9. Dual-Polarized Square Waveguide Radiating Element Geometry and Lattice [3-41].

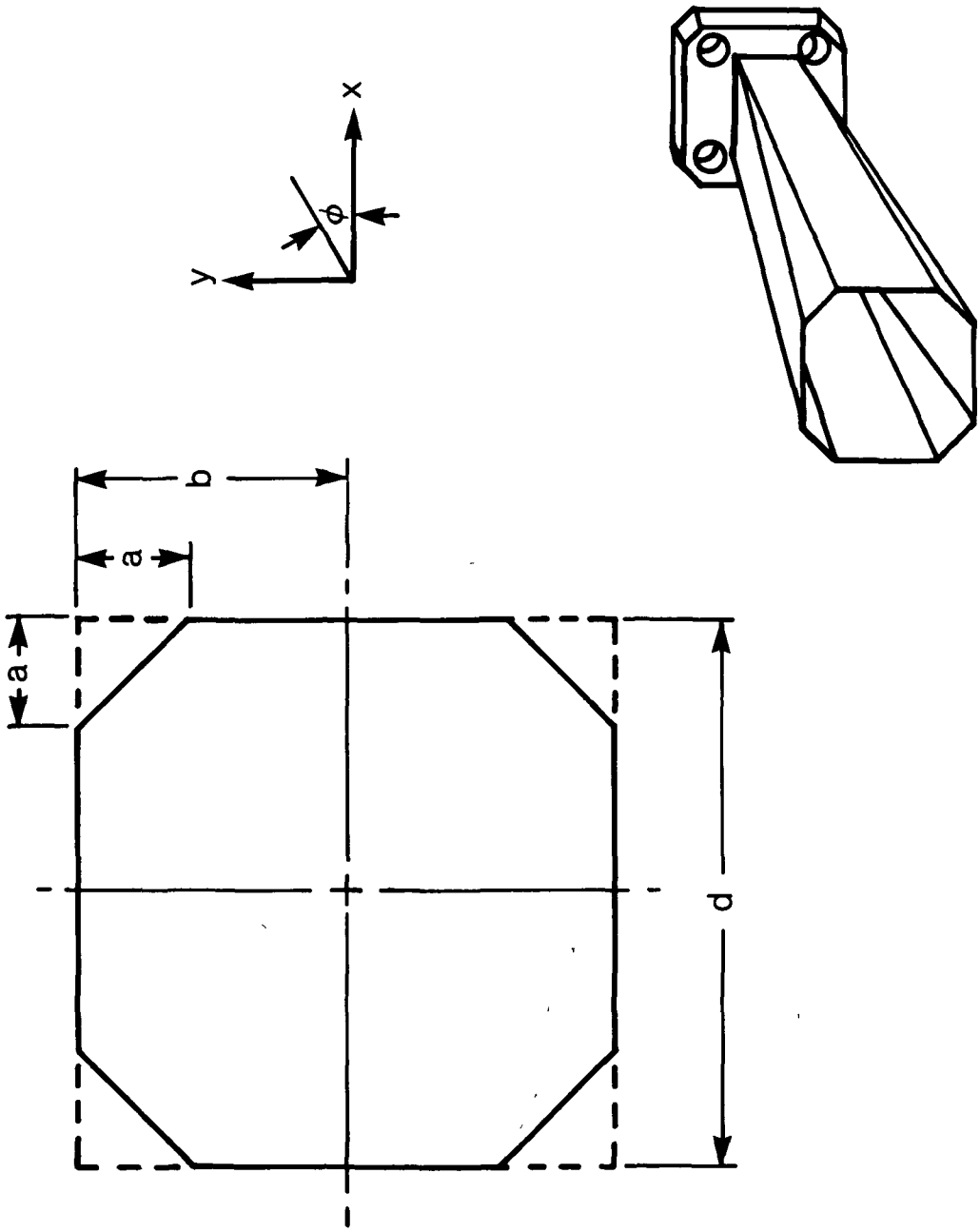

Figure 3-10. 8-Sided Primary Feed Horn [3-42]

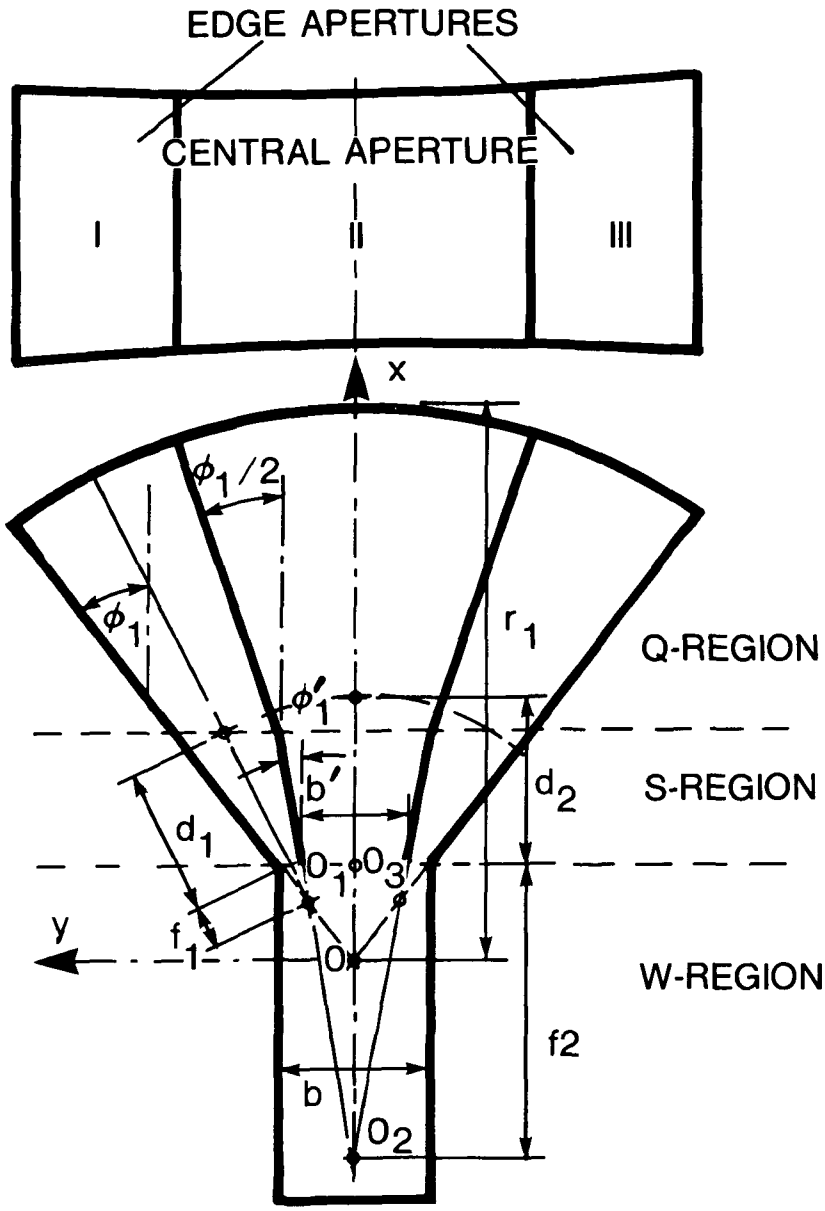

Figure 3-11. Theoretical Model of a Spherical Horn With a Sectoral Waveguide Power Divider [3-43]

to analyzing phased arrays is the modal approach, which is based on solving the boundary value problem at the array plane [3-20],[3-21],[3-52]. The effects of mutual coupling are implicitly accounted for in this formulation. Diamond [3-53] has presented another method based on matching the complex power flow across the aperture of a waveguide array. Stark [3-54] employed complex power matching to analyze a planar array of dipoles.

Another method to solve two-dimensional waveguide array problems applies a generalized scattering matrix [3-55],[3-56], in which a set of waveguide walls is extended by a certain amount to create a fictitious parallel-plate region. The rows of rectangular waveguides radiate into these parallel plate regions, and then the regions radiate into space, resulting in a cascade of two discontinuities. The central idea of the unit-cell approach is to have every array element radiate into a corresponding fictitious waveguide [3-57],[3-45],[3-26]. A unit cell is centered around each element in the periodic array and defines the cross-section of the corresponding unit-cell waveguide, whose axis is perpendicular to the plane of the array. Thus, all mutual coupling effects are automatically accounted for.

For the special case of arrays of rectangular waveguides with thin walls, Wu and Galindo [3-58] used the Wiener-Hopf or residue calculus technique to solve the boundary value problem. Lee and Mittra [3-59] relaxed the restriction of the thin waveguide wall assumption and presented a modified residue calculus method. A more general way of formulating the phased array problem is the integral equation technique, in which the tangential electric field is expressed in terms of the tangential magnetic field, or vice versa, before the continuity conditions are imposed. The resulting integral equation is then solved by a Galerkin method. This approach was used extensively by Amitay, Galindo, and Wu [3-12].

The moment method has also been used to solve for the mutual coupling effects in phased arrays. Harrington and Mautz [3-60] presented a general formulation for aperture problems. Recently Luzwick and Harrington [3-61] extended the method to evaluate the mutual coupling coefficients of finite planar arrays of rectangular waveguides. Mailloux [3-62] used the moment method to evaluate couplings between waveguides propagating two orthogonal modes, and Steyskal [3-63] applied this method to arrays of open-ended circular waveguides.

Another method, developed at COMSAT Laboratories to evaluate mutual coupling between elements in a planar array [3-64], is based on the correlation matrix technique [3-65],[3-66]. The relationship of the cross-correlation function between aperture fields to the mutual power density is used to calculate the mutual admittance matrix, which leads to the scattering matrix of the elements in the array. Figure 3-12 shows the results of calculating the mutual admittance and mutual coupling coefficients between two collinear rectangular apertures. A comparison with previous results published by Galejs [3-67] is also given.

3.6 SPACE-FED (LENS) PHASED ARRAYS

The microwave lens has been postulated as a way of achieving a scanning beam antenna by Rotman and Turner [3-68] in what is now known as the Rotman lens. This two-dimensional trifocal lens has a flat secondary surface with zero phase error in three directions in the lens plane. Figure 3-13 is a schematic diagram of a parallel plate lens of this type, in which the coaxial microwave lens elements are connected directly to a straight line of radiators to form a line source. The phase errors at the nonfocal points can be reduced by moving the feed position radially,

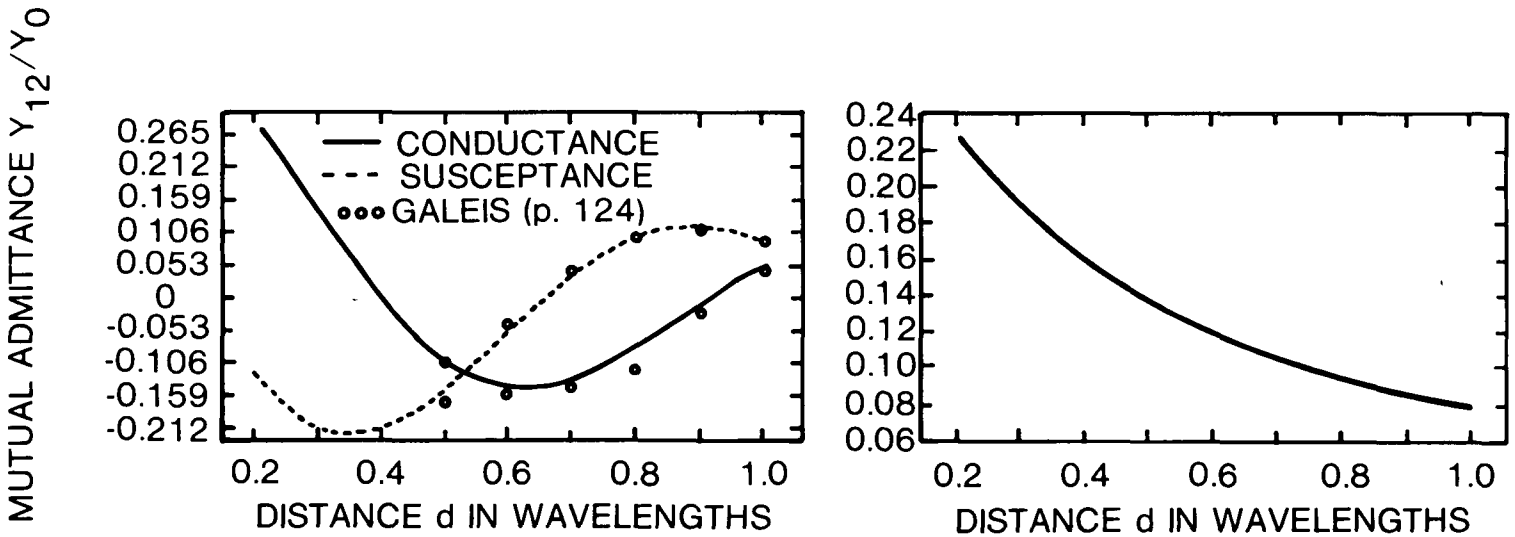

Figure 3-12. Mutual Admittance and Mutual Coupling Between Collinear Apertures of a = 0.6λ, b = 0.2λ [3-64]

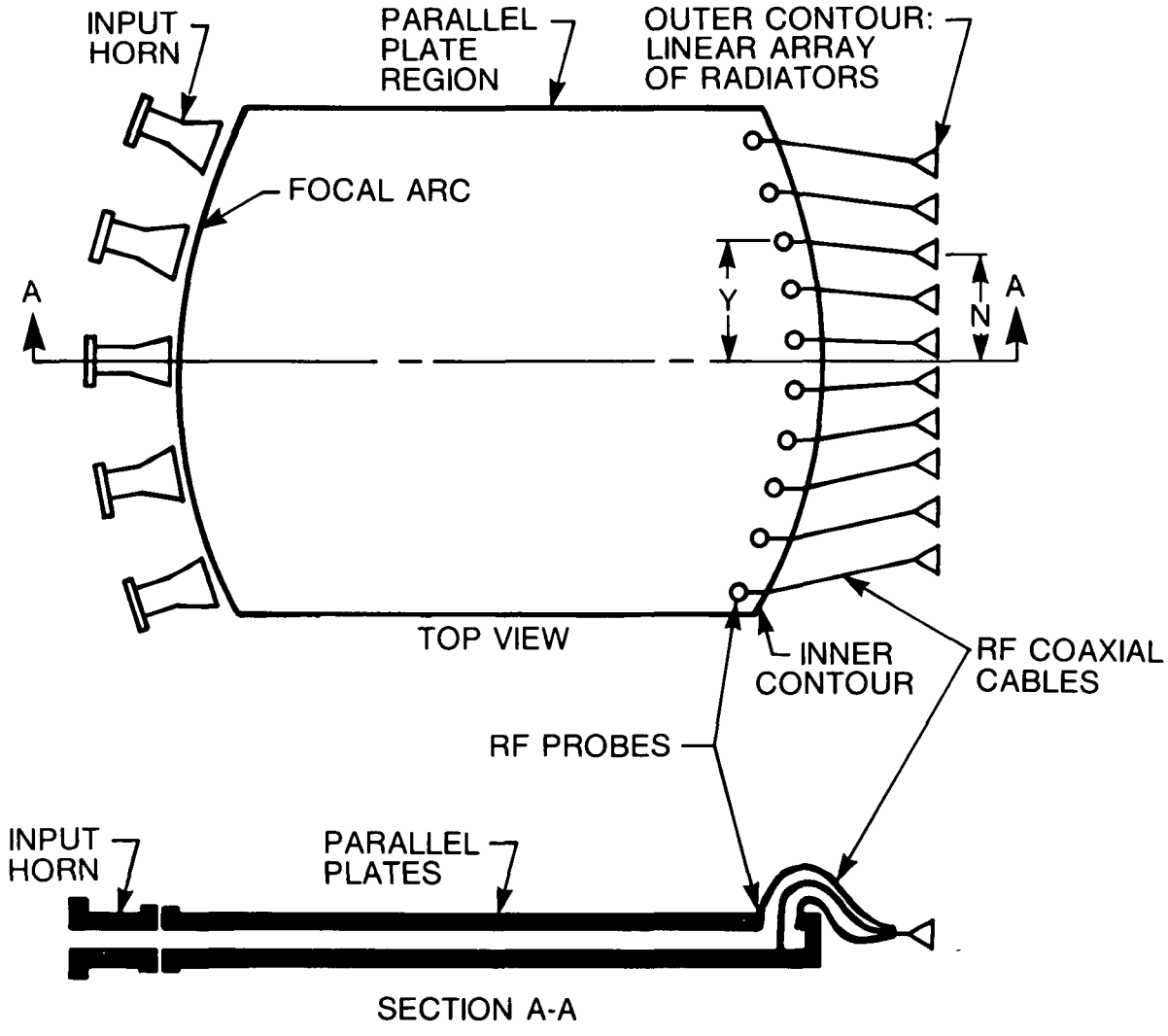

Figure 3-13. Parallel-Plate Microwave Lens [3-68]

as described earlier by Ruze [3-69]. A more general three-dimensional analysis of such a lens has been reported recently by Rao [3-70],[3-71], who included path length error assessments of bifocal, trifocal, and quadrufocal lenses. The analysis included scanning in two orthogonal planes. Figures 3-14 and 3-15 show the maximum path length error for single focus, bifocal, trifocal, and quadrufocal lenses when the main beam is scanned in two planes.

The use of a bifocal lens for variable coverage satellite applications was proposed by Dion and Ricardi [3-72]. The geometry of this lens is shown in Figure 3-16. The feed cluster is composed of circular apertures, while the bifocal lens is composed of square waveguides. The secondary surface is stepped to reduce weight and volume; however, this introduces shadowing and blockage problems. The pattern of the five central individual beams is shown in Figure 3-17, and an example of a composite coverage is given in Figure 3-18 as a contour plot of the radiation pattern superimposed on an orthographic projection of the western hemisphere. An earlier discussion of the shadowing problems in lenses was given by Peeler and Gabriel [3-73]. Another use of lenses for multiple beam antenna systems was proposed by Luh et al. [3-74], who used TEM elements for dual band application.

Considerable effort has also been expended in the study of other types of microwave lenses. The equal group delay waveguide lens [3-75] offers a wideband application, which is achieved by using half-wave-plate phase shifters in each waveguide element, oriented to produce a planar phase front. Figure 3-19 shows the geometry of this lens. Another lens type known as the R-2R [3-76] produces a perfect focal circle in a two-dimensional lens. The symmetrically configured bootlace lens (Figure 3-20) was introduced by Shelton [3-77], with the added restriction of a symmetric feed-curve/lens-curve configuration. The Rotman lens has also been proposed in microstrip form [3-78],[3-79].

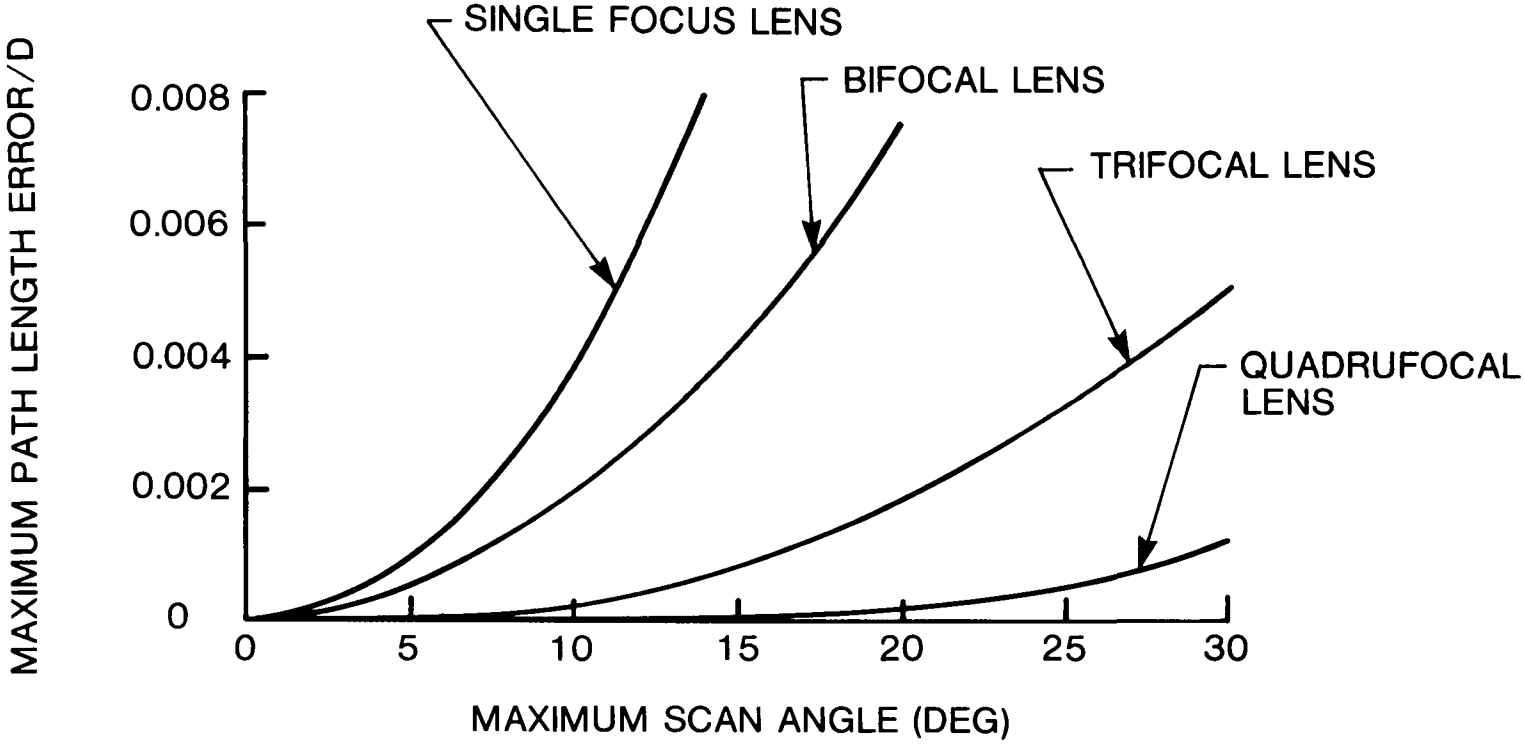

Figure 3-14. Maximum Scan Angle vs Maximum Path Length Error in Principal Plane [3-70]

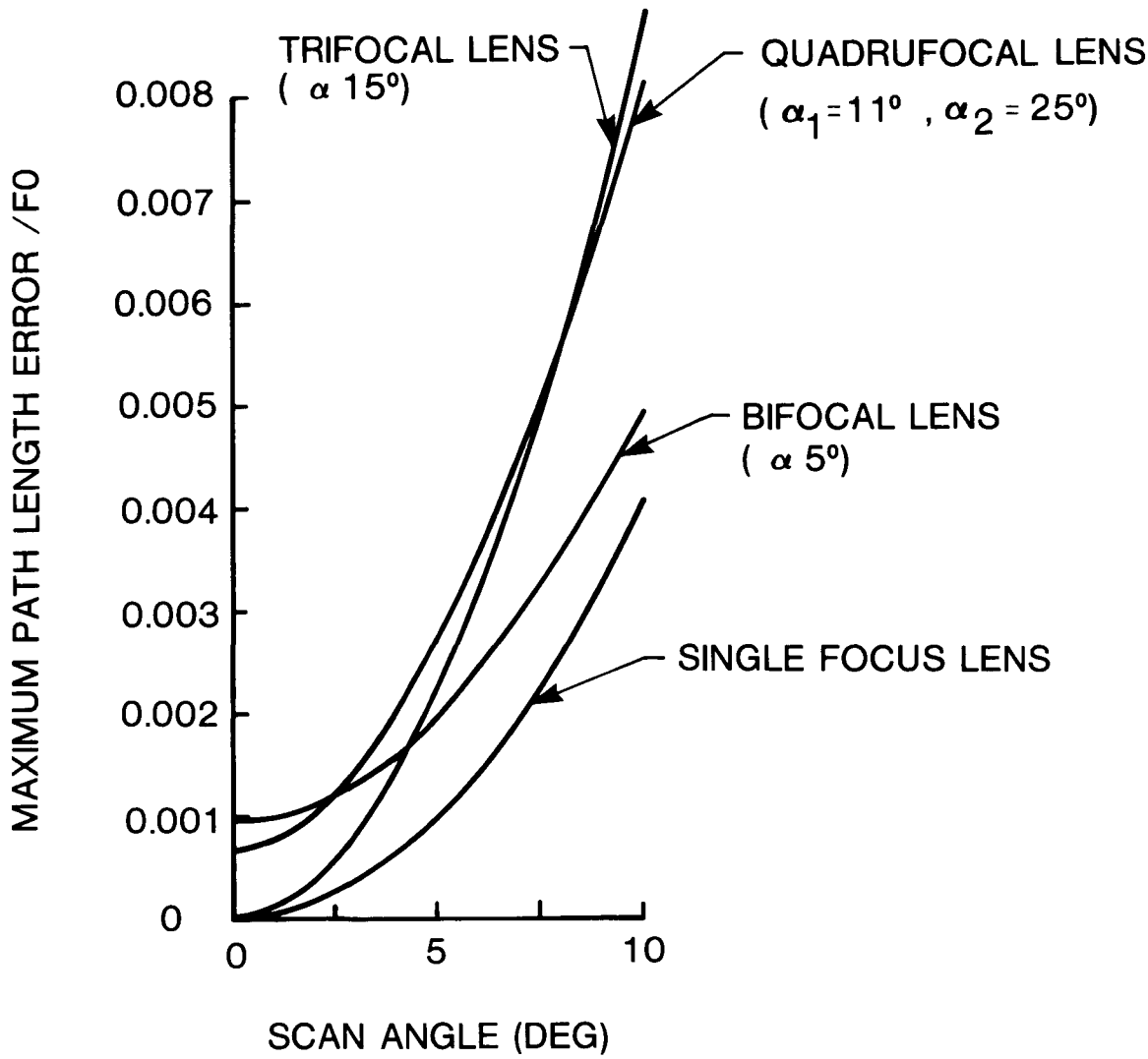

Figure 3-15. Maximum Path Length Error vs Scan Angle in Orthogonal Plane [3-70]

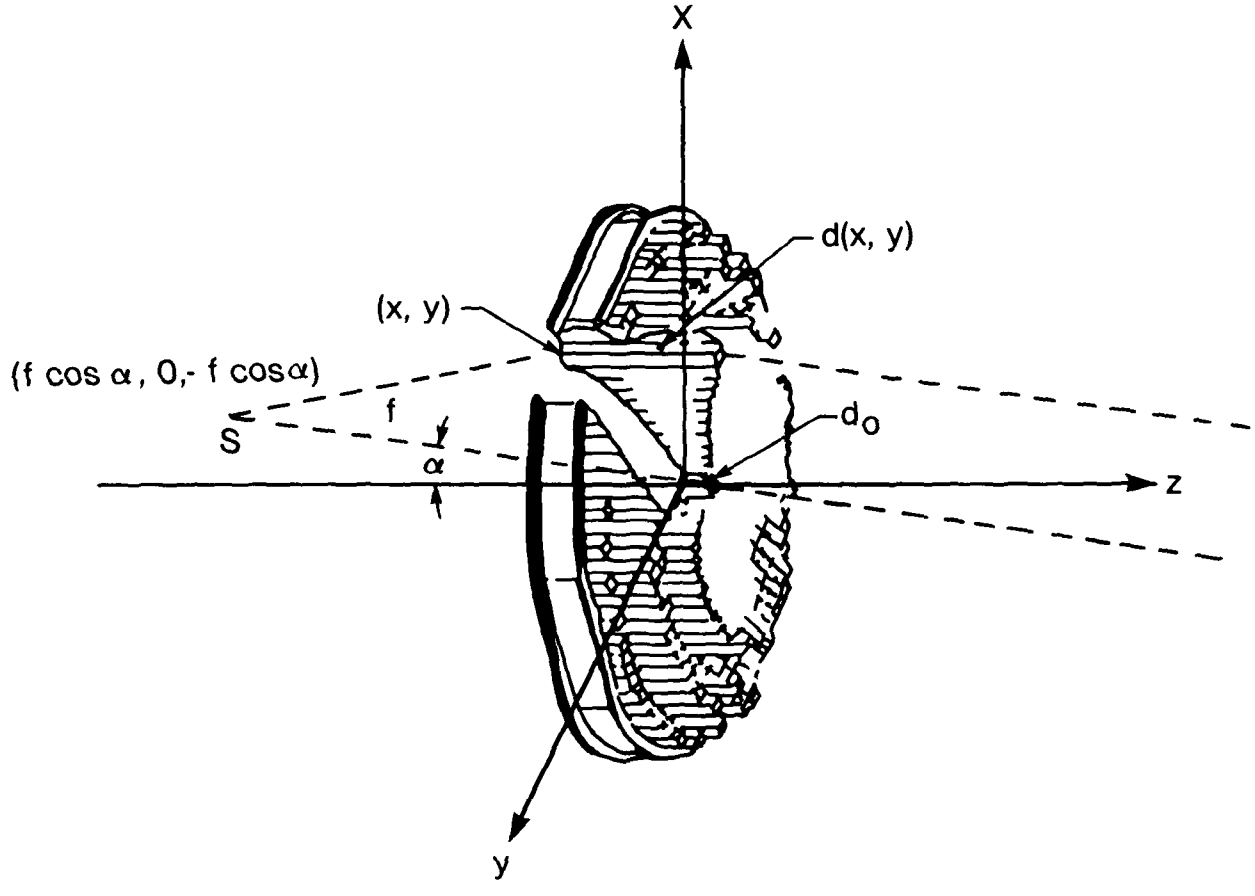

Figure 3-16. Lens Geometry for a Multiple-Beam Antenna System [3-72]

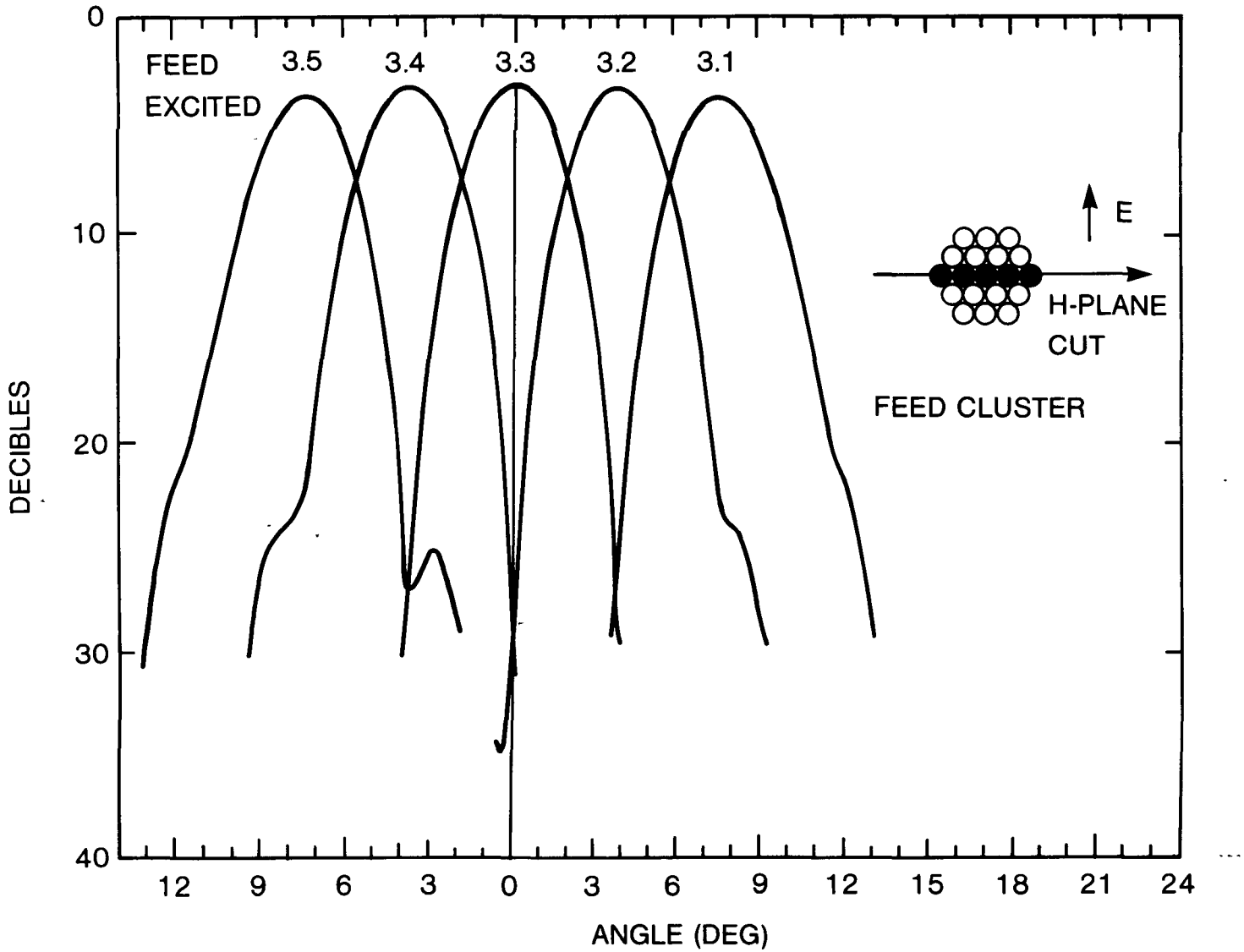

Figure 3-17. Superimposed Beams for Scanning in the H-Plane [3-72]

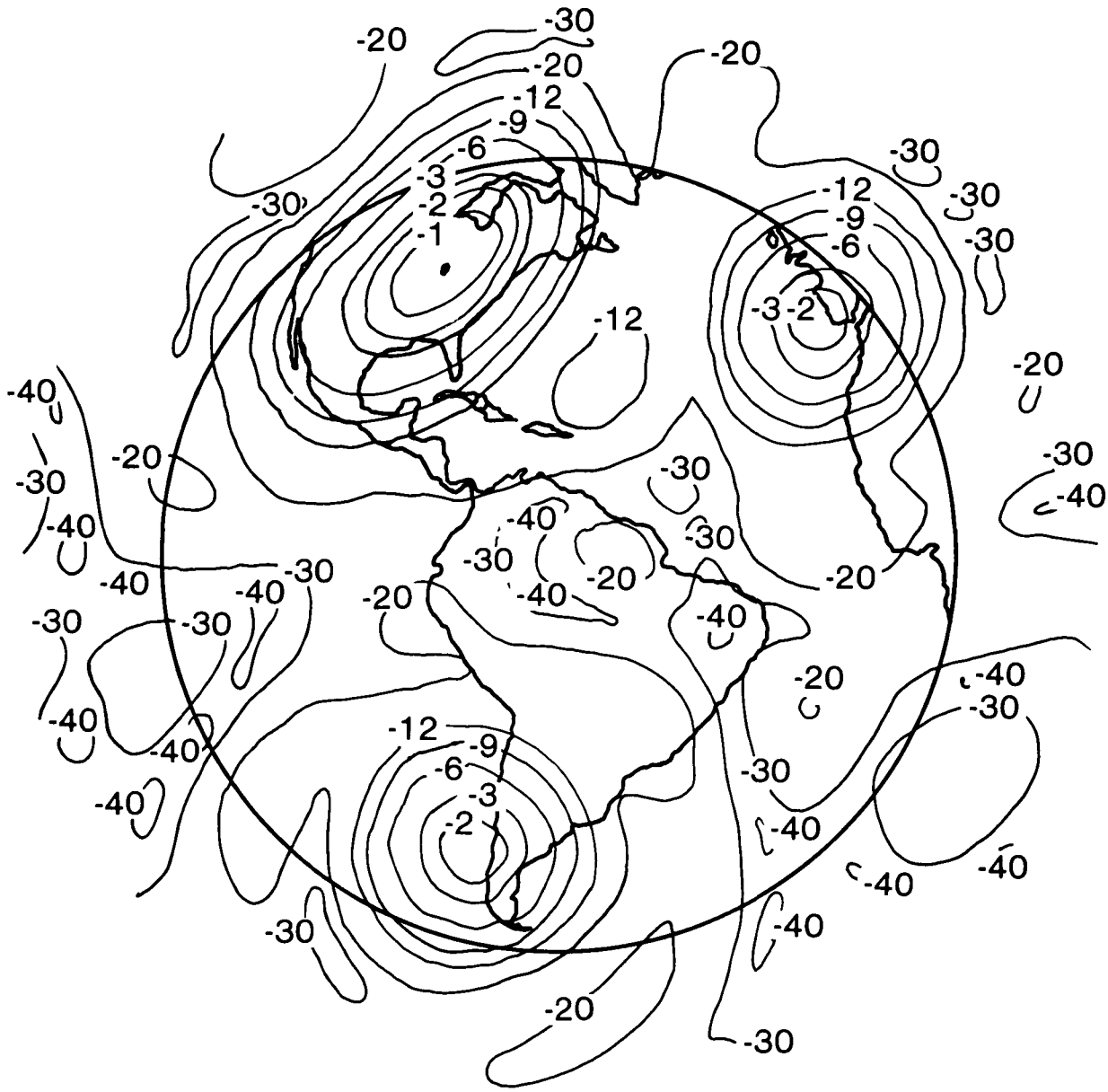

Figure 3-18. Pattern Contour for Compound Coverage [3-72]

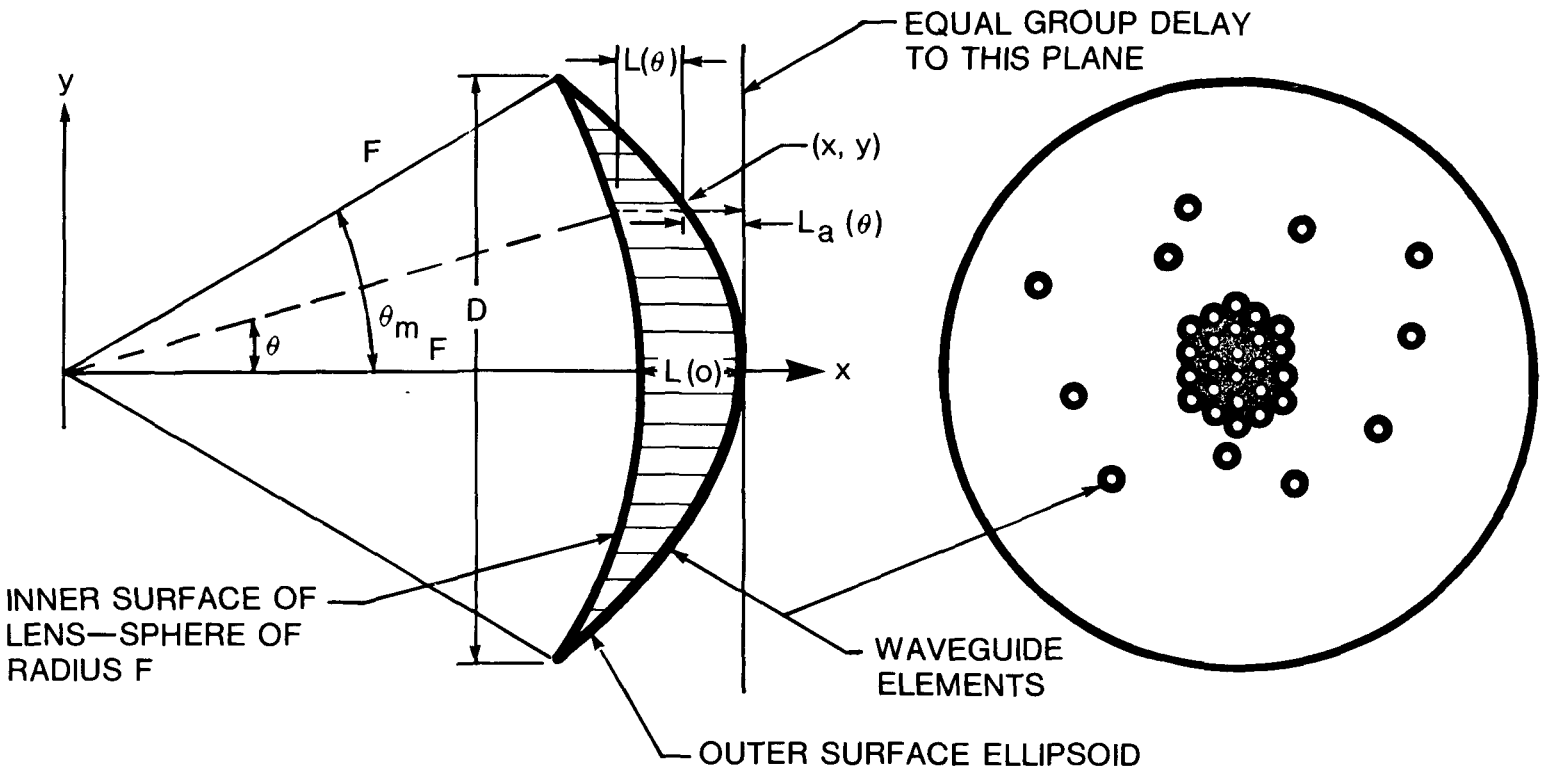

Figure 3-19. Geometry of the Group Delay Waveguide Lens [3-75]

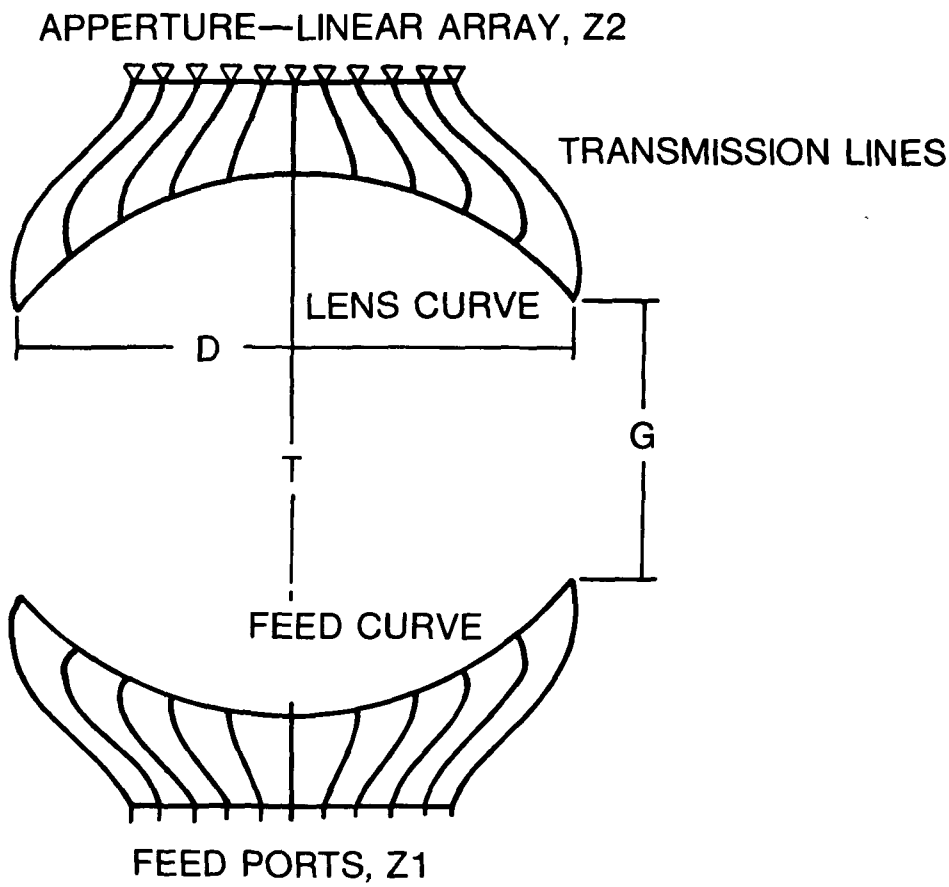

Figure 3-20. Symmetrically Configured Bootlace Lens [3-77]

Design problems in lenses have also been given some attention. Studies have addressed the effects of phase errors on gain and sidelobe levels [3-80] and array synthesis to produce low-sidelobe patterns [3-81]. Recently, an analytical account was given for the refraction at a curved interface [3-82]. This analysis used a geometrical optics solution for the transmission coefficient and the divergence factor of the lens surface.

3.7 FUTURE TRENDS IN PHASED ARRAYS

Understanding of the fundamental electromagnetic aspects of phased arrays has matured over the years; however, technological advances in the design of array components have been the determining factor in the overall development of phased arrays. With the advent of significant advances in solid-state array modules, monolithic fabrication, digital processing, and optical-fiber technology, phased array design is on the verge of tremendous growth and change. Monolithic fabrication will make possible the affordable phase shifters and amplifiers that are needed in large quantities to construct large arrays. Monolithic array fabrication is also a definite possibility. The implementation of these technologies will be the subject of ongoing research projects, including the present study. The application of MMIC modules in future satellite antenna systems has already been reported [3-83].

4. BEAM-FORMING NETWORKS

4.1 INTRODUCTION

The purpose of a beam-forming network (BFN) is to provide the necessary amplitude and phase distribution across the array antenna aperture to yield the required beam shape. In the case of multiple beams, the "network" has several input ports connected to the aperture, one for each beam. In a general sense, there are two types of feeding networks. The first employs transmission line techniques entirely in routing signals from the element array to the central feed point (input port). This type of network is known as a constrained feed network. The second method utilizes free-space propagation to spread the signal out from the central terminal to the individual elements, and is known as space feed. Because both types of networks have advantages and limitations, and depending on the intended application, care must be taken in the design to realize their ultimate capabilities.

The major advantage of a constrained feed is that it can provide precise amplitude and phase control to each element of the array. To achieve this, the various interconnections must be matched; otherwise they could yield large amplitude and phase errors. Amplitude and phase control in space feed is not optimum, but it does not differ significantly. It may be made to approach the optimum with a degree of precision by utilizing an increasingly larger feed array illuminating the secondary aperture. While space feed is subject to spillover loss, constrained feed is subject to transmission loss (insertion loss) which may exceed the spillover loss. The following subsections briefly describe the advantages

and disadvantages of the two types of feeding systems. Hill [4-1] has described these systems in greater detail.

4.2 CONSTRAINED FEED BFN TYPES

In constrained feeding networks, each element of the array is fed from some kind of transmission line. The characteristics of the array then depend both on the element and on the transmission line feeding it. Various array designs require different feeding methods, which fall into two distinct classes: parallel feeds and series feeds.

4.2.1 PARALLEL FEEDS

In parallel feeds, a number of power dividers are joined by equal lengths of line to form an input-output device with a single input port and several output ports. A phase shifter or a time-delay device is added to each output port to provide the proper phase taper.

4.2.1.1 Corporate Feed

Figure 4-1 shows examples of n'ary parallel feed systems. The n'ary systems is also known as corporate feed. The major problem in this type of feed network is the error effect on the excitation coefficients of the elements caused by reflections within the feed and from the elements. These reflections introduce sidelobes in the space pattern [4-2]. The use of separately matched components throughout the feed helps to reduce these errors.

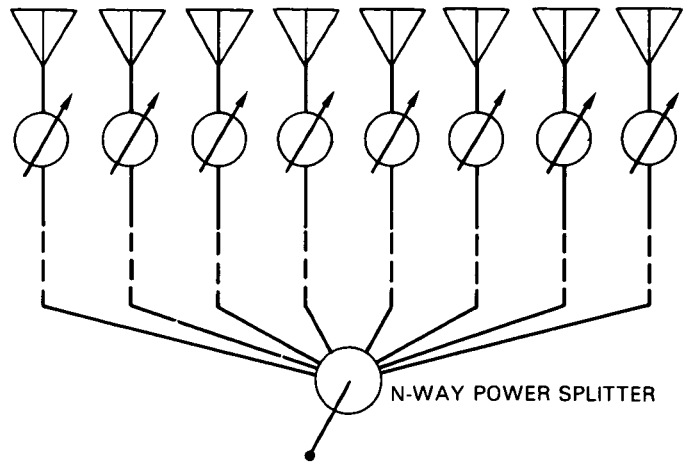

(a) PARALLEL RF FEED USING
N-WAY POWER DIVIDER

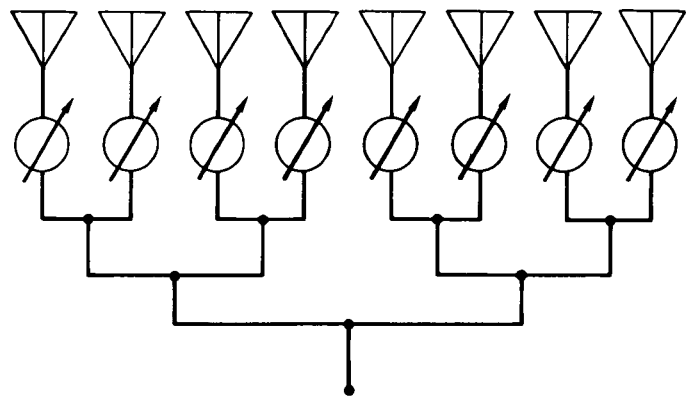

(b) PARALLEL RF FEED USING
CORPORATE STRUCTURE

Figure 4-1. Parallel RF Feed Using an N-Way Power Divider

Another technique, which practically eliminates these error effects, employs 4-port dividers in the feed network wherein the arm not connected to one of the transmission lines is terminated in a load. This is shown in Figure 4-2. The reflected wavefront (from the elements) passes through the phase shifter bank and impresses signals on the side arms of a 4-port junction. For a finite wave tilt, the reflected signal results in symmetric signals connected to the sum arm and antisymmetric signals connected to the difference arm, which is terminated in a load. This method reduces cross coupling and reflections. A magic-T and a directional coupler are examples of devices used in such a junction. Another example is the in-phase divider developed by Parad and Moynihan [4-3].

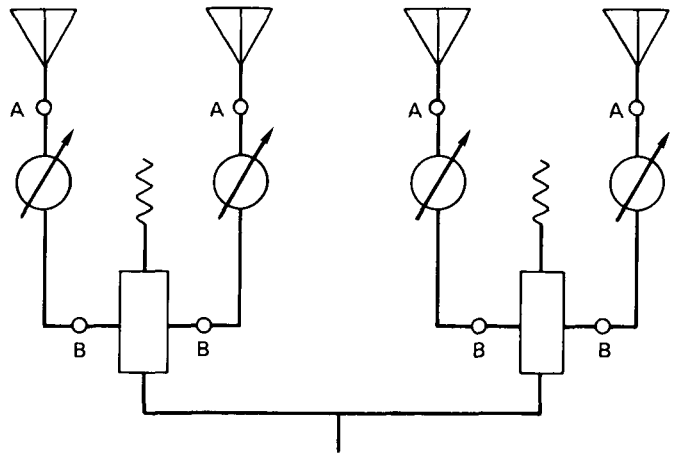

Figure 4-2. Corporate Feed Network Using 4-Port Dividers

The impedance bandwidth of a corporate feed system is almost entirely determined by the impedance bandwidth of the individual power dividing junctions. The corporate feed system also produces virtually zero beam squint as a function of frequency, because equal line lengths exist in each arm. When the number of

elements increases, the parallel feed network becomes complex and bulky. Another drawback is that, when power splits are unequal, performance bandwidth narrows.

4.2.1.2 Butler Matrix

The Butler matrix feed network is a variation of the parallel feed network and is used to produce simultaneous beams that overlap and can potentially cover the half space in front of the array aperture. This network is implemented by employing hybrid junctions and fixed phase shifters. There is no interaction or intercoupling loss to reduce the gain of any beam. The 8-input, 8-output Butler matrix shown in Figure 4-3 produces eight beams with a 4-dB crossover point and covers the entire sector, as illustrated in Figure 4-4. The beam positions are not independent of frequency.

In their original work [4-4], Butler and Lowe constructed a 4-element BFN at 3 GHz that had coaxial-fed dipole radiators, an operating bandwidth of 0.05 GHz, and couplers built on tri-plate. This work was followed by both theoretical and experimental analysis of the Butler matrix [4-5]-[4-9], which determined that maximum efficiency is obtained by uniform illumination of all elements by all inputs. This results in lossless simultaneous beams with high sidelobe levels. In the case of tapered illuminations (to reduce sidelobes), the beams have low crossover levels for the lossless network. In effect, for a lossless passive antenna radiating multiple beams from a common aperture, the radiation pattern and the crossover levels cannot be specified independently. To overcome this limitation, some transmission loss must be tolerated in the network. For example, to achieve a -3-dB crossover level instead of -4 dB (lossless case), the network becomes lossy.

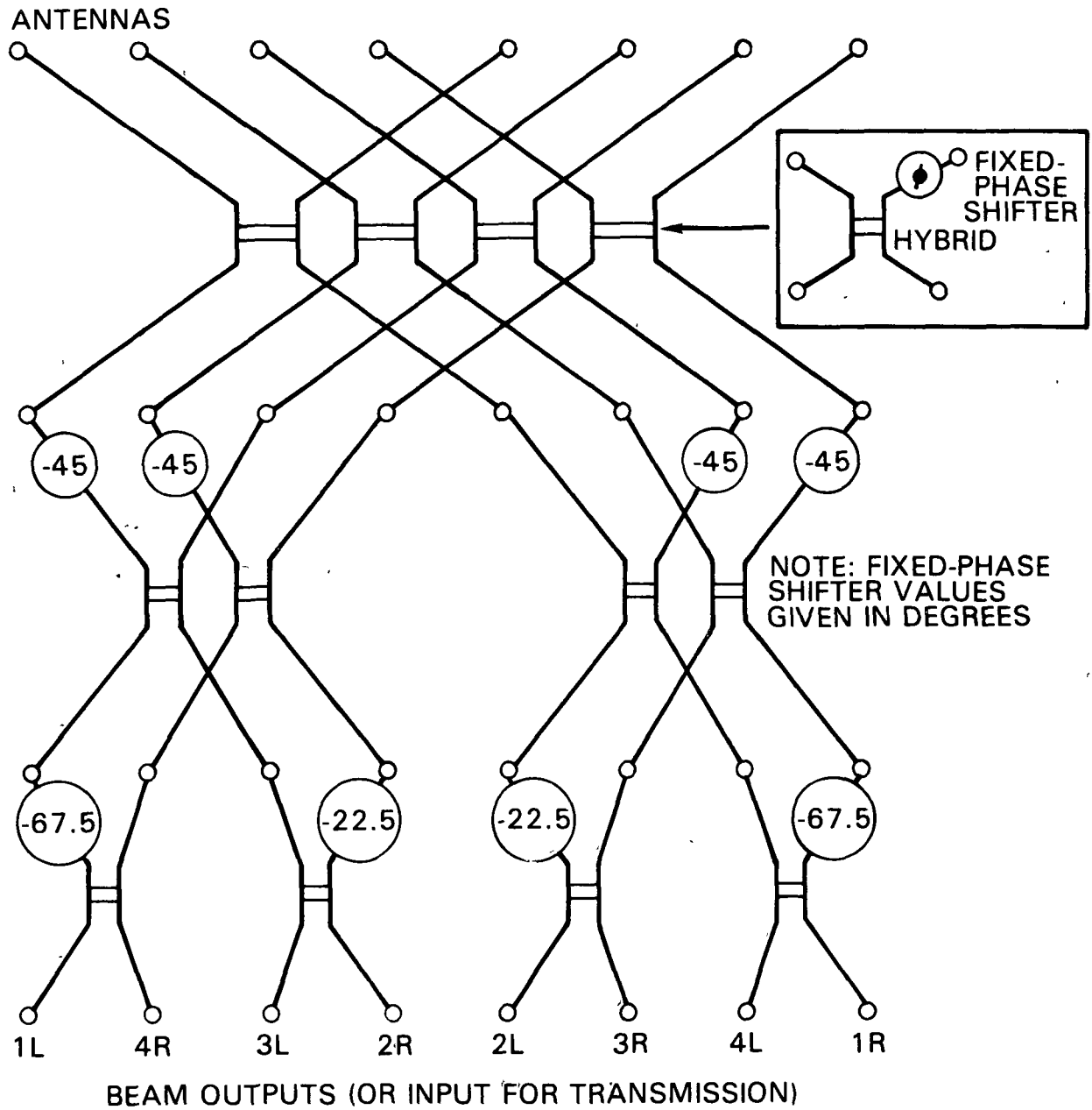

Figure 4-3. 8-Input, 8-Output Butler Matrix

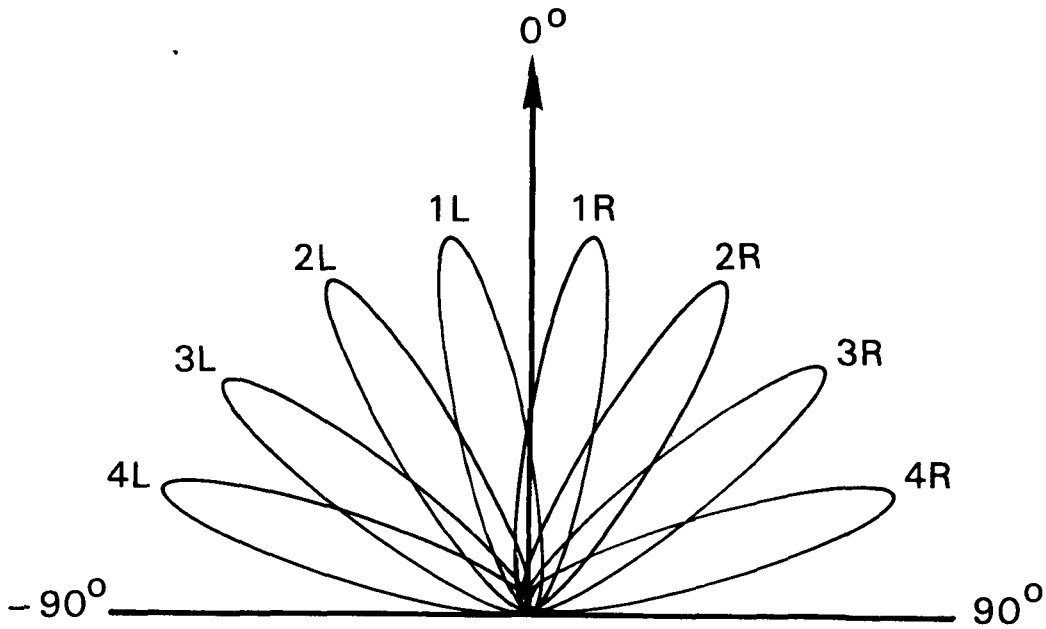

Figure 4-4. Resulting Beam Pattern of the 8-Input, 8-Output Butler Matrix

In a mathematical analysis [4-8], the magnitude of coupling between beam terminals to the complex cross-correlation coefficient of the corresponding beam patterns in space has been determined for the no-loss case. Experimental analysis [4-9] has revealed some drawbacks, such as the complexity involved in these networks for large arrays and their limited power-handling capability (from a transmitting standpoint). The bottom directional couplers and phase shifters are required to handle higher powers than the upper couplers and phase shifters in this matrix, as in all parallel feed networks. A systematic design procedure for a Butler matrix has been reported by Moody [4-10] and Jaeckle [4-11].

A one-to-one correspondence exists between fast Fourier transforms and Butler matrices, as shown in Reference 4-12. A more detailed approach to the same idea has been reported by Veno [4-13], in which the scattering matrix of the hybrid couplers is taken into account.

Butler matrices usually have the same number of input ports as output ports; however, some applications require additional output ports (more elements). Foster and Hailt [4-14] have shown that, by using a smaller number of hybrids, the Butler matrix can be extended to its next larger size. For example, an N x N matrix is extended to have N + M output ports by using only M additional hybrids, instead of $(N \ell n N)/(2 \ell n 2)$ for the case when N = M. This extension is at the expense of departure from the orthogonality of the beams (lower crossover levels) and an increase in network loss.

The beams produced by a Butler matrix are generally not in phase. In some applications, the phase relationship between beams is important. Pelletier et al. [4-15] have described a method of feed network design in which the phase relations between the beams can be known and controlled.

When networks are designed to achieve higher crossover levels (>-4 dB), losses are introduced in the network. Winter [4-16] has described a technique to maximize the available antenna gain at the beam crossover points by using specific illumination functions with a lossy network design.

4.2.2 SERIES FEEDS

Two basic feed network designs are shown in Figure 4-5a and b which have different phase shifter locations. In a series feed system, as contrasted to a parallel feed system, the lengths of transmission lines between input terminals and array elements are not equal. This system also has a similar problem of multiple reflections from couplers producing sidelobes if 4-port couplers are not used. A configuration using such a coupling junction is shown in Figure 4-6. Some of the disadvantages of such feeds are beam squinting as a function of frequency and the power handling limitation of the couplers on the main line.

An advanced form of series feed is the dual series feed [4-17] shown in Figure 4-7. In a linear array of this design, the "sumbeam" is excited by the front row of directional couplers by conventional center feeding with a magic-T. Feeding at a different port of the same magic-T produces an asymmetrical aperture distribution that yields a difference pattern. However, it also produces a large discontinuity in passing through the center of the aperture, which results in high sidelobes. This condition is corrected by modifying the distribution produced by the first line of couplers with a distribution produced by the second line of couplers to provide a Bayliss distribution.

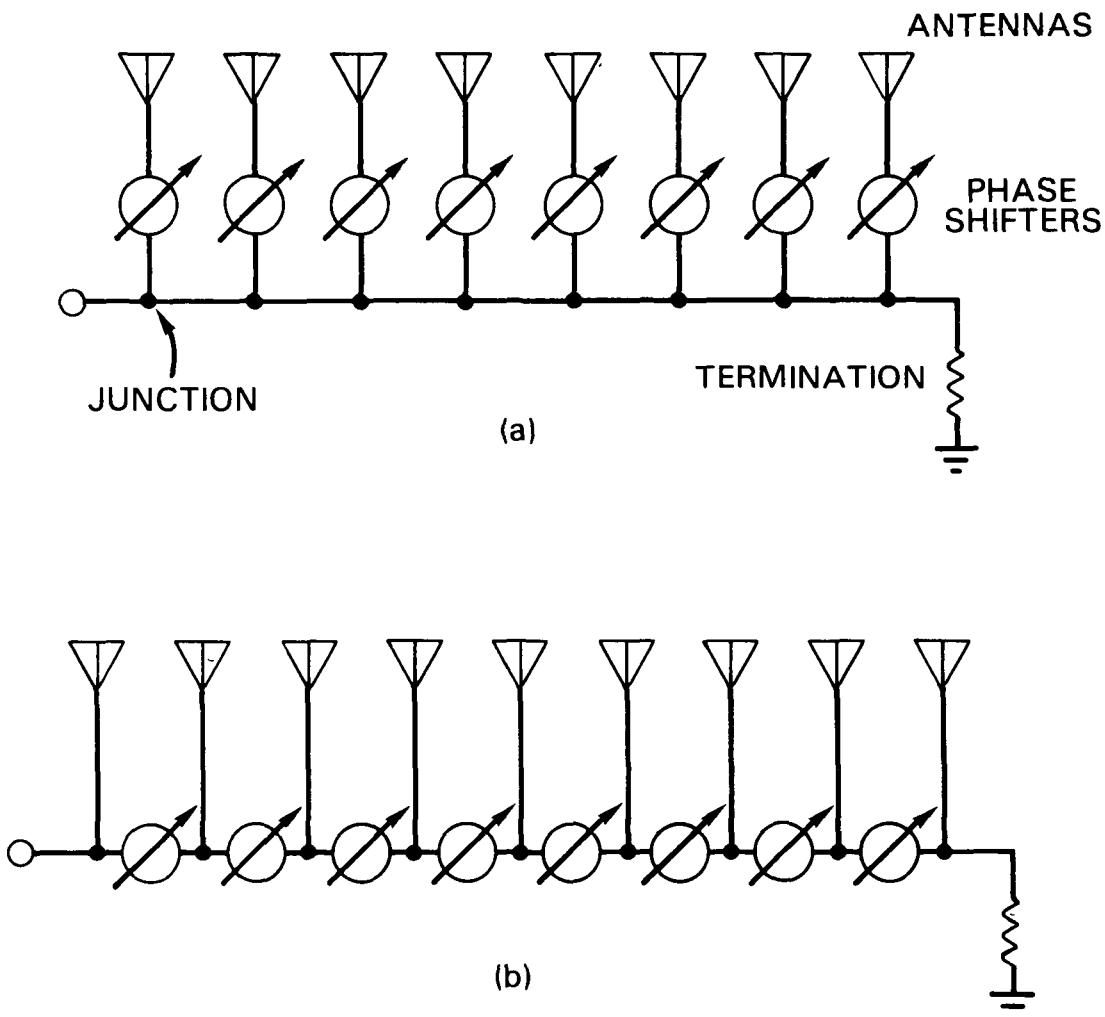

Figure 4-5. Series Feed Networks With Different Phase-Shifter Locations

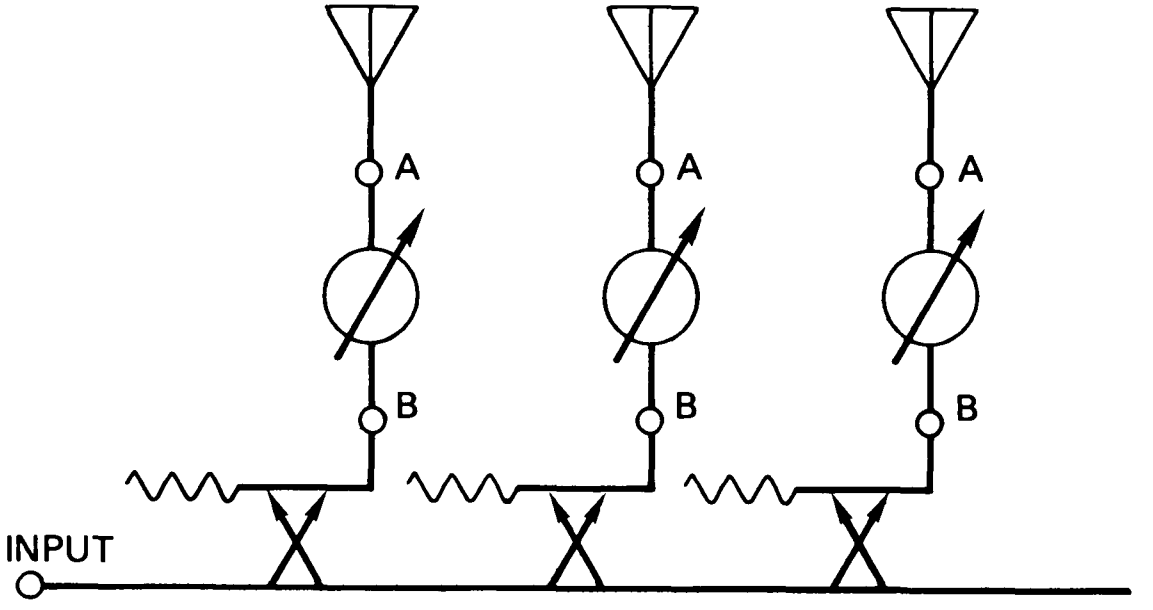

Figure 4-6. Series Feed Network With 4-Port Couplers

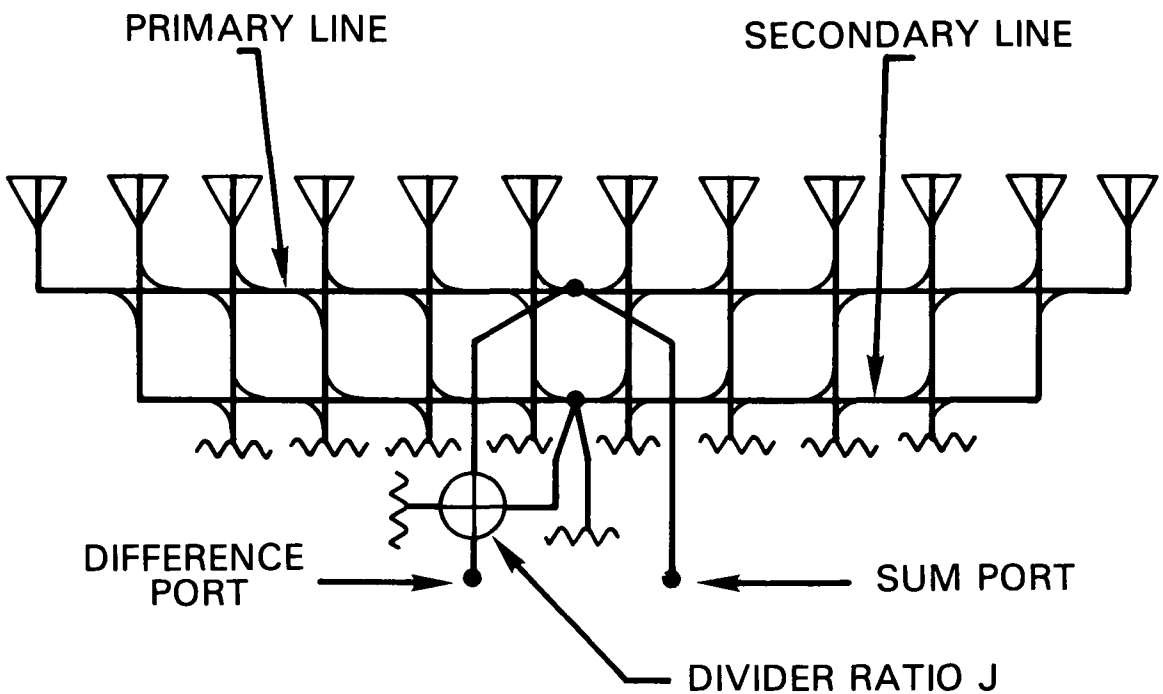

Figure 4-7. Dual Series Feed Network [4-17]

The multiple beam forming serial-type feed system shown in Figure 4-8 is the Blass matrix [4-18]. It consists of a number of main feeder lines which are excited by auxiliary feed lines through directional couplers. Each auxiliary feed line is tilted at an appropriate angle to the main feeder line to produce a beam pointing in a different direction. The same beam orthogonality criterion for maximum aperture efficiency applies as in the Butler matrix case.

4.2.3 SPACE FEED TECHNIQUES

The concept of space feed for a phased array antenna is to distribute the energy from a central feed point to the array element lattice by allowing the energy to spread through space, as in the case of a horn feed for a parabolic dish antenna. The degree of control obtainable by the constrained feed may be approached by using a feed aperture which approaches the size and number of elements of the phased array aperture. This entails proper accounting for the near-field diffraction from the feed array.

4.3 CURRENT BFN TECHNOLOGY

Power dividing networks for array feeds have different requirements for different applications. Some are required to synthesize extremely precise aperture distributions for low sidelobe radiation patterns; while in other applications, BFNs are required to handle high power levels or to be lightweight and compact. In ambitious programs, BFNs are required to have all these

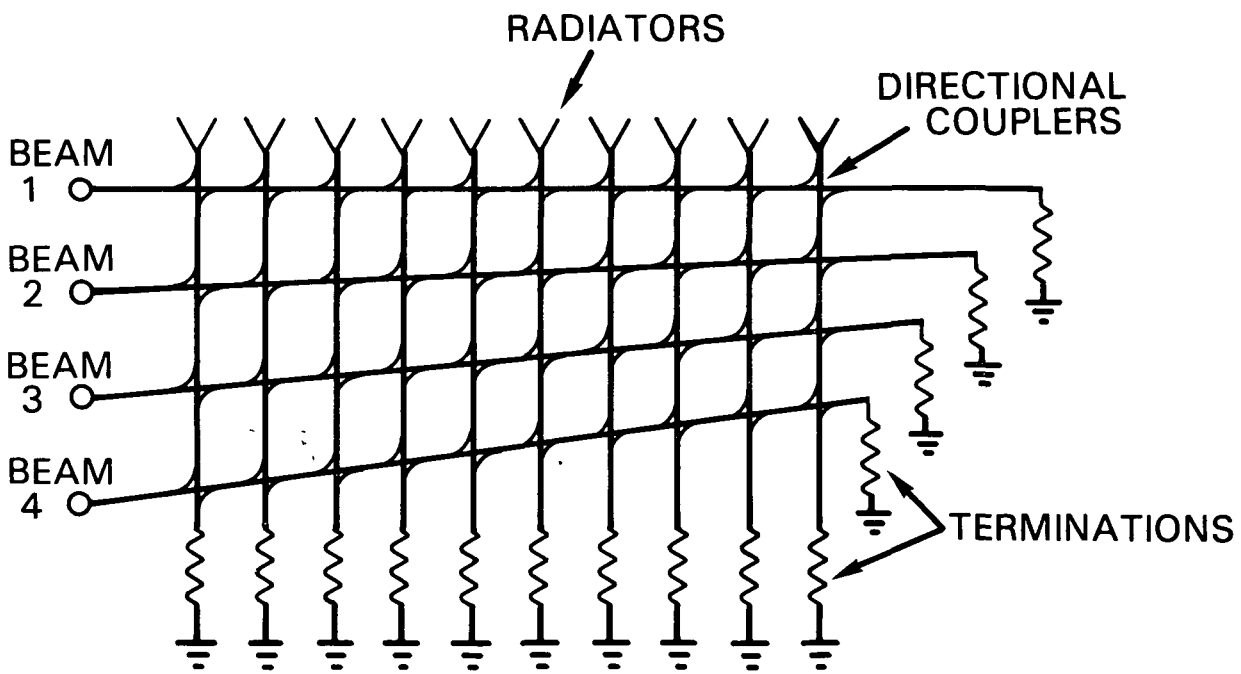

Figure 4-8. Multiple Beam-Forming Serial Network--Blass Matrix

features. Over the years, BFN technology has evolved from waveguide and coaxial line feed networks to printed-circuit (stripline) types of networks. Waveguide and coaxial line networks are most often used for high-power arrays. However, the increasing ease and quality of stripline construction has made stripline the medium of choice for many new array developments. A hybrid combination of waveguide, coaxial line, and stripline is used, depending on the application requirements. Stripline networks cannot handle very high power, but can be made compact and lightweight.

The selection of power division networks is critical to array design, and the choice can vary substantially with the intended application. Hanley and Perini [4-19] have designed a stripline array feed for a dual-shaped beam column array. This column network, shown in Figure 4-9, is composed of 2- and 3-branch stripline power dividers, some with interchanged output lines to give a wide range of coupling values. The bandwidth of this series-fed branch line coupler network was broadened by adding line lengths before each element. This network formed the requisite beams with less than 1.05-dB loss over 15-percent bandwidth at 1.3 GHz. Winchell and Evans [4-20],[4-21] have developed a corporate stripline feed for a low sidelobe fixed beam array at L-band. In this example of modern feed technology, the corporate feeds were constructed of stripline with the center conductor machined by a computer-controlled mill to produce a -55-dB Chebychev taper. The completed array demonstrated better than -36-dB peak and -48-dB rms sidelobes over about 45-percent bandwidth.

The phase control in BFNs is most often implemented at the RF operating frequency; although, there are instances where phase shifters have been used at intermediate frequencies [4-22], [4-23]. Generallly, diode phase shifters dominate the frequency range below 2 GHz, and ferrites are selected above 5 GHz. Diode

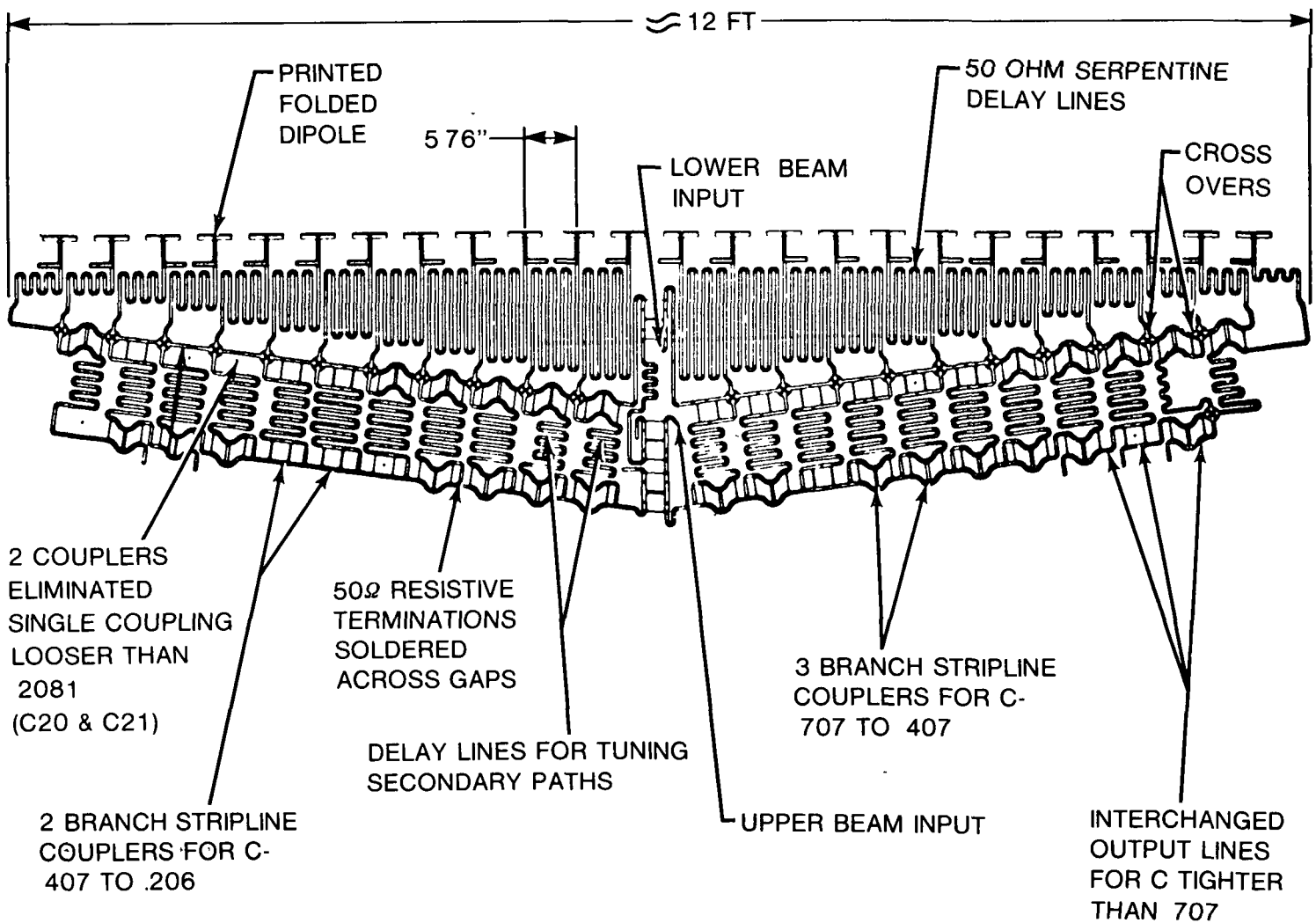

Figure 4-9. Column Network [4-19]

phase shifters are most often used in lightweight array configurations because they are easy to implement in printed circuits and networks. Tsandoulas [4-24] has developed a BFN for a low sidelobe array by using 6-bit diode phase shifters. The power division network was designed with careful tolerance control and the array achieved extremely low sidelobe levels.

Ferrite phase shifters have been used in BFNs for operation up to 60 GHz. These BFNs possess excellent characteristics for many applications. Power handling capability in such BFNs is high, on the order of 1 kW to as much as 150-kW peak. In the fire-finder system developed by Hughes Aircraft Co. in AN/TPQ-36, ferrite phase shifters were used to achieve scanning; whereas, in AN/TDQ-37, diode phase shifters achieve the scan capability. The electronically agile radar developed by Westinghouse used 1,818 phase shifters which, along with drivers, were integrated into the radiating elements. General Electric has developed a solid-state planar array with row feed networks. The row feed is a lightweight, single layer stripline circuit that is followed by transistorized power amplifier modules. For the Navy Aegis program, RCA developed a C-band phased array system that used a waveguide power divider network to feed 4,480 elements. Phase shifters were used at the element and array levels, and transmit and receive functions utilized different array illuminations and subarrays. This subarraying was done to accommodate high-power amplifiers in the transmit network.

Complex feed networks are required to feed circular and cylindrical arrays. These techniques include mechanical or electronic switching, lens-switch combinations, and hybrid matrix phase shifter combinations, and are described in detail in Reference 4-25. Shelag [4-26] has developed a BFN to feed a circular array. This BFN uses a power dividing network, followed by fixed phase shifters and variable phase shifters that feed a Butler matrix. More

recently, Skahil and White [4-27] demonstrated this technique by using an 8 x 8 Butler matrix and 8-phase shifters implemented in a combination of stripline and coaxial-line hybrids and power dividers. Hazeltine Corporation has developed a low-profile array at 8 GHz, with a BFN that used ferrite phase shifters and low-loss radial power dividers to provide a 21-way power split.

Printed-circuit arrays satisfy light weight and low profile requirements. Such arrays are usually fed with BFNs that are printed on the same substrate. Some advances have been made in this area, including an L-band array that was developed for aircraft tests with ATS-6 [4-28]. The BFN was printed on the same substrate as the radiating elements, and the power dividing network was followed by 3-bit switched line phase shifters. Munson [4-29] has developed a 16-element array at 4-6 GHz with the elements, phase shifters, and feed lines all on one side of the board. Huebner [4-30] used a technique to gain real estate by separating the elements and the feed with multiple layer construction. The feed network consisted of an input 3-way power divider followed by three binary power dividers, and was electromagnetically coupled to the radiating elements.

In phase-scanned arrays, additional space is required for diode phase shifters; consequently, they are often set apart from the elements on a separate board. Yee et al. [4-31] used this method to develop a 2 x 16 element array with a 16-way stripline power divider followed by 4-bit phase shifters. The circuit was printed on alumina ceramic substrate as a single integrated module. This technique lends itself to high-volume production, reduces fabrication costs, and improves reliability.

Printed-circuit technology for large arrays presents special problems, such as high feed network loss. This technology has been used to construct a 1,024-element L-band planar array

for the Seasat program. A low-loss substrate with a honeycomb structure was used for most of the circuit, and coaxial cabling was used in other parts of the feed. Overall losses were 2.3 dB.

4.4 BFN COMPONENTS

A BFN can have many components, such as power dividers, phase shifters, switches, amplifiers, polarizers, and OMTs, depending on the requirements of a particular application. Figure 4-10 shows the layout of a BFN that utilizes all these components. This subsection will discuss each component and the impact of characteristics such as form-factor, losses, weight, heat dissipation capacity, reliability, reproducibility in large-scale production, and cost.

4.4.1 POWER DIVIDERS

The power divider is one of the main components in a BFN. Various types of power dividers can be classified either by the type of transmission medium they are built in, or by the type of coupling mechanism used (codirectional, aperture, interference, waveguide, coax, printed, or intrinsic). This study will discuss classification by transmission medium, because this approach provides information on many features needed for a direct comparison.

Power dividers built in waveguide have been in existence for many years and are popular for their intrinsic, extremely small insertion loss. Because these dividers generally have a form-factor restriction (on the location of the output ports), their use in large BFNs is limited. They can handle high power levels (kilowatts), but have the disadvantage of becoming heavy. New lightweight materials, such as copper plated graphite, are currently

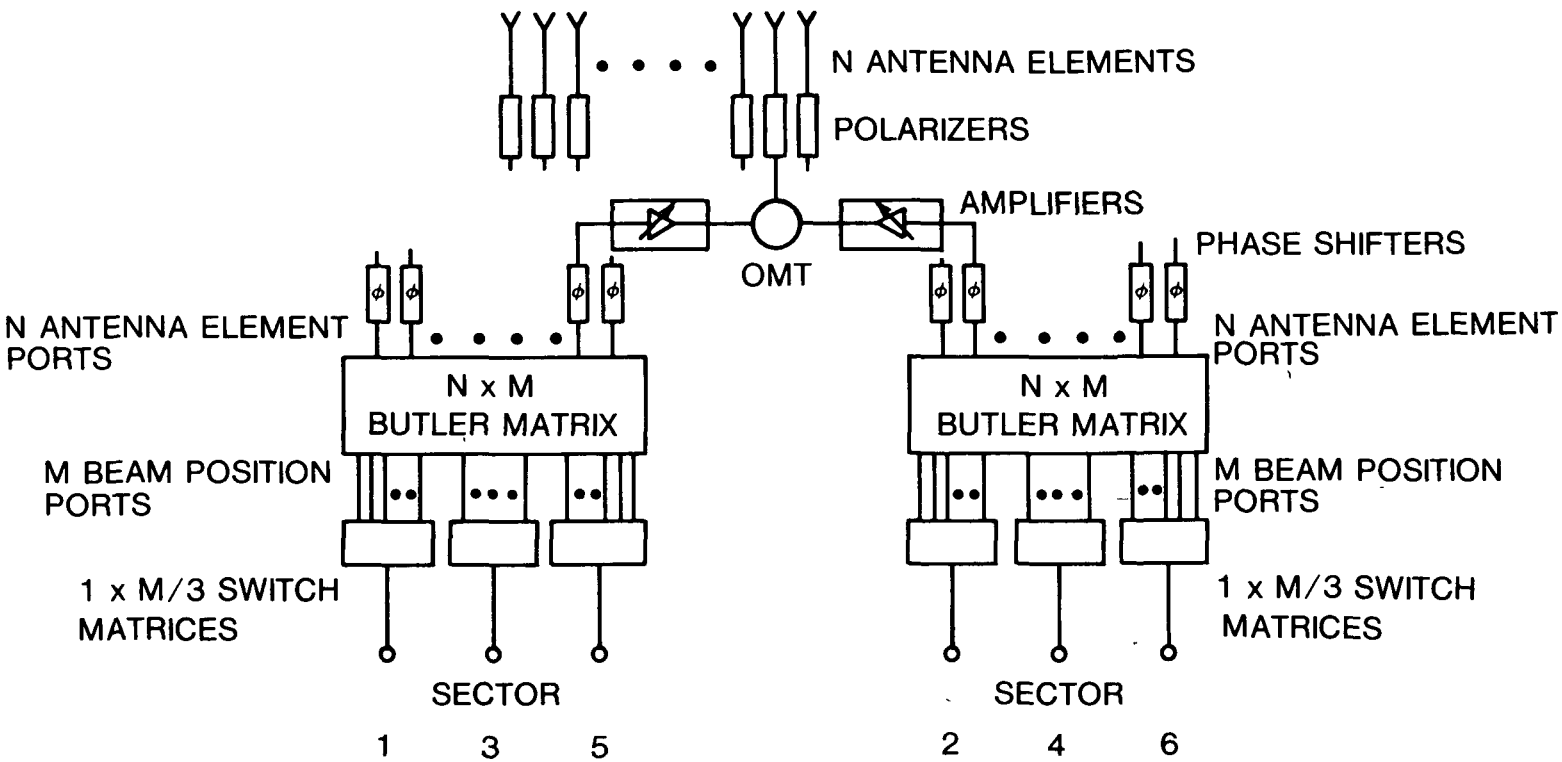

Figure 4-10. Generalized BFN

used in their construction. Heat dissipation is usually not a problem if techniques are developed to radiate it efficiently. In general, the reliability and reproducibility of these power dividers is very high while the manufacturing cost is moderately high. The advent of stripline line circuits has led to the replacement of waveguide power dividers in some applications.

The increasing demand for lightweight and compact BFNs, coupled with their size, has led to the development of planar circuit technology. Coaxial power dividers have been used in BFNs; however, they tend to get lossy as the frequency increases. Also, reproducibility and reliability are generally not high. An extension of coaxial power dividers is the squareax power divider developed by Hughes Aircraft Company. This transmission medium has lower loss and allows a greater degree of freedom in the design of complex networks. The transmission line combines the layout-design features of conventional etched-circuit stripline with the performance features of waveguide microwave networks. The attenuation loss of this line is claimed by Hughes to be about 0.015 dB/m at 4 GHz, whereas a regular waveguide is about 0.03 dB/m. For INTELSAT VI, a BFN using power dividers in this transmission medium is being constructed by Hughes to feed as many as 79 antenna elements with an estimated total insertion loss of 0.9 dB.

The most commonly used power dividers in stripline medium are the reactive tee, branch line, parallel coupled, and in-line types. Although the simplest and least expensive to construct, reactive-tee power divider networks have no isolated ports, and hence present serious mismatch and isolation problems when used to feed mismatched elements. Therefore, reactive corporate feed networks are used mainly in fixed beam arrays. Branch-line couplers are easily fabricated and are most useful for coupling ranges from 3 to 9 dB. Parallel coupled stripline couplers are generally useful for loose coupling (>10 dB). The Wilkinson

divider [4-32] can be designed for n-way division in a radial fashion. By using a circular symmetry principle, n^2 elements can be made in two layers. An extension of this in-line power divider to stripline is given in Reference 4-33. Both equal and unequal splits are possible. These in-line power dividers are usually employed, because they possess excellent broadband characteristics.

In the recent past, many planar n-way power dividers have been proposed [4-34]-[4-37]. Of particular interest is the 4-way and 7-way combiner [4-36] at 12 GHz, which was fabricated in microstrip employing duroid substrate with chip resistors used between output ports. Measured interport isolation has a nominal value of 20 dB. A 5-way power divider, constructed in microstrip at 2 GHz, has resulted in 0.5-dB loss and 13.5-dB interport isolation [4-37].

Microwave integrated circuit (MIC) power combiners for FET amplifiers have been reported in the literature. Quine et al. [4-38] have developed a 6-way radial waveguide combiner for use at 7.5 GHz. The circuit is etched in a fused silica disc, and measured insertion loss is 0.25 dB. In another report [4-39] of a radial power combiner, microstrip lines were connected to active devices (Gunn diodes) and coupled to a tabular dielectric cavity acting as a combiner circuit. A combining efficiency of 70 percent was achieved at 10.3 GHz.

With the advent of monolithic microwave integrated circuits (MMICs), power dividers are being fabricated on semiconductor substrates. Couplers have also been fabricated on GaAs substrate, which is the most commonly used for MMICs. Pucel et al. [4-40] reported the design, fabrication, and band performance of a monolithic 3-port Wilkinson coupler and a monolithic interdigital Lange coupler at X-band frequencies. At 9.5 GHz, the Wilkinson divider occupied an area of 0.08 mm^2 with a 0.25-dB loss. For the Lange coupler, the loss is 0.75 dB at 15 GHz with an isolation of -15 dB.

In another report [4-41], a 3-dB Lange coupler fabricated on GaAs substrate had a 0.7-dB loss at 9.5 GHz. The dimensions of this coupler were 0.11 x 3.2 mm. To reduce the loss in a Lange coupler, Hobdell et al. [4-42] have used air-bridge straps in place of bond wires on a 3-dB Lange coupler built on alumina substrate. This technique resulted in a 0.3-dB reduction of loss. It can be employed for Lange couplers on GaAs substrates.

A new development in power divider design, still in the preliminary stage, is the use of active devices. The loss associated with passive power dividers is eliminated, and a gain is introduced. Pan [4-43] has reported a power division technique that employs a GaAs dual-gate MESFET. The active combiner/divider is constructed on alumina substrate operable at 7.25-7.75 GHz. This device has the advantage of variable power division, which is accomplished by variable bias control. For equal power division, a gain of 4.5 dB and a reverse isolation of 18 dB have been measured.

BFNs constructed using GaAs power dividers are very compact. The present problems with such BFNs are the high loss, and, in the case of passive circuits, the extremely low yield in mass production and reliability.

4.4.2 PHASE SHIFTERS

Diode phase shifters generally dominate the frequency range below 2 GHz, while ferrites are selected above 5 GHz. Also, diode phase shifters are more compact and significantly lighter in weight than the ferrite devices.

Currently, the most popular types of diode phase shifter designs are the hybrid-coupled, switched-line, and loaded-line phase shifters using p-i-n diodes. Switched-line hybrids have

greater insertion loss and undesirable frequency sensitivity; however, they possess distinct advantages in weight and compactness and have been used successfully in monolithic BFNs. Hybrid and transmission phase shifters have lower loss and better bandwidth performance. White [4-44] has reported an S-band stripline hybrid phase shifter with an average 0.8-dB loss and 3° phase error. At X-band and K_u-band, the losses are 2 dB and 3 dB, respectively. These devices have handled up to 4 kW of peak power. Schiffman phase shifters produce nearly constant phase shift over a broad range of frequencies [4-45]. Another class of diode phase shifters is the high pass/low pass type [4-46]. This circuit can be made small on GaAs by using lumped elements. A phase shift of 180° over 20-percent band has been achieved. Since dual-gate FETs are used as switches, gain can be obtained from these devices.

Ferrite phase shifters have been built to operate up to 60 GHz and possess excellent electrical characteristics. Nonreciprocal ferrite phase shifters include the dual slab and the toroid designs. These types of phase shifters presently have a bandwidth in excess of 10 percent and insertion loss of 0.5-1 dB. Power levels can vary from 1 kW to as much as 150-kW peak, and average to 400 W. Latching phase shifters have switching times on the order of 1 μs. Flux drive circuits allow for analog phase settings.

Of the several varieties of reciprocal phase shifters, dual-mode phase shifters have been found to have lower values of phase shift per wavelength than Reggia-Spencer phase shifters. These values are competitive with toroid phase shifters. Dual-mode phase shifters have average power levels up to 1.5 kW at S-band and peak powers to 150 kW. Insertion loss can be 0.6 dB through X-band. In Reference 4-47, specific examples of phase shifters are compared.

Another important reciprocal phase shifter is the analog rotary-field phase shifter of Boyd [4-48]. Although this circuit requires a large amount of drive power and has long switching times (≅200 μs), its advantage is its nearly dispersionless phase shifting capability. It can handle high power levels, with an insertion loss under 1 dB.

Recently, phase shifters have been built by using monolithic fabrication technology. In one case, four dual-gate FET amplifiers and an in-phase, 4-way combiner were used to achieve a continuous phase shift [4-49]. In another case, three dual-gate FET amplifiers and quadrative couplers were used to achieve the same result [4-50]. These phase shifters have several advantages, such as light weight, fast response, low loss, and octave bandwidth capability.

4.4.3 SWITCH

Semiconductor diode switches have been the most commonly used switches in BFNs because of their high speed, small size, and low driving power. The power-handling capacity of diodes is limited by reverse breakdown voltage, which has greatly increased over the years with the introduction of p-i-n diodes. These switches have an associated insertion loss which can be high at higher frequencies.

Presently, use of both single and dual-gate GaAs FETs in a conventional amplifier configuration has received considerable attention. Gaspari and Yee [4-51] have reported an 8-way switch utilizing a tuned series-connected FET switch; Vorhaus [4-52] has reported a multithrow dual-gate FET switch with isolation in excess of 25 dB at X-band; and Garver [4-53] has proposed a "control" FET, which is capable of handling several watts of RF power.

4.4.4 POLARIZER

The polarizer usually connects the BFN output to the antenna array element. It is used to convert a linearly polarized wave to a circularly polarized wave.

Various types of polarizers have been built in waveguide. The most commonly used are the pin type [4-54], which have been built to operate over 50 percent bandwidth at 4-6 GHz and inherently have no limit. An axial ratio of 0.1 dB or less is achievable. This design is suitable for circular waveguides, but can also be used for square waveguides. The design is easily extendable to higher frequency by scaling techniques. COMSAT Laboratories has built and tested the same polarizer at 12 GHz.

An improvement on the pin polarizer design is the cavity-compensated polarizer, in which an axial ratio of 0.05 dB has been achieved over the same band. Nippon Electric Corporation developed a 4- to 6-GHz frequency reuse polarizer with a low axial ratio by using a quartz dielectric vein, a resonant cavity, a multihole coupler, and a ridge located within the circular waveguide [4-54].

Another type of waveguide polarizer is the septum polarizer built by Ford Aerospace for the INTELSAT V satellite antenna system. This design is suited for square waveguides. A typical polarizer has a 0.2-dB maximum axial ratio over a 3.7-4.1 GHz range.

In horns, circular polarization can also be achieved by exciting the horn throat with four in-plane orthogonal probes. A network is used to generate equal amplitude and phase progression. This scheme is being implemented by Hughes Aircraft in INTELSAT VI satellites. The feed network is a hybrid squareax type, with a demonstrated axial ratio of 0.2 dB over 3.7-4.0 GHz. These polarizers have the advantage of compactness.

Another class of polarizers is the transmission type [4-55]. In these devices, a TEM linearly-polarized wave is phased through a layer of printed-circuit meander line inclined at 45° to the electric field, and the emerging wave is circularly polarized. Transmission polarizers are inherently narrowband and have an associated high insertion loss. They are also of limited application.

4.5 BFN CONTROLLERS

The major function of a BFN controller is to provide the proper drive signals, accurately synchronized across a large distributed BFN. Data sequencing for scanning beams, while not currently done, is virtually identical in concept to SS-TDMA matrix control, and as such represents no great technical innovation. The main consideration is the logic family used. Semistatic multibeam antenna controllers are far simpler than scanning beam controllers, since no sequencer or sequencer memory are required (although a beam to phase/amplitude look-up memory might be desirable).

Little information has been published specifically relating to multibeam antenna controllers. Most work thus far appears to have been performed by Bell Laboratories [4-56]-[4-59]. Because of the great similarity to SS-TDMA control, appropriate work has been done for the advanced WESTAR spacecraft and at COMSAT Laboratories as part of SS-TDMA projects [4-60],[4-61].

4.6 TRENDS IN TECHNOLOGY

In the past decade or two substantial advances have been made in antenna array technology, including advances in components, phase shifters, and feed networks. Many new antenna elements have been developed, most notably microstrip and stripline elements. The aim of this work has been to reduce the size and weight of the antenna arrays to achieve cost reduction. With the advent of printed-circuit technology, microstrip arrays are becoming suitable for many applications requiring narrow bandwidth, low power, and extremely light weight. Multilayer techniques facilitate wideband and high-power operation and integration with solid-state amplifiers for increased efficiency. This dictates the development of printed-circuit BFNs in parallel for integration with the antenna array. State-of-the-art BFNs are being fabricated in planar structures using squareax transmission medium and microstrip or stripline transmission medium. Extremely low loss substrates are available, thus extending the size of BFNs. In this hybrid form, with active devices (amplifiers, phase shifters, and switches) mounted on the substrates or as separate modules in the BFN, the network loss can be high and the BFNs can become bulky. The trend is toward monolithic BFNs, much work is being done to develop power dividers on GaAs substrates so that active devices can be etched directly on the substrate, thus reducing any connection losses. It is envisioned that a completely monolithic BFN module integrated with printed-circuit antennas, also on GaAs substrates could become the state of the art within the next 20 years.

Presently, development of most components on GaAs substrates are at X-band. These MMICs have a performance comparable to circuits in hybrid technology. It is expected that the frequency band of operation will move into the K-band in a few years.

In the context of this project, the two technologies best suited for BFNs of various configurations are squareax and waveguide transmission media. Both have been demonstrated at low frequencies and are extendable to 20-30 GHz.

5. MICs AND MMICs IN PHASED ARRAYS

The large-scale application of MICs to phased arrays began with the initiation of the Molecular Electronics for Radar Application (MERA) program at Texas Instruments in 1964, funded by the Air Force Avionics Laboratory [5-1]. The need for an electronically scannable and reconfigurable radar was the prime motivation for this effort, and the availability of compact, low-power dissipation control circuitry in MIC form made the system realizable. The need for smaller and more reliable phased array modules has been the main driving force behind the development of advanced MICs, and more recently MMICs, in the 20 years since MERA.

5.1 HYBRID MICs

For the past 15 years, the predominant form of microwave circuit realization has been the hybrid MIC. In this technology, circuits are etched onto either ceramic or "soft" substrate material, and all or most components, such as active devices, resistors, and capacitors, are attached to the circuit with solder, epoxy, or wire bonds. As this technology has progressed, a greater number of passive components have been incorporated into the photolithographic process, so that today it is possible to fabricate a hybrid circuit in which the only "hybrid" component is the FET or diode.

The various transmission media currently used in the fabrication of hybrid MICs include microstrip, coplanar waveguide (CPW), and slotline. Of these, microstrip is the most commonly

used because of its relatively low loss and the substantial amount of design information available for it. The CPW medium is lossier than microstrip and is prone to moding problems unless care is taken in fabrication. Its advantage is that access to ground is easier, which may improve the performance of circuits that depend on a low inductance path to ground. This is especially important at high frequencies, where a small parasitic inductance may contribute a large unwanted reactance to the circuit. The slotline medium has had limited use because of its problems with loss and stray coupling. It is used primarily in circuits that require a balanced transmission medium, such as push-pull amplifiers or dipole radiators, and thus it requires an additional balun circuit to properly match unbalanced circuits like microstrip or CPW.

5.2 MONOLITHIC MICROWAVE INTEGRATED CIRCUITS

The development of MMICs has followed a sequence of milestones similar to those achieved in the development of lower frequency silicon devices. First, the appearance of discrete devices were designed, followed by the development of simple integrated circuits, and finally the combination of several circuits on a common chip to function as a subsystem or system. These similarities, however, should not mask the fundamental differences between the development of the two technologies, such as different frequency ranges, semiconductor materials, fabrication technologies, and applications. GaAs MMICs are fabricated using epitaxy or ion implantation, operate in the 1- to 60-GHz range, and are used for the typical communications functions of low noise and power amplification, mixing, detection, and switching [5-2]. The definition of a "monolithic" circuit has been debated since its appearance; however, there is no argument that an MMIC contains

at least one FET or diode fabricated in situ on a GaAs substrate, along with a matching circuit composed of passive or active circuit elements. The major advantages of MMICs, as noted by Pucel [5-3], are as follows:

a. low cost,
b. improved reliability and reproducibility,
c. small size and weight,
d. broadband performance, and
e. design flexibility and multifunction performance on a chip.

These attributes are obviously not equally important for all applications. Some circuits may be required to emphasize low cost, while others may be designed to optimize performance or some other characteristic. The potential for a low-cost technology derives from the same reasons that silicon integrated circuits have achieved that goal, namely, automated processing and small size. The maturity of GaAs processing has still not reached that of silicon, so the cost benefits have yet to be realized. There is no reason, however, to expect that GaAs will not reach that point. Improved reliability and reproducibility arise from the fact that virtually all manual bonding and assembly operations have been eliminated. Small size and weight will allow greater redundancy and the application to new systems, such as phased arrays. The elimination of many parasitic reactances allows the realization of broader bandwidth circuits and also of circuits capable of operating at higher frequencies.

Some of the problem areas should also be mentioned. The losses associated with smaller circuits on a GaAs substrate are higher than in a well-designed hybrid circuit. The inability to select devices for parameters such as low noise, high gain, or

power output means that performance may not be easily optimized. Furthermore, the lack of tuning ability in the fabricated circuit restricts circuit yield and performance. From a physical viewpoint, GaAs circuits are very fragile and must be handled and mounted carefully to avoid breakage.

Although the technology is relatively young, much progress has already been made in realizing many different types of circuits in GaAs MMIC form. Among these are power amplifiers generating 1.0 W at 9 GHz [5-4], low-noise amplifiers with 6.2-dB noise figure at 21 GHz [5-5], phase shifters [5-6], switches [5-7], and oscillators [5-8].

The potential of MMICs in digital circuits may be even greater than that in analog circuits because of the high speed of GaAs FETs and the high density with which they can be packed in a typical digital circuit. Digital frequency dividers have been fabricated in MMIC form with input frequencies up to 5 GHz [5-9].

One of the fundamental questions that remains to be answered is what level of integration will be optimal for a given application. The limitations will probably be controlled by unacceptable reductions in yield or unacceptable loss of performance, such as by interaction.

5.3 MIC/MMIC-WAVEGUIDE TRANSITIONS

A basic problem encountered in the design of phased array systems is how to integrate the RF module with the radiating element in a way which minimizes loss and impedance mismatch and yet allows physical access and heat dissipation. The traditional technique has been to combine all or most of the RF circuitry in one partitioned housing with coaxial connections to both input and output. At the output, a transition to the radiating element,

which can be a waveguide horn or a dipole (as was the case in MERA), is required.

If we assume a waveguide radiating element, transitioning between microstrip and waveguide can be accomplished in the following ways:

a. microstrip-coax-waveguide,
b. microstrip-ridge transformer-waveguide, and
c. microstrip-finline-waveguide.

The choice among the three is based on the specifications for maximum insertion loss, ease of fabrication and assembly, and array structure. At frequencies above about 12 GHz, insertion loss becomes an important criterion; and it may have great influence on the choice. The ridge transformer transition will generally have the lowest loss [5-10]; however, it suffers from a relatively complex mechanical structure and the inability to appear transparent to the orthogonal propagating mode. The coaxial transition generally has the greatest insertion loss becuase of the losses associated with the coaxial section itself.

The finline transition has moderate insertion loss but has two properties which make it superior to either of the former transitions for certain applications. First is its simplicity. The entire circuit can be photolithographically etched on a ceramic substrate, which is mounted vertically across the E-plane of the waveguide. Circuits such as amplifiers, phase shifters, or attenuators can be either deposited on the same substrate as the transition or can be mounted on the surface of the substrate, as for MMIC. Two different types of finline transitions have been investigated. One is a field-rotation version developed by Van Heuven [5-11] which takes the vertical electric field in the waveguide and rotates it by 90°, and the other is a planar version

developed at COMSAT Laboratories in which the orientation of the electric field is preserved and, consequently, is transparent to orthogonally-polarized field components. This is discussed in detail in Volume II of this report.

With the increased application of MMICs to phased arrays, mounting techniques and transitions will play a larger role because of their mechanical fragility and the desire to take maximum advantage of their small size and weight. It is for these reasons that the finline transition should find application for both single and dual polarization systems.

6. ANTENNA REFLECTOR TECHNOLOGY

This section highlights current reflector technology and future trends as applicable to 20/30-GHz phased arrays [6-1]-[6-4]. Both solid-surface and unfurlable reflectors are discussed from the viewpoint of offset dual reflector applications. Contour and pointing accuracy resulting from manufacturing errors, repeated deployments, alignments, launch environment, and in-orbit thermal distortion are reviewed. The problems associated with the various aspects are indicated.

6.1 CURRENT TECHNOLOGY

6.1.1 SOLID SURFACE

Fixed-diameter solid-surface axisymmetric and offset reflectors up to 2.5 m in diameter have been produced in graphite, graphite-Kevlar, and Kevlar epoxy composites [6-5],[6-6]. These have been sandwich constructions with aluminum or composite material cores of various thicknesses. Most applications have been for 4-6 GHz, some for 11-14 GHz, but none have been made for 20-30 GHz. The contour tolerances that can be achieved in fabrication are proportional to diameter. The best tolerance that has been accomplished to date for a 1.98-m graphite epoxy composite (GEC) sandwich reflector appears to be 0.08 mm rms. Some studies have been done on unfurlable solid-surface reflectors. Developmental work is currently underway at TRW on their Sunflower design [6-7], [6-8].

6.1.2 MESH SURFACE

Several contractors have produced unfurlable rib-and-mesh reflectors in proprietary designs [6-9]-[6-18]. All of these have been axisymmetric; however, work is currently underway on an offset configuration. All rib-and-mesh designs are near approximations of the paraboloidal shape. Both woven and knitted mesh made with metallized polymeric fibers or gold plated metal, such as copper-plated polyester and gold-plated molybdenum, have been used. The diameter Tracking and Data Relay Satellite System (TDRSS) has 18 tubular ribs made of GEC and a 4.79-m RF aperture [6-15]. The as-fabricated contour error of 0.37 mm rms is the best contour accuracy achieved to date for a mesh construction. The best accuracy which can be achieved with the TDRSS design is 0.33 mm rms; however, improved contour accuracy can be expected by using more ribs, more intercostal mesh supports, or both. A development program would be required to determine the maximum contour accuracy that could be achieved with a radial-rib offset configuration. INTELSAT currently has an RFP outstanding for a 4- to 6-GHz offset design.

6.2 REQUIREMENTS FOR 20/30-GHz REFLECTORS

6.2.1 UNFURLABLE OR FIXED-DIAMETER

The specific arrangement of the dual offset reflector relative to the overall satellite configuration will determine whether a fixed-diameter or unfurlable main reflector can be used. With some configurations, a fixed-diameter reflector can be fitted into the missile shroud or shuttle bay. In other cases, an

unfurlable reflector will be required. Achievement of the required reflector contour accuracy will be difficult with an unfurlable reflector.

6.2.2 CONTOUR ACCURACY REQUIREMENTS

6.2.2.1 Main Reflector

The fabricated contour accuracy required for a 20/30-GHz main reflector is estimated at 0.05-0.08 mm rms within the size range of 2.74-4.27 m diameter. This estimate is based on scaling the accuracy required for the INTESLAT V 4- and 6-GHz multibeam antennas. Accuracies of this magnitude have not previously been achieved for a GEC solid-surface reflector in the size range indicated. It is likely that they can be achieved, or closely approached, with available technology; however, some developmental effort will be required to determine details of construction and processing [6-6].

6.2.2.2 Subreflector

For a solid-surface subreflector, 0.04-0.05 mm rms are required and achievable with current technology in the range of 0.93-1.43 m diameter. With appropriate tooling and attention to processing detail, the smaller value could be produced. The surface accuracy of the subreflector is more critical because of the magnification inherent in the dual reflector configuration.

6.2.3 DESIGN REQUIREMENTS

6.2.3.1 Solid Surface

To achieve the required surface accuracy, the reflector sandwich must be fabricated of all-graphite epoxy faceskins on an aluminum honeycomb core. It is estimated that the sandwich thickness required will be $\geq$1.27 cm, and the sandwich density will be $\geq$0.258 gm/cm^2 of surface area. (The density of the INTELSAT V reflector is 0.097 gm/cm^2.) Backside stiffening ribs will also be needed. The resulting reflector will be a rigid construction, resistant to local flexibility and launch vibration effects. Nonetheless, reflector thermal distortion will be higher than desired, contributing a beam pointing error of about 0.02°. Automatic beam steering will be required to keep this error within system requirements.

6.2.3.2 Mesh Surface

Since mesh can only approximate the ideal paraboloid, a rib-and-mesh reflector cannot equal the surface accuracy of the solid-surface type. The best that can be expected is about 0.005 mm rms. In contrast to the solid-surface reflector (the contour accuracy of which is determined by that of the mold) the mesh surface must be adjusted into position. One to two weeks of effort with a computerized measuring system is required to achieve the final result. If a fixed-diameter reflector could be used, it would be possible to use rigid (GEC) rather than flexible (quartz fiber) intercostal supports, thereby increasing contour accuracy. The density of the rib-and-mesh construction should be

about half that of the GEC solid surface. Thermal distortion of the former should also be less.

6.3 THERMAL DISTORTION

Beam pointing error and gain loss will result from thermal distortion of the reflectors and the antenna support structure [6-5]. The feed or reflectors may be displaced, the reflectors may rotate, or localized reflector distortions may occur. Support structure and reflector distortions are additive for concurrent conditions during the annual cycle. Several exposure conditions must be examined to determine the maximum distortion. The change in focal length and the increase in contour and beam pointing errors are usually determined for each condition. Offset reflector configurations are more sensitive to thermal distortions than are axisymmetric configurations. Dual-offset reflector configurations will be still more sensitive.

6.3.1 MAIN REFLECTOR

Thermal distortion test and analytical results have not yet been effectively correlated. Computer analysis is usually based on simplified models, which omit discontinuities. Consequently, error margins are not well defined. Nonetheless, previous analyses of solid-surface and rib-and-mesh reflectors at geosynchronous orbit provide some indication of the magnitude of the cnanges to be expected as a result of reflector thermal distortion. These values are given in Table 6-1. Concurrent thermal distortions caused by the antenna support structure will increase these values.

Table 6-1. Estimated Maximum Changes Due to Reflector Thermal Distortion at Geosynchronous Orbit

Parameter	Solid-Surface GEC	Rib-and-Mesh Unfurlable
Contour error rms (mm rms)	0.025	0.292
Focal length (%)*	±0.05	±2.0
Beam pointing error (deg)	±0.0225	±0.0165

*f/D = 1.0-1.3

Beam pointing error can be reduced by RF sensing and beam steering devices. The effect of defocusing must be evaluated on an individual basis. Increased contour errors resulting from thermal distortion are based on BFP calculations, which provide mean values. While the increased contour error of a solid-surface reflector will be small, local thermal distortion (for example, at the reflector edges) could be large enough to affect some beam sidelobes or beam isolation. If this should be the case, reflector shaping would have to be considered. This technique has been studied, but is undeveloped at this time.

6.3.2 SUBREFLECTOR

A lightweight, rigid structure with an extremely accurate contour is required for the subreflector. Maximum contour accuracy cannot be achieved with a conventional GEC sandwich. Further, if a conventional GEC sandwich were used with conventional passive cooling, thermal distortion of the subreflector would produce errors of about the same magnitude as those previously

described for the main reflector. Since these errors would be magnified by the dual reflector configuration, active cooling with heat pipes should be considered for the subreflector.

Some design investigations will be required to optimize contour accuracy, minimize weight, and achieve satisfactory cooling. A sandwich construction with integral active cooling is a desirable approach. An all-aluminum sandwich with the reflecting surface machined and polished after bonding is one possible way to achieve the required contour accuracy. The use of GEC faceskins with an epoxy gel coat finished after bonding and then metallized is another. Metal matrix materials are discussed in Subsection 6.5.2.

6.4 BEAM POINTING ERROR DUE TO ALIGNMENT

Antenna pointing error results from alignment errors associated with the following:

a. Spacecraft master cube
b. Reflector RF boresight
c. Reflector deployment repeatability
d. Zero-gravity devices
e. Earth sensor
f. Momentum wheel
g. Alignment variation due to launch environment

The RSS total of these errors may vary from a maximum of $\pm 0.043°$ pointing error under average conditions with each axis having a single pair of hinges, to a minimum of $\pm 0.025°$ for a best-conditions alignment. The latter would include use of positive

latching devices and improved alignment techniques. The smaller value is still unacceptable from a systems viewpoint. It was previously noted that beam steering would be required to offset mispointing due to thermal distortion. The most economical design and the simplest alignment procedure should be used, consistent with a beam steering range that maintains pointing within the maximum systems pointing error [6-19].

6.5 MATERIALS

6.5.1 GRAPHITE EPOXY COMPOSITE

The reflectivity of GEC is about 98 percent parallel to the fiber direction and near zero perpendicular to it. Graphite cloth, rather than unidirectional tape, should be used on the reflecting surface of the main dish to obtain satisfactory reflectivity and eliminate metallization. Ultra-high modulus graphite (GY-70 or P75S) should be used in the composite to obtain the lowest CTE of the reflector sandwich. Strict control of materials and processes will be required to achieve a relatively uniform CTE in all segments of the reflector [6-20]-[6-23].

The epoxy matrix is hygroscopic, and non-uniform absorption of moisture may produce reflector distortions equal to or greater than those caused by heat [6-24]-[6-27]. The effect of moisture on GEC reflectors has not been thoroughly investigated. It has usually been assumed that exposing such components to 50-percent relative humidity on the ground does not result in excessive in-orbit distortions. In view of the greater accuracy requirements of the 20/30-GHz reflectors, this assumption is questionable, and appropriate testing is recommended. Several methods

of sealing the composite to prevent moisture absorption have been investigated, but none is completely satisfactory [6-28], [6-29]. Any sealing material will increase the CTE and weight of the composite.

6.5.2 METAL MATRIX COMPOSITES

Materials such as graphite aluminum and graphite magnesium are currently in the experimental stage [6-30]-[6-33]. Nevertheless, they have been projected as candidates for both solid-surface reflectors and the rib elements of mesh reflectors. While the metal matrix eliminates the moisture and viscoelastic problems associated with epoxy, the CTE of these materials are somewhat larger than that of GEC, about 3.0-4.5 ppm/C vs 0.5-1.0 ppm/C. These materials are more likely candidates for use in subreflectors, where the temperature would be controlled with active cooling.

6.5.3 MESH

Both woven and knitted mesh fabricated of metallized polymeric fibers and gold-plated metal have been used in rib-and-mesh reflectors. Copper-plated polyester and gold-plated molybdenum were cited above as examples. The characteristics of the woven and knitted materials are quite different. One advantage of the knitted material for unfurlable reflectors is its lower stiffness, two or three orders of magnitude lower than that of a weave. On the other hand, after deployment, the higher stiffness of the woven mesh is advantageous for retaining the desired paraboloid shape. For a fixed-diameter rib-and-mesh reflector, woven material would be preferable.

The reflectivity of the mesh is related to the operating frequency of the antenna, which determines the fineness of the weave or knit required. At 14 GHz, a knitted mesh with 10 openings per inch is satisfactory. At 20 GHz, 18 openings per inch are required. Reflectivity may vary from 95 to 99 percent.

The advantages of mesh construction are reduced weight and lower solar pressure. The disadvantages of the unfurlable type include the larger contour error associated with mesh shaping and successive deployments. Although the as-fabricated contour error of a fixed-diameter mesh reflector would be smaller than that of an unfurlable reflector, substantial developmental effort is required to determine whether the accuracy necessary for 20/30 GHz implementation could be achieved. Additionally, while stowed mesh has withstood the launch environment, it has not been determined that deployed mesh can withstand the same conditions.

7. REFLECTOR DEPLOYMENT TECHNIQUES

The mechanisms considered here are articulated devices used to position an antenna reflector in its in-orbit configuration from its launch/stowed position. Typically, large reflectors (>1.5 m) on spacecraft require mechanisms not only for their deployment, but also to accomplish efficient packaging of the antenna farm in a given launcher payload envelope.

A survey was conducted to investigate current techniques and devices used in deployment mechanisms and to identify future trends.

7.1 MECHANISMS

The mechanisms under consideration can be divided into three classes: stowage, deployment, and latching. The stowage mechanism holds and protects the antenna components during the launch phase and absorbs the increased loads induced by the launch vehicle. The deployment mechanism deploys the antenna in its in-orbit configuration. Commonly, the reflector is the only antenna component deployed, as deployment of the feed array poses complex problems, such as rotary joints in waveguides and alignment errors. Finally, the latching mechanism locks in, or constrains the deployed antenna to maintain proper alignment of the antenna components.

The principal requirements of these mechanisms are reliability, accuracy, stiffness, and alignment. Low mass/inertia and power consumption are also desirable.

7.2 CURRENT TECHNOLOGY

A review of some current spacecraft programs, namely, INTELSAT V, Satellite Business System (SBS), Tracking and Data Relay Satellite (TDRS), and Defense Satellite Communications System III (DSCS III) indicated the predominance of two basic reflector deployment techniques: the mechanical hinge and the electromechanical device. Choosing between these two approaches entails a tradeoff between overall pointing accuracy and mass/power limitations, as discussed below.

7.2.1 MECHANICAL HINGE

This first approach employs a purely mechanical device, which includes a support bracket with bearings to tie the reflector to the spacecraft body; a hinge pin; and a torsional spring. The energy stored in the spring actuates rotation of the reflector about the hinge pin axis for deployment. Typically, a second part is included in this mechanism to provide for reflector latching at the end of deployment. The latching device is designed to restrict reflector freedom and minimize hinge error, which influences reflector pointing. Hence, these types of mechanisms are custom-designed for particular applications. They possess the advantages of low mass, good reliability, compact packaging, and low cost. The main disadvantage is that they limit the overall pointing accuracy that can be achieved.

7.2.2 ELECTROMECHANICAL DEVICE

The second approach requires electrical power input for the operation of the mechanism. This design is functionally more

sophisticated, involving stepper motors, gear drives, and gimbal supports all integrated into a single unit. These components require dedicated electronic circuits for their operation.

This type of design has the advantage of greater pointing accuracy (<0.05°) and the capability of in-orbit pointing adjustments. Also, an antenna tracking function incorporated in this design eliminates the mechanical and thermal errors caused by the reflector supporting structure. As compared to the first approach, this design is bulkier and requires power which could be in limited supply.

7.3 EXAMPLES OF MECHANISMS

Table 7-1 summarizes the overall beam pointing accuracy achieved or attempted by several current spacecraft programs. The deployment mechanisms used on the INTELSAT V, SBS, and TDRS spacecraft illustrate typical techniques.

7.3.1 INTELSAT V

In the INTELSAT V spacecraft antenna 4-GHz subsystem, the 2.44-m reflector was supported by two arm assemblies. The reflector was stowed during launch and deployed in orbit by spring actuators. The spring action also latched the arm at the end of deployment, thus limiting reflector movement. The latch was held in position by a latch spring.

Table 7-1. Antenna Survey

Spacecraft Program	Beam Diameter (m)	Actuator Type	Latch Type	Design Status	Beam Pointing Accuracy (Pitch/Roll) (deg)
INTELSAT V	2.4	Spring-actuated hinge	Spring-loaded	In orbit	0.21
TDRS	4.0 S.A.	Spring-actuated for deployment reflector on two-axis gimbal	Spring-loaded boom latch	Ground testing	<0.04 (RF tracking)
	2.0 SGL	Motor-driven gimbal	None	Ground testing	<0.04
SBS	1.8	Motor-driven hinge	None	In orbit	±0.04 (RF tracking)
DSCS III	1.3	Motor-driven gimbal	None		--
T.V. Sat.	1.5	Spring-actuated hinge (APM optional)	Positive latch	Model tested	<0.1
INTELSAT VI (Projected)	3-4	Spring-actuated hinge	Positive latch	Projected	0.15

7.3.2 SATELLITE BUSINESS SYSTEM

The SBS reflector deployment mechanism, also referred to as the antenna positioner mechanism (APM), is an example that utilizes an electromechanical device. The APM consists of redundant motors driving a single-axis hinge assembly. The output shaft supports and rotates the reflector assembly from the stowed to the deployed position by using the motor (actuator) and a gear drive assembly. The operation can be effectively controlled by the power input to the motor. This antenna system also employs RF tracking, which assists in correcting reflector orientation in one axis.

7.3.3 TRACKING AND DATA RELAY SATELLITE

The TDRS single-axis antenna deployment mechanism is an example that may indicate a trend toward the combination of both the mechanical hinge and APM. This deployment system consists of two 4.9-m center-fed mesh type reflectors mounted on two separate truss booms and deployed on either side of the spacecraft body. Each reflector is attached to an APM, which can rotate in two orthogonal axes and perform in-orbit RF tracking. The APM, in turn, is supported by a boom which is attached to a spring-mechanical hinge on the spacecraft body. The spring-actuated hinge is similar in operation to that used on INTELSAT V, but is more complex. The spring-actuated hinge deploys and latches the truss boom/reflector assembly from the stowed position, and the APM actively controls on-orbit reflector pointing and tracking. The overall mechanism system also contained stowage/caging devices.

7.4 ERROR SOURCES

Typical error sources are those that contribute to the misalignment between a reflector and the antenna platform. The principal error sources are alignment errors and thermal distortion errors.

Alignment errors arise from the following sources:

a. eccentricity among rotating/sliding elements and their mating parts,
b. linkage tolerances,
c. bearing clearances, and
d. actuator malfunction.

Thermal distortion error is caused by the thermal effect on the mechanism elements and the reflector support structure.

7.5 ERROR REDUCTION

Practical methods for reducing alignment error can only be analyzed and suggested by considering particular cases, as it is dependent upon the peculiarities of the design. However, the following general guidelines can help to minimize errors:

a. Place hinge supports far apart.
b. Use ball bearings in duplex pairs, as opposed to simple sleeve bearings.
c. Build adequate flexural stiffness into the support structure.
d. Incorporate an active latching device.
e. Maintain minimum deployment distances.

To reduce the effects of thermal distortion, materials with low coefficients of thermal expansion should be used. The most common material for antenna applications is the "Graphite . Fibre" epoxy construction. Also, differential thermal expansions of the mating parts in the assembly should be matched.

7.6 FUTURE TRENDS

Based on this survey, two approaches, the mechanical hinge and the electromechanical APM, appear to be the current technology in antenna deployment mechanisms. The electrical APM provides a higher overall pointing accuracy than the mechanical hinge. However, the future trend is toward a combination of the two approaches.

8. REFERENCES

[2-1] B. R. A. Nijboer, "The Diffraction Theory of Aberrations," Parts 1 and 2, Physica X, October 1943, pp. 679-692; Physica XIII, December 1947, pp. 605-620; with K. Nienhuis, Part 3, Physica XIV, January 1949, pp. 590-608.

[2-2] R. Kingslake, "The Diffraction Structure of the Elementary Coma Image," Proc. Phys. Soc. (London), Vol. 6, 1948, pp. 147-158.

[2-3] M. Born and E. Wolf, Principles of Optics, Chapters 5 and 9, New York: Pergamon Press, 1969.

[2-4] S. Silver and C. S. Pao, "Paraboloidal Antenna Characteristics as a Function of Feed Tilt," Report 479, Radiation Laboratory, Massachusetts Institute of Technology, February 1944.

[2-5] K. S. Kelleher and H. P. Coleman, "Off-Axis Characteristics of the Paraboloidal Reflector," NRL Report 4088, Naval Research Laboratory, Washington, D.C., December 31, 1952.

[2-6] Y. T. Lo, "On the Beam Deviation Factor of a Parabolic Reflector," IRE Transactions on Antennas and Propagation, (Commun.), Vol. AP-8, May 1960, pp. 347-349.

[2-7] S. S. Sandler, "Paraboloidal Reflector Patterns for Off-Axis Feed," IRE Transactions on Antennas and Propagation, Vol. AP-8, July 1960, pp. 368-379.

[2-8] J. Ruze, "Lateral Feed Displacement in a Paraboloid," IEEE Transactions on Antennas and Propagation, Vol. AP-13, September 1965, pp. 660-665.

[2-9] M. S. Afifi, "Aberration and Dispersion Off the Focus of a Parabola," IEEE G-AP Symposium, Los Angeles, 1971, Digest, p. 219.

[2-10] W. A. Imbriale, P. G. Ingerson, and W. C. Wong, "Large Lateral Feed Displacements in a Parabolic Reflector," IEEE Transactions on Antennas and Propagation, Vol. AP-22, November 1974, pp. 742-743.

[2-11] A. V. Mrstik, "Scan Limits of Off-Axis Fed Parabolic Reflectors," IEEE Transactions on Antennas and Propagation, Vol. AP-27, September 1979, pp. 647-651.

[2-12] A. W. Rudge, "Multiple-Beam Antennas: Offset Reflectors With Offset Feeds," IEEE Transactions on Antennas and Propagation, Vol. AP-23, May 1975, pp. 234-239.

[2-13] P. G. Ingerson and W. C. Wong, "Focal Region Characteristics of Offset Fed Reflectors," International IEEE/AP-S Symposium, Atlanta, June 10-12, 1974, Program and Digest, pp. 121-123.

[2-14] V. N. Krichevsky and D. F. DiFonzo, "Optimum Feed Locus for General Three-Dimensional Beam Scanning in Offset Cassegrain Antennas," International IEEE/AP-S Symposium, Los Angeles, June 16-19, 1981, Digest, pp. 700-703.

[2-15] V. N. Krichevsky, "Optimum Beam Scanning in Offset Single and Dual Reflector Antennas," COMSAT Laboratories Final Report on INTELSAT Contract INTEL-222, March 1983.

[2-16] P. G. Ingerson, "Off-Axis Scan Characteristics of Offset Fed Parabolic Reflectors," IEEE International AP-S Symposium, University of Illinois, Urbana-Champaign, June 2-4, 1975, Digest, pp. 382-386.

[2-17] A. Zaghloul and R. R. Persinger, "INTELSAT VI Antenna Subsystem Studies," COMSAT Laboratories, Final Report for INTELSAT Task T4-81-100, August 1981.

[2-18] A. W. Rudge et al., The Handbook of Antenna Design, Vol. 1, London: Peter Peregrinus, Ltd., 1982.

[2-19] T. Takeshima, "Beam Scanning of Parabolic Antenna by Defocusing," Electronic Engineering, 1969, pp. 70-72.

[2-20] P. C. Loux and R. W. Martin, "Efficient Aberration Correction With a Transverse Focal Plane Array Technique," IEEE International Convention Record, Vol. 12, 1964, p. 125.

[2-21] A. W. Rudge and M. J. Withers, "New Technique for Beam Steering With Fixed Paraboloid Reflectors," IEE Proceedings, Vol. 118, No. 7, July 1971, pp. 857-863.

[2-22] P. Balling, R. Jorgensen, and K. Pontoppidan, "Study of Techniques for Design of High Gain Antennas With Contoured Beams," TICRA Final Report for ESTEC Contract 3371/77/NL/AK, December 1978.

[2-23] V. Galindo-Israel, S. W. Lee, and R. Mittra, "Synthesis of a Laterally-Displaced Feed Cluster for a Reflector Antenna With Application to Multiple Beams and Contoured Patterns," IEEE Transactions on Antennas and Propagation, Vol. AP-26, 1978, pp. 220-228.

[2-24] D. F. DiFonzo, "The Evolution of Communications Satellite Antennas," IEEE AP Symposium, University of New Mexico, Albuquerque, Digest, Vol. 1, May 1982, pp. 358-361.

[2-25] P. W. Hannan, "Microwave Antenna Derived From the Cassegrain Telescope," IRE Transactions on Antennas and Propagation, Vol. AP-9, March 1961, pp. 140-153.

[2-26] W. D. White and L. K. DeSize, "Focal Length of a Cassegrain Reflector," IRE Transactions on Antennas and Propagation, Vol. AP-9, January 1961, p. 412.

[2-27] W. C. Wong, "On the Equivalent Parabola Technique to Predict the Performance Characteristics of a Cassegrainian System With an Offset Feed," IEEE Transactions on Antennas and Propagation, Vol. AP-21, May 1973, pp. 335-339.

[2-28] H. Gniss and G. Ries, "Remarks on the Concept of Equivalent Parabolas for Cassegrain Antennas," Electronics Letters, Vol. 6, November 12, 1970, pp. 737-739.

[2-29] Y. Y. Rahmat-Samii and V. Galindo-Israel, "Scan Performance of Dual Offset Reflector Antennas for Satellite Communications," Radio Science, Vol. 16, No. 6, November-December 1981, pp. 1093-1099.

[2-30] D. F. DiFonzo and B. S. Lee, "Wide-Angle Beam Scanning Performance of Dual Reflector Antennas," URSI Meeting, Houston, Texas, May 1983, Digest, p. 22.

[2-31] W. V. T. Rusch, "Scattering From a Hyperboloidal Reflector in a Cassegrainian Feed System," IEEE Transactions on Antennas and Propagation, Vol. AP-11, July 1963, pp. 414-421.

[2-32] P. D. Potter, "Application of Spherical Wave Theory to Cassegrainian-Fed Paraboloids," IEEE Transactions on Antennas and Propagation, Vol. AP-15, November 1967, pp. 727-736.

[2-33] J. B. Keller, "Geometrical Theory of Diffraction," Journal of the Optical Society of America, Vol. 52, 1962, pp. 116-130.

[2-34] R. G. Kouyoumjian and P. H. Pathak, "A Uniform Geometrical Theory of Diffraction for an Edge in a Perfectly Conducting Surface," Proceedings of the IEEE, Vol. 62, 1974, pp. 1448-1461.

[2-35] C. A. Mentzer and L. Peters, "A GTD Analysis of the Far-Out Sidelobes of Cassegrain Antennas," IEEE Transactions on Antennas and Propagation, Vol. AP-23, September 1975, pp. 702-709.

[2-36] O. Sorensen and W. V. T. Rusch, "Application of the Geometric Theory of Diffraction to Cassegrain Subreflectors With Laterally Defocused Feeds," IEEE Transactions on Antennas and Propagation, Vol. AP-73, September 1975, pp. 698-701.

[2-37] N. A. Adatia, "Diffraction Effects in Dual Offset Cassegrain Antenna," International IEEE/G-AP Symposium, Washington, D.C., May 1978, Digest, pp. 235-238.

[2-38] R. Graham, "The Polarization Characteristics of Offset Cassegrain Aerials," IEEE International Conference on Radar--Present and Future, October 1973, paper 105. Also U.S. Patent 3 792 480.

[2-39] H. Yokoi and T. Mizuguchi, "Low Sidelobe Aperture Antennas," Patent Application 47-94628, Patent Disclosure 49-52953.

[2-40] E. Ogawa, Ushijima, and T. Takano, "Radiation Characteristics of Offset Cassegrain Antennas," National Convention Record of IECE, Vol. 70, 1976.

[2-41] T. Mizuguchi, M. Akagawa, and H. Yokoi, "Radiation Characteristics of Offset Gregorian Antennas," (2), National Convention Record of IECE, Vol. 70, AP75-45, October 1975.

[2-42] M. Akagawa and T. Mizuguchi, "Radiation Characteristics of Offset Gregorian Antennas," (3), National Convention Record of IECE, Vol. 70, AP76-22, June 1976.

[2-43] M. Akagawa, "Application of Offset Dual Reflectors of Spacecraft Antennas," COMSAT Laboratories Technical Memorandum CL-42-78, September 26, 1978.

[2-44] T. Mizuguchi, M. Akagawa, and H. Yokoi, "Offset Gregorian Antenna," Electronics and Communications in Japan, Vol. 61-B, No. 3, 1978, pp. 58-66.

[2-45] M. Akagawa and D. F. DiFonzo, "Beam Scanning Characteristics of Offset Gregorian Antennas," International IEEE/G-AP Symposium, Digest, June 1979.

[2-46] E. A. Ohm and M. J. Gans, "Numerical Analysis of Multiple-Beam Offset Cassegrainian Antennas," AIAA/CASI 6th Communications Satellite Conference, Montreal, April 5-8, 1976.

[2-47] E. A. Ohm, "System Aspects of a Multibeam Antenna for Full U.S. Coverage," International Conference on Communications, Boston, June 10-14, 1979, Conference Record, pp. 49.2.1-49.2.5.

[2-48] C. Dragone, "A First Order Treatment of Aberrations in Cassegrainian and Gregorian Antennas," IEEE Transactions on Antennas and Propagation, Vol. AP-30, No. 3, May 1982, pp. 331-339.

[2-49] N. G. Ponomarev, "Graphical Method for the Design of Profile of Aplanatic Antennas," Radio Engineering and Electronic Physics, Vol. 6, 1961, p. 42.

[2-50] W. D. White and L. K. DeSize, "Scanning Characteristics of Two-Reflector Systems," IRE Convention Record, Part I, 1962, pp. 44-70.

[2-51] B. Claydon, "The Schwarzschild Reflector Antenna With Multiple or Scanned Beams," The Marconi Review, First Quarter 1975, pp. 14-43.

[2-52] J.H.A.W. van de Sande, M.H.A.J. Herbeu, and E. J. Maanders, "Designing Schwarzschild Antenna Systems," IEE 2nd International Conference on Antennas and Propagation, York, U.K., April 1981, Conference Publication 195, pp. 153-157.

[2-53] G. E. Roberts, "Parametric Solution of the Equations of the Schwarzschild Two-Reflector Optical System," Journal of the Optical Society of America, Vol. 54, No. 9, September 1964, pp. 1111-1114.

[2-54] C. M. Rappaport, "The Offset Bifocal: A New Concept in Scanning Dual Reflector Antennas," COMSAT Laboratories Technical Report CL-TR-4-82, January 1983.

[2-55] D. C. Hogg and R. A. Semplak, "An Experimental Study of Near-Field Cassegrainian Antennas," Bell System Technical Journal, November 1964, pp. 2677-2704.

[2-56] W. D. Fitzgerald, "Limited Electronic Scanning With a Near-Field Cassegrainian System," Technical Report 484, MIT Lincoln Laboratory, September 24, 1971.

[2-57] E. A. Dudkovsky, "A System for Exciting Large Parabolic Antennas," Russian Patent No. 146365, 1962.

[2-58] G. E. Skahill, L. K. DeSize, and P. J. Wilson, "Electronically Steerable Field Reflector Antenna Techniques," Technical Report RADC-TR-66-354, August 1966.

[2-59] W. D. Fitzgerald, "Limited Electronic Scanning With an Offset Feed Near-Field Gregorian System," Technical Report 486, MIT Lincoln Laboratory, September 24, 1971.

[2-60] R. W. Kreutel and D. F. DiFonzo, "A Dual Reflector Antenna With Phased Array Feed," Memorandum TCLT/74-2061, COMSAT Laboratories, June 12, 1974.

[2-61] M. H. Chen and G. N. Tsandoulas, "A Dual-Reflector Optical Feed for Wideband Phased Arrays," IEEE Transactions on Antennas and Propagation, Vol. AP-22, No. 4, July 1974, pp. 541-545.

[2-62] K. Woo and P. Cramer, "Limited Scan Near-Field Cassegrainian Antenna," IEEE International Symposium, University of Massachusetts at Amherst, October 1976, Digest, pp. 323-325.

[2-63] C. Dragone and M. J. Gans, "Imaging Reflector Arrangements to Form a Scanning Beam Using a Small Array," Bell System Technical Journal, Vol. 58, No. 2, February 1979, pp. 501-515.

[2-64] C. Dragone and M. J. Gans, "Satellite Phased Arrays: Use of Imaging Reflectors With Spatial Filtering in the Focal Plane to Reduce Grating Lobes," Bell System Technical Journal, Vol. 59, No. 3, March 1980, pp. 449-461.

[2-65] K. Woo, "Array-Fed Reflector Antenna Design and Applications," IEE 2nd International Conference on Antennas and Propagation, York, U.K., April 1981, Conference Publication 195, pp. 209-213.

[2-66] Y. Hwang and C. C. Han, "A Scanning Offset-Fed Near-Field Gregorian Reflector Antenna," IEEE Antennas and Propagation Symposium Digest, 1981, pp. 716-719.

[2-67] M. Tanaka and M. Mizusawa, "Elimination of Cross Polarization in Offset Dual-Reflector Antennas," Electronics and Communications in Japan, Vol. 58-B, No. 12, 1975, pp. 71-78.

[3-1] C. Dragone and M. Gans, "Satellite Phased Arrays: Use of Imaging Reflectors With Spatial Filtering in the Focal Plane to Reduce Grating Lobes," Bell System Technical Journal, Vol. 59, No. 3, March 1980, pp. 449-461.

[3-2] N. Amitay and M. Gans, "Design of Arrays of Oversized Aperture, Tapered Waveguide Horn Elements," IEEE International Symposium on Antennas and Propagation, Seattle, Washington, June 1979, Digest, pp. 356-359.

[3-3] N. Amitay and M. Gans, "Design of Rectangular Horn Arrays with Oversized Aperture Elements," IEEE Transactions on Antennas and Propagation, Vol. AP-29, November 1981, pp. 871-884.

[3-4] J. Fratamico, M. Gans, and G. Owens, "A Wide Scan Quasi-Optical Frequency Diplexer," IEEE Transactions on Microwave Theory and Techniques, Vol. MTT-30, January 1982, pp. 20-27.

[3-5] K. Woo, "Array-Fed Reflector Antenna Design and Applications," IEE International Conference on Antennas and Propagation, York, U.K., 1981, Conference Publication 195, pp. 209-213.

[3-6] M. H. Chen and G. N. Tsandoulas, "A Dual-Reflector Optical Feed for Wide-Band Phased Arrays," IEEE Transactions on Antennas and Propagation, Vol. AP-22, July 1974, pp. 541-545.

[3-7] D. O. Reudink and Y. S. Yeh, "A Scanning Spot-Beam Satellite System," Bell System Technical Journal, Vol. 56, No. 8, October 1977, pp. 1549-1560.

[3-8] W. H. Von Aulock, "Properties of Phased Arrays," Proceedings of the IRE, Vol. 48, October 1960, pp. 1715-1727.

[3-9] R. S. Elliott, "Beamwidth and Directivity of Large Scanning Arrays," Part I, Microwave Journal, Vol. 6, No. 12, December 1963, pp. 53-60; Part II, Microwave Journal, Vol. 7, No. 1, January 1964, pp. 74-82.

[3-10] P. W. Hannan, "The Element Gain Paradox for a Phased-Array Antenna," IEEE Transactions on Antennas and Propagation, Vol. AP-12, July 1964, pp. 423-433.

[3-11] R. C. Hansen, Ed., Microwave Scanning Antennas, 3 Volumes, New York: Academic Press, 1966.

[3-12] N. Amitay, V. Galindo, and C. P. Wu, Theory and Analysis of Phased Array Antennas, New York: Wiley-Interscience, 1972.

[3-13] L. Stark, "Microwave Theory of Phased-Array Antennas - A Review," Proceedings of the IEEE, Vol. 62, December 1974, pp. 1661-1703.

[3-14] R. J. Mailloux, "Phased Array Theory and Technology," Proceedings of the IEEE, Vol. 70, March 1982, pp. 246-291.

[3-15] R. Mailloux et al., "Grating Lobe Control in Limited Scan Arrays," IEEE Transactions on Antennas and Propagation, Vol. AP-27, January 1979, pp. 79-85.

[3-16] R. Mailloux and G. Forbes, "An Array Technique with Grating Lobe Suppression for Limited-Scan Applications," IEEE Transactions on Antennas and Propagation, Vol. AP-21, September 1973, pp. 597-602.

[3-17] A. I. Zaghloul and R. H. MacPhie, "Effects of Positioning Errors on Grating-Lobe Reduction in Uniform Linear Arrays," Radio Science, Vol. 6, March 1971, pp. 407-419.

[3-18] R. H. T. Bates, "Mode Theory Approach to Arrays," IEEE Transactions on Antennas and Propagation, Vol. AP-13, March 1965, pp. 321-322.

[3-19] J. L. Allen, "On Surface-Wave Coupling Between Elements of Large Arrays," IEEE Transactions on Antennas and Propagation, Vol. AP-13, July 1965, pp. 638-639.

[3-20] G. F. Farrell, Jr. and D. H. Kuhn, "Mutual Coupling Effects of Triangular-Grid Arrays by Modal Analysis," IEEE Transactions on Antennas and Propagation, Vol. AP-14, September 1966, pp. 652-654.

[3-21] G. F. Farrell, Jr. and D. H. Kuhn, "Mutual Coupling in Infinite Planar Arrays of Rectangular Waveguide Horns," IEEE Transactions on Antennas and Propagation, Vol. AP-16, July 1968, pp. 405-414.

[3-22] P. W. Hannan, "Discovery of an Array Surface Wave in a Simulator," IEEE Transactions on Antennas and Propagation, Vol. AP-15, July 1967, pp. 574-576.

[3-23] R. F. Frazita, "Surface-Wave Behavior of a Phased Array Analyzed by the Grating-Lobe Series," IEEE Transactions on Antennas and Propagation, Vol. AP-15, November 1967, pp. 823-824.

[3-24] H. A. Wheeler, "The Grating-Lobe Series for the Impedance Variation in a Planar Phased-Array Antenna," IEEE Transactions on Antennas and Propagation, Vol. AP-14, November 1966, pp. 707-714.

[3-25] L. W. Lechtreck, "Effects of Coupling Accumulation in Antenna Arrays," IEEE Transactions on Antennas and Propagation, Vol. AP-16, January 1968, pp. 31-37.

[3-26] G. H. Knittel, A. Hessel, and A. A. Oliner, "Element Pattern Nulls in Phased Arrays and Their Relation to Guided Waves," Proceedings of the IEEE, Vol. 56, November 1968, pp. 1822-1836.

[3-27] G. H. Knittel, "The Relation of Blindness in Phased Arrays to Higher-Mode Cutoff Conditions," IEEE International Symposium on Antennas and Propagation, Los Angeles, California, September 1971, Digest, pp. 69-72.

[3-28] Y. T. Lo and V. D. Agrawal, "A Method for Removing Blindness in Phased Arrays," Proceedings of the IEEE, Vol. 56, September 1968, pp. 1586-1588.

[3-29] A. I. Zaghloul and R. H. MacPhie, "On the Removal of Blindness in Phased Antenna Arrays by Element Positioning Errors," IEEE Transactions on Antennas and Propagation, Vol. AP-20, September 1972, pp. 637-641.

[3-30] P. W. Hannan and S. P. Litt, "Capacitive Ground Plane for Phased Array Antenna," IEEE International Symposium on Antennas and Propagation, Boston, 1968, Digest, pp. 115-123.

[3-31] A. Hessel and G. H. Knittel, "A Loaded Ground Plane for the Elimination of Blindness in a Phased-Array Antenna," IEEE International Symposium on Antennas and Propagation, Austin, Texas, December 1969, Digest, pp. 163-169.

[3-32] S. W. Lee and W. R. Jones, "On the Suppression of Radiation Nulls and Broadband Impedance Matching of Rectangular Waveguide Phased Arrays," IEEE Transactions on Antennas and Propagation, Vol. AP-19, January 1971, pp. 41-51.

[3-33] N. Goto and D. Cheng, "Phase-Shifter Thinning and Sidelobe Reduction for Large Phased Arrays," IEEE Transactions on Antennas and Propagation, Vol. AP-24, March 1976, pp. 139-143.

[3-34] B. R. Hatcher, "Granularity of Beam Positions in Digital Phased Arrays," Proceedings of the IEEE, Vol. 56, November 1968, pp. 1795-1800.

[3-35] N. Amitay, P.E. Butzien, and R. C. Heidt, "Match Optimization of a Two-Port Phased Array Antenna Element," IEEE Transactions on Antennas and Propagation, Vol. AP-16, January 1968, pp. 47-57.

[3-36] C. O. Hemmi, W. F. Hayes, and R. C. Voges, "Practical Impedance Matching of Phased Array Radiating Element," Proceedings of the IEEE, Vol. 56, November 1968, pp. 1963-1967.

[3-37] B. L. Diamond, "Small Arrays--Their Analysis and Their Use for the Design of Array Elements," Phased Array Antennas, A. A. Oliner and G. H. Knittel, Editors, Dedham, Massachusetts: Artech House, 1972, pp. 127-131.

[3-38] H. A. Wheeler, "A Systematic Approach to the Design of a Radiator Element for a Phased Array Antenna," Proceedings of the IEEE, Vol. 56, November 1968, pp. 1940-1951.

[3-39] H. A. Wheeler, "A Survey of the Simulator Techniques for Designing a Radiating Element," Phased Array Antennas, A. A. Oliner and G. H. Knittel, Editors, Dedham, Massachusetts: Artech House, 1972, pp. 132-148.

[3-40] B. L. Diamond and G. H. Knittel, "A New Procedure for the Design of a Waveguide Element for a Phased Array Antenna," Phased Array Antennas, A. A. Oliner and G. H. Knittel, Editors, Dedham, Massachusetts: Artech House, 1972, pp. 149-156.

[3-41] G. N. Tsandoulas and G. H. Knittel, "The Analysis and Design of Dual-Polarization Square-Waveguide Phased Arrays," IEEE Transactions on Antennas and Propagation, Vol. AP-21, November 1973, pp. 796-808.

[3-42] A. W. Rudge, G. Y. Philippou, and N. Williams, "Low Cross-Polar Waveguide Horns for Multiple-Feed Reflector Antennas," IEE International Conference on Antennas and Propagation, London, November 1978, Conference Publication 169, pp. 360-363.

[3-43] A. S. Marincic and Z. Petrovic, "A New Design of Horn With Improved Radiation Pattern," IEE International Conference on Antennas and Propagation, November 1978, Conference Publication 169, pp. 364-368.

[3-44] P. S. Hall and J. R. James, "Survey of Design Techniques for Flat Profile Microwave Antennas and Arrays," Radio Electronics Engineering, Vol. 48, 1978, pp. 549-565.

[3-45] A. A. Oliner and R. G. Malech, "Mutual Coupling in Infinite Scanning Arrays," Microwave Scanning Antennas, Vol. II, Chapter 3, R. C. Hansen, Editor, New York: Academic Press, 1966.

[3-46] P. S. Carter, Jr., "Mutual Impedance Effects in Large Beam Scanning Arrays," IRE Transactions on Antennas and Propagation, Vol. AP-8, May 1960, pp. 276-285.

[3-47] L. A. Kurtz et al., "Mutual Coupling Effects in Scanning Dipole Arrays," IRE Transactions on Antennas and Propagation, Vol. AP-9, September 1961, pp. 433-443.

[3-48] W. Wasylkiwskyj and W. K. Kahn, "Mutual Coupling and Element Efficiency for Infinite Linear Arrays," Proceedings of the IEEE, Vol. 56, November 1968, pp. 1901-1907.

[3-49] P. W. Hannan, "The Ultimate Decay of Mutual Coupling in a Planar Array Antenna," IEEE Transactions on Antennas and Propagation, Vol. AP-14, March 1966, pp. 246-248.

[3-50] V. Galindo and C. P. Wu, "Asymptotic Behavior of the Coupling Coefficient for an Infinite Array of Thin-Walled Rectangular Waveguides," IEEE Transactions on Antennas and Propagation, Vol. AP-14, March 1966, pp. 248-249.

[3-51] V. Galindo and C. P. Wu, "On the Asymptotic Decay of Coupling for Infinite Phased Arrays," Proceedings of the IEEE, Vol. 56, November 1968, pp. 1872-1880.

[3-52] G. V. Borgiotti, "Modal Analysis of Periodic Planar Phased Arrays of Apertures," Proceedings of the IEEE, Vol. 56, November 1968, pp. 1881-1892.

[3-53] B. L. Diamond, "A Generalized Approach to the Analysis of Infinite Planar Array Antennas," Proceedings of the IEEE, Vol. 56, November 1968, pp. 1837-1851.

[3-54] L. Stark, "Radiation Impedance of a Dipole in an Infinite Planar Phased Array," Radio Science, Vol. 1, March 1966, pp. 361-377.

[3-55] E. C. DuFort, "A Scattering Matrix Method for Solving Waveguide Array Impedance Problems," Radio Science, Vol. 3, May 1968, pp. 475-485.

[3-56] S. W. Lee, N. S. Wong, and R. Tang, "Analysis of Infinite Planar Array of Rectangular Waveguides by Generalized Scattering Matrix Approach," Phased Array Antennas, A. A. Oliner and G. H. Knittel, Editors, Dedham, Massachusetts: Artech House, 1972, pp. 91-103.

[3-57] S. Edelberg and A. A. Oliner, "Mutual Coupling Effects in Large Antenna Arrays: Part I - Slot Arrays," IRE Transactions on Antennas and Propagation, Vol. AP-8, May 1960, pp. 286-297.

[3-58] C. P. Wu and V. Galindo, "Properties of a Phased Array of Rectangular Waveguides With Thin Walls," IEEE Transactions on Antennas and Propagation, Vol. AP-14, March 1966, pp. 163-173.

[3-59] S. W. Lee and R. Mittra, "Radiation from Dielectric-Loaded Arrays of Parallel-Plate Waveguides," IEEE Transactions on Antennas and Propagation, Vol. AP-16, September 1968, pp. 513-519.

[3-60] R. F. Harrington and J. R. Mautz, "A Generalized Network Formulation for Aperture Problems," IEEE Transactions on Antennas and Propagation, Vol. AP-24, November 1976, pp. 870-873.

[3-61] J. Luzwick and R. F. Harrington, "Mutual Coupling Analysis in a Finite Planar Rectangular Waveguide Antenna Array," Electromagnetics, Vol. 2, January 1982, pp. 25-42.

[3-62] R. J. Mailloux, "Radiation and Near-Field Coupling Between Two Collinear Open-Ended Waveguides," IEEE Transactious on Antennas and Propagation, Vol. AP-17, January 1969, pp. 49-55.

[3-63] H. Steyskal, "Mutual Coupling Analysis of a Finite Planar Waveguide Array," IEEE Transactions on Antennas and Propagation, Vol. AP-22, July 1974, pp. 594-597.

[3-64] A. I. Zaghloul and M. R. Chartoff, "Correlation Matrix Solution to Mutual Coupling Between Rectangular Apertures," IEEE International Symposium on Antennas and Propagation, Quebec, June 1980, Digest, pp. 170-173.

[3-65] A. I. Zaghloul and R. H. MacPhie, "Cross-Correlation Formulation of the Complex Power from Planar Apertures," Radio Science, Vol. 10, June 1975, pp. 619-624.

[3-66] R. H. MacPhie and A. I. Zaghloul, "Radiation From a Rectangular Waveguide With Infinite Flange - Exact Solution by the Correlation Matrix Method," IEEE Transactions on Antennas and Propagation, Vol. AP-28, July 1980, pp. 497-503.

[3-67] J. Galejs, Antennas in Inhomogeneous Media, London: Pergamon Press, 1969, pp. 121-127.

[3-68] W. Rotman and R. Turner, "Wide-Angle Microwave Lens for Line Source Applications," IEEE Transactions on Antennas and Propagation, Vol. AP-11, November 1963, pp. 623-632.

[3-69] J. Ruze, "Wide-Angle Metal-Plate Optics," Proceedings of the IRE, Vol. 38, January 1950, pp. 53-59.

[3-70] J. B. L. Rao, "Multifocal Three-Dimensional Bootlace Lenses," IEEE Transactions on Antennas and Propagation, Vol. AP-30, November 1982, pp. 1050-1056.

[3-71] J. B. L. Rao, "Multifocal Three-Dimensional Bootlace Lenses," Naval Research Laboratories Report 8465, March 1981.

[3-72] A. Dion and L. Ricardi, "A Variable Coverage Satellite Antenna System," Proceedings of the IEEE, Vol. 59, February 1971, pp. 252-262.

[3-73] G. D. M. Peeler and W. F. Gabriel, "Volumetric Scanning GCA Antenna," IRE Convention Record, Part I, 1955, pp. 20-27.

[3-74] H. H. S. Luh, T. M. Smith, and W. G. Scott, "A Dual-Band TEM Lens for a Multiple Beam Antenna System," IEEE Transactions on Antennas and Propagation, Vol. AP-30, March 1982, pp. 224-229.

[3-75] J. S. Ajioka and V. W. Ramsey, "An Equal Group Delay Waveguide Lens," IEEE Transactions on Antennas and Propagation, Vol. AP-26, July 1978, pp. 519-527.

[3-76] R. E. Collin and F. J. Zucker, Editors, Antenna Theory, Part II, Chapter 18, New York: McGraw-Hill, 1969.

[3-77] J. P. Shelton, "Focusing Characteristics of Symmetrically Configured Bootlace Lenses," IEEE Transactions on Antennas and Propagation, Vol. AP-16, July 1978, pp. 513-518.

[3-78] A. Y. Niazi, M. S. Smith, and D. E. N. Davies, "Microstrip and Triplate Rotman Lenses," Military Microwaves Conference, London, October 1980, Proceedings, pp. 3-12.

[3-79] A. Niazi, "Rotman Lens Fed Multiple Beam Array," IEE International Conference on Antennas and Propagation, York, U.K., 1981, Conference Publication 195, pp. 93-97.

[3-80] E. Jacobs, "Phase Error Effects on Gain and Sidelobe Level of a Space-Fed Array," IEEE Transactions on Antennas and Propagation, Vol. AP-28, March 1980, pp. 243-246.

[3-81] D. Thomas, "Multiple Beam Synthesis of Low Sidelobe Patterns in Lens Fed Arrays," IEEE Transactions on Antennas and Propagation, Vol. AP-26, November 1978, pp. 883-886.

[3-82] S. W. Lee et al., "Refraction at a Curved Dielectric Interface: Geometrical Optics Solution," IEEE Transactions on Microwave Theory and Techniques, Vol. MTT-30, January 1982, pp. 12-19.

[3-83] J. Smetana, "Application of MMIC Modules in Future Multiple Beam Satellite Antenna Systems," NASA Technical Memorandum 83344, September 1982.

[4-1] R. T. Hill, "Phased Array Feed Systems, A Survey," Phased Array Antennas, A. A. Oliver and G. H. Knittel, Editors, Dedham, Massachusetts: Artech House, 1972, pp. 197-211.

[4-2] J. L. Allen and B. L. Diamond, "Mutual Coupling in Array Antennas," Lincoln Laboratory, Massachusetts Institute of Technology, Technical Report 424, 1966.

[4-3] L. Parad and R. Moynihan, "Split Tec Power Divider," IEEE Transactions on Microwave Theory and Techniques, Vol. MTT-13, January 1965, pp. 91-96.

[4-4] J. Butler and R. Lowe, "Beam Forming Matrix Simplifies Design of Electronically Scanned Antennas," Electronic Design, Vol. 9, 1961, pp. 170-173.

[4-5] J. L. Allen, "A Theoretical Limitation on the Formation of Lossless Multiple Beams in Linear Arrays," IEEE Transactions on Antennas and Propagation, Vol. AP-9, July 1961, pp. 350-352.

[4-6] W. D. White, "Pattern Limitations in Multiple Beam Antennas," IRE Transactions on Antennas and Propagation, Vol. AP-10, July 1962, pp. 430-436.

[4-7] J. P. Shelton and K. S. Kelleher, "Multiple Beams From Linear Arrays," IRE Transactions on Antennas and Propagation, Vol. AP-9, 1961, pp. 154-161.

[4-8] S. Stein, "On Cross Coupling in Multiple-Beam Antennas," IEEE Transactions on Antennas and Propagation, Vol. AP-10, September 1962, pp. 548-557.

[4-9] W. P. Delaney, "An RF Multiple Beam Forming Technique," Lincoln Laboratory, Massachusetts Institute of Technology, Report 41G-0012, August 1961.

[4-10] H. J. Moody, "The Systematic Design of the Butler Matrix," IEEE Transactions on Antennas and Propagation, Vol. AP-12, November 1964, pp. 786-788.

[4-11] W. G. Jaeckle, "Systematic Design of a Matrix Network Used for Antenna Beam Steering," IEEE Transactions on Antennas and Propagation, Vol. AP-15, March 1967, pp. 314-316.

[4-12] J. P. Shelton, "Fast Fourier Transforms and Butler Matrix," Proceedings of the IEEE, March 1968, p. 350.

[4-13] M. Veno, "A Systematic Design Formulation for Butler Matrix Applied FFT Algorithm," IEEE Transactions on Antennas and Propagation, Vol. AP-29, May 1981, pp. 496-501.

[4-14] H. E. Foster and R. E. Hialt, "Butler Network Extension to Any Number of Antenna Ports," IEEE Transactions on Antennas and Propagation, Vol. AP-18, November 1970, pp. 818-820.

[4-15] M. Pelletier et al., "Phase Control in Multibeam Arrays," IEEE Transactions on Aerospace and Electronic Systems, Vol. AES-13, May 1977, pp. 318-321.

[4-16] C. Winter, "Lossy-Feed Networks in Multiple-Beam Arrays," IEEE Transactions on Antennas and Propagation, Vol. AP-27, January 1979, pp. 122-126.

[4-17] J. Blass, "Multidirectional Antenna--A New Approach to Stacked Beams," IRE National Convention Record, Part 1, 1960, pp. 48-50.

[4-18] A. R. Lopez, "Monopulse Networks for Series Feeding an Array Antenna," IEEE Transactions on Antennas and Propagation, Vol. AP-16, July 1968, pp. 436-440.

[4-19] G. R. Hanley and H. R. Perini, "Column Network Study for a Planar Array Used With an Unattended Radar," Final Report, RADC-TR-80-191, March 1980.

[4-20] S. G. Winchell, "A Performance Analysis of Broadband Low Sidelobe Array Antennas," Report N60921-79-C-A236-100, Naval Surface Weapons Center, Pahlgren, Virginia, 1979.

[4-21] G. E. Evans and S. G. Winchell, "A Wideband Ultra-Low Sidelobe Antenna," 1979 Antennas Applications Symposium, University of Illinois, Urbana-Champaign, 1979.

[4-22] Military Standardization Handbook, U.S. Radar Equipment, MIL-HDBK-1628, December 15, 1973, pp. 558-559.

[4-23] G. C. Bandy, L. J. Hardeman, and W. F. Hayes, "MERA Modules, How Good in an Array," Microwaves, 1969, pp. 39-49.

[4-24] G. N. Tsandoulas, "Unidimensionally Scanned Phased Arrays," IEEE Transactions on Antennas and Propagation, Vol. AP-28, 1980, pp. 86-98.

[4-25] J. H. Provencher, "A Survey of Circular Symmetric Arrays," Phased Antennas, A. Oliner and G. Knittel, Editors, Dedham, Massachusetts: Artech House, 1972, pp. 292-300.

[4-26] B. Sheleg, "A Matrix-Fed Circular Array for Continuous Scanning," Proceedings of the IEEE, Vol. 56, 1968, pp. 2016-2027.

[4-27] G. Skahil and W. D. White, "A New Technique for Feeding a Cylindrical Array," IEEE Transactions on Antennas and Propagation, Vol. AP-13, 1975, pp. 253-256.

[4-28] G. G. Sanford, "Conformal Microstrip Phased Array for Aircraft Tests With ATS-6," IEEE Transactions on Antennas and Propagation, Vol. AP-26, 1981, pp. 642-646.

[4-29] R. Munson and G. Sanford, "Microstrip Phased Array Developed for 5 GHz Application," International IEEE AP-S Symposium, Stanford University, California, 1977, Digest, pp. 72-75.

[4-30] D. Huebner, "An Electrically Small Microstrip Dipole Planar Array," Workshop on Printed Circuit Antenna Technology, New Mexico State University, 1979, Proceedings, Paper 17.

[4-31] J. Yee and W. Furlong, "An Extremely Lightweight Fuselage Integrated Phased Array for Airborne Applications," Workshop on Printed Circuit Antenna Technology, New Mexico State University, 1979, Proceedings, Paper 15.

[4-32] E. J. Wilkinson, "A N-Way Hybrid Power Divider," IRE Transactions on Microwave Theory and Techniques, Vol. MTT-8, January 1969, pp. 116-118.

[4-33] H. Howe, Stripline Circuit Design, Dedham, Massachusetts: Artech House, 1974, p. 94.

[4-34] H. Y. Yee et al., "N-Way TEM Mode Broadband Power Dividers," IEEE Transactions on Microwave Theory and Techniques, Vol. MTT-18, October 1970, pp. 682-688.

[4-35] N. Nagai, E. Mackawa, and K. Ono, "New n-Way Hybrid Power Dividers," IEEE International Microwave Symposium Digest, 1981, pp. 503-504.

[4-36] Z. Galani and S. J. Temple, "A Broadband n-Way Combiner/Divider," IEEE International Microwave Symposium Digest, 1981, pp. 499-502.

[4-37] C. L. Chao, "N-Way Branch-Line Directional Couplers," IEEE International Microwave Symposium Digest, 1974, pp. 93-95.

[4-38] J. P. Quine et al., "MIC Power Combiners for FET Amplifiers," 9th European Microwave Conference, Brighton, England, September 1979, Proceedings, pp. 661-664.

[4-39] J. O. Bregon et al., "New Radial Power Combiner Using Tubular Dielectric Cavities," Electronics Letters, September 1982, Vol. 18, No. 18, pp. 771.

[4-40] R. A. Pucel et al., "GaAs Monolithic Lange and Wilkinson Couplers," IEEE Transactions on Electron Devices, Vol. ED-28, February 1981, pp. 212-216.

[4-41] G. A. Brehm et al., "Monolithic GaAs Lange Coupler at X-Band," IEEE Transactions on Electron Devices, Vol. ED-28, February 1981, pp. 217-218.

[4-42] J. Hobdell et al., "Low-Loss Lange Coupler," Electronics Letters, Vol. 18, No. 19, 1982, pp. 815-816.

[4-43] J. J. Pan, "Active Microwave Power Combiner/Divider Using a Dual-Gate MESFET," IEEE International Microwave Symposium Digest, 1981, pp. 434-435.

[4-44] J. F. White, Semiconductor Control, Dedham, Massachusetts: Artech House, 1977.

[4-45] J. F. White, "Review of Semiconductor Microwave Phase Shifters," Proceedings of the IEEE, Vol. 56, 1968, pp. 1924-1930.

[4-46] R. V. Garver, "Broadband Diode Phase Shifters," IEEE Transactions on Microwave Theory and Techniques, Vol. MTT-20, 1972, pp. 314-423.

[4-47] W. J. Ince, "Recent Advances in Diode and Ferrite Phaser Technology for Phased-Array Radars, Part I, Microwave Journal, Vol. 15, No. 9, 1972, pp. 36-46; Part II, Micro-Wave Journal, Vol. 15, No. 10, 1972, pp. 31-36.

[4-48] C. R. Boyd, "Analog Rotary-Field Ferrite Phase Shifters," Microwave Journal, Vol. 20, 1977, pp. 41-43.

[4-49] M. Kumar et al., "Broadband Dual-Gate FET Continuously Variable Phase Shifter," IEEE International Microwave Symposium Digest, 1981, pp. 431-433.

[4-50] Y. Gazit and H. C. Johnson, "A Continuously Variable K_u-Band Phase/Amplitude Control Module," IEEE International Microwave Symposium Digest, 1981, pp. 436-437.

[4-51] R. A. Gaspari and H. H. Yee, "Microwave GaAs FET Switching," IEEE MTT-S International Microwave Symposium Digest, Ottawa, Canada (78CHI355-7 MTT), 1978, pp. 58-60.

[4-52] W. Fabian et al., "Dual-Gate GaAs FET Switches," GaAs IC Symposium, Lake Tahoe, September 1979, Research Abstracts, Paper 28.

[4-53] R. V. Garver, "Microwave Semiconductor Control Devices," IEEE Transactions on Microwave Theory and Techniques, Vol. MTT-27, 1979, pp. 523-529.

[4-54] "Earth Station Antenna Technology Seminar," COMSAT Laboratories, Clarksburg, Maryland, April 17, 1980, pp. 142-154.

[4-55] Leo Young, "Meander-Line Polarizer for Converting Linear to Circular Polarization," IEEE Transactions on Antennas and Propagation, Vol. AP-21, May 1973, pp. 376-378.

[4-56] D. O. Reudink and Y. S. Yeh, "The Organization and Synchronization of a Switched Spot-Beam System," 4th International Conference on Digital Communications, Montreal, Canada, October 1978, Conference Record, pp. 191-196.

[4-57] A. S. Acampora, C. Dragone, and D. O. Reudink, "A Satellite System With Limited-Scan Spot Beams," IEEE Transactions on Communications, Vol. COM-27, No. 10, October 1979, pp. 1406-1415.

[4-58] W. L. Aranguren, R. E. Langseth, and C. B. Woodworth, "Sequencer Designs for Scanning Beam Satellite," Bell System Technical Journal, Vol. 58, No. 9, November 1979, pp. 1999-2011.

[4-59] A. S. Acampora and B. R. Davis, "Efficient Utilization of Satellite Transponders Via Time Division Multibeam Scanning," Bell System Technical Journal, Vol. 57, No. 8, October 1978.

[4-60] F. T. Assal, K. Betaharon, A. I. Zaghloul, and R. Gupta, "Wideband Microwave Switch Matrix for SS/TDMA Systems," 5th International Conference on Digital Satellite Communications, Genoa, Italy, 1980, Conference Record, pp. 421-428.

[4-61] F. Assal, R. Gupta, K. Betaharon, A. Zaghloul, and J. Apple, "A Wideband Satellite Microwave Switch Matrix for SS/TDMA Communications," IEEE Journal on Selected Areas in Communications, Vol. SAC-1, January 1983, pp. 223-231.

[5-1] D. N. McQuiddy, "Solid State Radar's Path to GaAs," IEEE MTT Symposium Digest, June 1982, pp. 176-178.

[5-2] B. Geller and F. Assal, "Impact of Monolithic Microwave Integrated Circuit Development on Communications Satellites," ICC Digest, June 1982, pp. IEI.1-IEI.5.

[5-3] R. A. Pucel, "Design Considerations of Monolithic Microwave Integrated Circuits," IEEE Transactions on Microwave Theory and Techniques, Vol. MTT-29, June 1981, pp. 513-534.

[5-4] H. Tserng et al., "Design, Fabrication, and Characterization of Monolithic Microwave GaAs Power FET Amplifier," IEEE Transactions on Electron Devices, Vol. ED-28, February 1981, pp. 183-190.

[5-5] A. Higashisaka and T. Mizuta, "20-GHz Band Monolithic GaAs FET Low Noise Amplifier," IEEE Transactions on Microwave Theory and Techniques, Vol. MTT-29, January 1981, pp. 1-6.

[5-6] Y. Ayasli et al., "A Monolithic X-Band Four Bit Phase Shifter," IEEE MTT Symposium Digest, 1982, pp. 486-488.

[5-7] W. McLevige and V. Sokolov, "Resonated GaAs FET Devices for Microwave Switching," IEEE Transactions on Electron Devices, Vol. ED-28, February 1981, pp. 198-204.

[5-8] B. Scott and G. Brehm, "Monolithic Voltage Controlled Oscillator for X- and K_u-Bands," IEEE MTT Symposium Digest, 1982, pp. 482-485.

[5-9] M. Cathelin et al., "5-GHz Binary Frequency Division on GaAs," Electronics Letters, July 3, 1980, pp. 535-536.

[5-10] M. V. Schneider, B. Glance, and W. F. Bodtmann, "Microwave and Millimeter Wave Hybrid Integrated Circuits for Radio Systems," Bell System Technical Journal, July-August 1969, pp. 1703-1726.

[5-11] J. Van Heuven, "A New Integrated Waveguide-Microstrip Transition," IEEE Transactions on Microwave Theory and Techniques, Vol. MTT-24, March 1976, pp. 144-147.

[6-1] "30/20 GHz Spacecraft, Multiple Beam Antenna System, Major Review Document for Tasks I and II," Document A030-3, November 12, 1981. Prepared for NASA-Lewis Research Center under Contract NAS3-22499 by TRW, Redondo Beach, California.

[6-2] "30/20 GHz Spacecraft, Multiple Beam Antenna Systems, Task I Report, Development of Operational Systems Concepts," Document A005, February 28, 1981. Prepared for NASA-Lewis Research Center under Contract NAS3-22499 by TRW, Redondo Beach, California.

[6-3] "30/20 GHz Spacecraft, Multiple Beam Antenna System, Task II Report, Antenna System Concept for Demonstration Satellite," April 22, 1981. Prepared for NASA-Lewis Research Center under Contract NAS3-22499 by TRW, Redondo Beach, California.

[6-4] "30/20 GHz Spacecraft, Multibeam Antenna System, Review #1," October-November 1980. Presented to NASA-Lewis Research Center under Contract NAS3-22498 by Ford Aerospace and Communications Corporation, Palo Alto, California.

[6-5] J. S. Archer, "High Performance Parabolic Antenna Reflectors," AIAA 7th Communications Satellite Systems Conference, San Diego, California, April 1978, Collection of Technical Papers, p. 442.

[6-6] TRW Defense and Space Systems Group, "Feasibility Study of Graphite Epoxy Antenna for a Microwave Limb Sounder Radiometer (MLSR)," Report 8710.7.79-3, Jet Propulsion Laboratory Contract 955258, February 1979.

[6-7] W. B. Palmer, "Deployable Antenna Reflector," TRW Defense and Space Systems Group, 12th Aerospace Mechanism Symposium, Moffett Field, California, April 1978.

[6-8] "Study of Advanced Sunflower Precision Deployable Antenna," Final Report MEL-79-B-126 for Jet Propulsion Laboratory Contract 955340, November 21, 1979, TRW Systems Group, Redondo Beach, California.

[6-9] J. A. Fager, Application of Graphite Composites to Future Spacecraft Antennas, AIAA Paper No. 76-238, 6th Communications Satellite Systems Conference, Montreal, Canada, April 5-8, 1976.

[6-10] A. A. Woods, Jr. and W. D. Wade, "On the Design of Self-Deploying Extremely Large Parabolic Antennas and Arrays," Lockheed Missiles & Space Company, Sunnyvale, California, IEEE Mechanical Engineering In Radar Symposium, Arlington, Virginia, November 1977.

[6-11] R. E. Freeland, "Industry Capability for Large Space Antenna Structures," Report No. 710-12, May 25, 1978, Jet Propulsion Laboratory, Pasadena, California.

[6-12] A. A. Woods, Jr. and M. Kural, "Considerations on the Use of Graphite-Reinforced Plastics for Space Erectable Antennas," Lockheed Missiles & Space Company, Sunnyvale, California, 7th AIAA Communications Satellite Systems Conference, San Diego, California, April 1978.

[6-13] A. A. Woods, Jr. and W. D. Wade, "An Approach Toward the Design of Large Diameter Offset-Fed Antennas," Lockheed Missiles & Space Company, Sunnyvale, California, AIAA/NASA Conference on Advanced Technology for Future Space Systems, Hampton, Virginia, May 1979.

[6-14] H. L. Staubs et al., "Advanced Antenna System Requirements and Implications on Material Characteristics," SAMPE National Symposium, San Francisco, California, May 1979.

[6-15] "Tracking and Data Relay Satellite System, System Design Report," March 26, 1979. Prepared under Subcontract 76159 to Western Union Space Communications, Inc. by TRW, Redondo Beach, California.

[6-16] M. B. Sullivan and B. E. McIntosh, "Advanced Composites Considerations in Design of Large Space Antennas," Conference on Advanced Composites--Special Topics, Harris Corporation, El Segundo, California, December 4-6, 1979, Proceedings, pp. 370-403.

[6-17] "Final Report for Study of Wrap-Rib Antenna Design," Report No. LMSC-D714613. Prepared for the Jet Propulsion Laboratory under Contract 955345 by Lockheed Missiles & Space Company, Sunnyvale, California, December 12, 1979.

[6-18] J. A. Fager, "Large Space Erectable Antenna Stiffness Requirements," AIAA 78-590R, Journal of Spacecraft and Rockets, Vol. 17, No. 2, March-April 1980, p. 86.

[6-19] S. H. Marx, "Precise Orientation of Multibeam Satellite," Report No. IAF-81-53. Ford Aerospace and Communications Corporation, Palo Alto, California, 1981.

[6-20] J. Prunty, "Dimensionally Stable Graphite Composites for Spacecraft Structures," 9th National SAMPE Conference, Atlanta, Georgia, October 4, 1977.

[6-21] D. D. Smith, "Design Considerations for Graphite Epoxy Laminates of Low Thermal Expansivity," Advanced Composites: Design and Applications, MFPG 29th Meeting, October 1979, National Bureau of Standards Special Publication 563, p. 60.

[6-22] S. Oken and D. E. Skoumal, "Design, Fabrication, and Test of a Full-Scale Graphite/Epoxy Metering Truss for the Space Telescope," 8th National SAMPE Technical Conference, Seattle, October 1976, Bicentennial of Materials, pp. 1-12.

[6-23] J. M. Miller, "Thermal Deformation Characteristics of a Six-Inch Graphite Epoxy and Ultra-Low Expansion Telescope," Journal of Spacecraft, Vol. 14, No. 5, May 1977, p. 315.

[6-24] C. C. Chamis et al., "An Integrated Theory for Predicting the Hygrothermomechanical Response of Advanced Composite Structural Components," Advanced Composite Materials - Environmental Effects, ASTM STP 658, September 1977, p. 160.

[6-25] R. Schapery et al., "Composite Materials for Structural Design," Report No. AFOSR-TR-79-0347, Contract F49620-78-C-0034, College Station, Texas, March 1979.

[6-26] F. W. Crossman and D. L. Flaggs, "Dimensional Stability of Composite Laminates During Environmental Exposure," Sampe Journal, July/August 1979, p. 15.

[6-27] D. F. Adams and D. E. Walrath, "Hygrothermal Response of Polymer Matrix Composite Materials," Report No. UWME-DR-901-102-1, Grant Nos. DAAG-29-76-G-0163 and DAAG-29-78-G-0053, University of Wyoming, Laramie, Wyoming, September 1979.

[6-28] C. J. Staebler, Jr. and B. F. Simpers, "Metallic Coatings for Graphite Epoxy Composites," Final Report under Contract N00019-77-C-0250, Grumann Aerospace Corporation, Bethpage, New York, May 1979.

[6-29] J. F. Haskins, "Recent Work on Techniques and Applications of Moisture Barriers to Graphite Epoxy Composites," Advanced Composites: Design and Applications, MFPG 29th Meeting, October 1979, National Bureau of Standards Special Publication 563, p. 47.

[6-30] J. J. Tribendis et al., "The Effect of Fiber Orientation and Thermal Treatment on the Mechanical Properties of Graphite-Aluminum Composites," AIAA, New York, Technical Information Service Paper No. A81-38597, 1981.

[6-31] A. Okurà et al., "Mechanical Properties of Carbon Fiber Reinforced Aluminum Composites," AIAA, New York, Technical Information Service Paper No. A81-40570, 1981.

[6-32] E. G. Wolff et al., "Thermal Expansion Measurements of Metal Matrix Composites," AIAA, New York, Technical Information Service Paper No. A81-40575, 1981.

[6-33] D. Webster, "Properties and Microstructure of Metal Matrix Composites," AIAA, New York, Technical Information Service Paper No. A81-40576, 1981.

COMSAT